NASA Technical Memorandum 80122

(NASA-TM-80122) SEASAT-A SATELLITE SCATTEROMETER MISSION SUMMARY AND ENGINEERING ASSESSMENT REPORT (NASA) 146 p HC A07/MF A01 CSCL 08C
N79-28645
Unclas
G3/43 29442

SeaSat-A Satellite Scatterometer
Mission Summary And Engineering
Assessment Report

James W. Johnson, Wendell H. Lee and Leon A. Williams

May 1979

NASA
National Aeronautics and
Space Administration

Langley Research Center
Hampton, Virginia 23665

ACRONYMS AND ABBREVIATIONS

ADWG	Algorithm Development Working Group
AGO	Santiago Ground Station
ALT	Altimeter
AOS	Acquisition of Signal
ASM	Antenna Switching Matrix
CRP	Command Request Profile
EU	Engineering Unit
GDR	Geophysical Data Record
GMT	Greenwich Mean Time
HVPS	High Voltage Power Supply
IDPS	Instrument Data Processing System
IGDR	Interim Geophysical Data Record
JPL	Jet Propulsion Laboratory
LaRC	Langley Research Center
LMSC	Lockheed Missiles and Space Company
LOS	Loss of Signal
MPT	Mission Planning Team
OAK	Oakhanger Ground Station
ORR	Orroral Ground Station
POCC	Project Operations Control Center
SAR	Synthetic Aperture Radar
SASS	SeaSat-A Satellite Scatterometer
SDR	Sensor Data Record
SMMR	Scanning Multifrequency Microwave Radiometer
SNR	Signal-to-Noise Ratio

SPAT	Spacecraft Performance Analysis Team
SPS	Sensor Performance Summary
SSS/LO	Solid State Source/Local Oscillator
TDA	Tunnel Diode Amplifier
VIRR	Visible and Infrared Radiometer

TABLE OF CONTENTS

INTRODUCTION

Scope

As the title suggests, the scope of this report is twofold. The primary topic is the SeaSat-A Satellite Scatterometer (SASS) engineering assessment as defined in the SASS Engineering Assessment Plan (Initial Phase) dated March 9, 1978. In addition, selected material and information, not required for engineering assessment per se but considered particularly interesting will be interspersed throughout, and an overview of significant mission events will be included. The purpose in not restricting the scope here to engineering assessment alone is to include information that needs to be documented and otherwise may not be.

In the Engineering Assessment Plan, the following tasks were outlined as Langley Research Center (LaRC) responsibilities.

1) Pre-launch support of the Mission Planning Team (MPT)
2) Pre and post launch support of the Spacecraft Performance Analysis Team (SPAT)
3) Pre and post launch support of the Algorithm Development Working Group (ADWG)
4) Validation of the Instrument Data Processing System (IDPS) software with respect to SASS status data handling and processing and engineering unit (EU) conversion of SASS analog data, excluding cell location processing.
5) The initial phase (Phase I) of the post launch engineering assessment or hardware evaluation of the SASS.

Items 1, 2 and 3 have been satisfactorily completed and require no further comment. The bulk of this report will deal with items 4 and 5.

Objective

The prime objective of Phase I Engineering Assessment was to assure the Project Office at the Jet Propulsion Laboratory (JPL) that SASS Sensor Data Records (SDR's) contain a correct engineering data base and that the instrument was operating properly so that SASS SDR's may be released for geophysical data processing. This objective was met by performing tasks 4 and 5 under the following basic conditions.

a) Data to be used must be restricted to the first 30 days of operation.

b) The hardware evaluation is based solely on SDR products. This does not include P_R/P_T and σ^o, where

   P_R/P_T = Ratio of received to transmitted power

   σ^o = Radar scattering coefficient.

c) Even though cell location processing is an IDPS function, its validation is dependent upon σ^o computations; therefore, it is being handled independently and for the purposes here will not be considered part of Phase I Engineering Assessment.

The Phase I objective has been met with a high level of confidence in spite of these constraints, and the primary purpose of this report is to demonstrate the work that has been done and the specific conclusions that have been drawn in the process. In general, it will be shown that the IDPS software is acceptable and the scatterometer operated properly in orbit.

Approach

The approach taken in Phase I Engineering Assessment differs somewhat from the original plan due to a pair of problems that developed after launch. First an acceptable flow of data from JPL was not established until three months after launch, and secondly the satellite power system failure terminated the mission after 3-1/2 months. These circumstances affected Engineering Assessment in that the σ^{o} algorithm was operational by the time data became available making some tasks that had been planned using only SDR products unnecessary, and with the satellite failure all evaluation was being done "after the fact" making the establishment of certain baseline performance criteria for future monitoring unnecessary. After the satellite failure, Phase II Engineering Assessment was deleted, therefore, the "Phase I" distinction will be dropped at this point.

A background overview of the scatterometer experiment itself and the instrument is included here in an effort to make this report as self contained as possible. The software and hardware evaluation tasks were independent of each other, and will be discussed separately. It was required that 2 sets of software be validated, namely that used at JPL by the IDPS and that used at Goddard Space Flight Center by the Project Operations Control Center (POCC). The POCC software assumed added importance after launch with the time lag in getting data to JPL. In parallel with this, an evaluation of the IDPS Sensor Performance Summary (SPS) Software was conducted. As confidence in the IDPS software developed, the hardware evaluation proceeded using continuous data listings (C-TABs) and SPS listings for both short term, frame-by-frame, and long term functional and engineering checks. Transmitter and receiver performance were studied in a limited fashion but no SASS end-to-end evaluation was possible since P_R and σ^o were not available for use in Engineering Assessment. Finally, a brief exercise to determine the usefulness of the SASS science voltage output at the SDR level in judging end-to-end instrument performance was included. The correlation between the science voltage output and σ^o at nadir and 8^o incidence was used since the true performance of the SASS as a wind sensor lies in its ability to measure σ^o.

BACKGROUND

Experiment

Microwave scatterometers have been shown to be sensitive to ocean surface wind speed and direction in previous aircraft programs and the Skylab S-193 experiment. Figures 1 and 2 are examples of data gathered by LaRC with an aircraft scatterometer and used as the basis for the satellite instrument and data inversion algorithm designs. Figure 1 demonstrates the dependence of σ^o on wind speed for given incidence angles, and the following equation couples σ^o to the parameter actually sensed by the scatterometer, P_R, plus other tractable terms.

$$\sigma^o = \frac{P_R}{P_T} \times \frac{(4\pi)^3 R^3}{\lambda^2 L \phi L_s G_o^2 (\frac{G}{G_o})^2}$$

P_R = received power

P_T = transmitted power

R = slant range

λ = free-space wavelength

L = footprint length in broad beam plane

ϕ = 3-dB beamwidth in narrow beam plane

G_o = peak antenna gain

G/G_o = relative gain at given incidence angle

Figure 2 shows the behavior of σ^o with wind direction for given wind speeds. The periodicity in σ^o vs wind direction will create ambiguities, primarily in wind direction, which must be removed from the satellite measurement. Figure 3 depicts the scatterometer swath and the nominal incidence angle distribution across the swath. The 4 SASS antennas illuminated patches on the surface that were further subdivided by doppler filtering. In this way, the following fundamental user requirements were met.

User Requirements
Wind Speed - 4 to 24 m/sec (±2 m/sec or ±10%)
Wind Direction - 360° (±20°)
Swath - 1000 km
Resolution - 50 × 50 km
Grid Spacing - 100 km

These requirements were derived from user interest in surface wind measurements as inputs to ocean wave forecast models and to weather forecasting models, and they formed the basis for defining instrument characteristics. A thorough description of the methods used to develop instrument performance requirements and design characterization for the SASS is given by Grantham, et. al.*

Instrument

The scatterometer electronics package and the 4 fully deployed antenna assemblies are situated on the SeaSat-A satellite as shown in Figure 4. Each antenna assembly is approximately 300 cm long and consists of 2 antennas, one horizontally polarized and the other vertically polarized. The electronics package is connected to the antennas through 8 independent waveguide sections. The scatterometer electronics manufacturer was the General Electric Company's Valley Forge Space Division, the antennas were provided by Aerojet ElectroSystems of Azusa, California, and the satellite

*Grantham, W. L., Bracalente, E. M., Jones, W. L., Johnson, J. W.: The SeaSat-A Satellite Scatterometer, IEEE J. Oceanic Eng., Vol. OE-2, pp. 200-206, April 1977.

contractor Lockheed Missiles and Space Company (LMSC) of Sunnyvale, California supplied the 8 waveguides interconnecting the electronics with the antennas. Figures 5 and 6 are photographs of one antenna assembly and the scatterometer electronics package respectively.

The conceptual block diagram of the scatterometer in Figure 7 shows the major components and subsystems. The SSS/LO is a frequency synthesizer that provides the transmitter excitation before upconversion to approximately 14.6 GHz and all required local oscillator signals at the receiver. Local oscillator signals at 2 different frequencies are provided for the second mixing stage so that selection of the proper one allows use of the same set of doppler filters for both forward looking (positive doppler) and aft looking (negative doppler) measurements. The transmitted signal is interrupted cw at 17% duty factor and 100 watts peak power out of the TWT, which is a Hughes 8294H from the Electron Dynamics Division in Torrance, California. The antenna switching matrix (ASM) selects the transmitting/receiving antenna for each backscatter measurement by switching in a periodic fashion as defined by the selected instrument operating mode. In all operating modes, a backscatter measurement is made every 1.89 sec. and an antenna switching cycle is completed every 7.56 sec. The noise source provides a periodic receiver gain calibration every 240 sec. A tunnel diode amplifier (TDA) is used for the first stage of amplification and sets the receiver noise figure at less than 5.7 dB over the full receiver temperature range. Using range gating and doppler filtering techniques in the Scat Processor, measurements of return signal from 15 contiguous cells on the ocean surface plus background noise power (S+N) and noise power only (N ONLY) are made. This amounts to 30 science data values every

1.89 sec. that, when corresponding pairs of S+N and N ONLY are processed, result in 15 measurements of P_R which are proportional to σ^o. The Digital Controller takes the spacecraft clock and generates the timing functions and commands required by the various subsystems, and it also assembles the scatterometer data stream and interfaces it with the block formatted satellite data system. The SASS uses both +28 VDC unregulated and +28 VDC regulated power from the spacecraft. The following table provides an overview of the instrument characteristics.

Instrument Characteristics	
Operating Frequency	14.59927 GHz
Receiver Noise Figure	5.7 dB*
Receiver Dynamic Range	>45 dB
Receiver Resolution	< 0.1 dB
RF Output Power	100 Watts
DC Input Power	136 Watts
Weight	63 kg
Envelope Dimensions	110 × 48 × 30 cm^3

*With baseplate temperature @ 33°C

The operational status of the scatterometer is determined by the position of latching, electromechanical relays and non-latching solid state switches located in the instrument itself. The diagram in Figure 8 shows the sequence of commands of both types conventionally required in operations. First, the SASS ENABLE and HVPS ENABLE* commands switch the latching relays to couple the regulated and unregulated 28 VDC spacecraft

*HVPS denotes the High Voltage Power Supply.

power to the instrument subsystems. Secondly, any one of the 10 nonlatching "MODE" commands may be selected to place the instrument in any one of 8 data modes, in the Continuous Calibrate mode or return it to the Standby mode. The 8 data modes are defined in Figure 9. They differ from one another only by the particular antenna switching scheme that is unique to each. The measurements in any of the 8 modes are periodic in 7.56 sec. Modes 1 and 2 offer single polarization measurements over the full swath, Modes 3 and 4 provide dual polarization over one half swath, and Modes 5 thru 8 provide single polarization measurements over one half swath but offer double the integration time for enhanced accuracy. The fundamental cycle is through antenna position such that in Modes 3 and 4 both horizontal and vertical polarization measurements are made before stepping to the next antenna. Table 1 outlines the nominal electrical behavior of the instrument in the various operating modes. Clearly, there are no differences in Modes 1 thru 8 and the changes that occur in Continuous Calibrate and Standby have only to do with the TWT and the HVPS. In Continuous Calibrate the TWT beam is inhibited and the output power goes to zero but the high voltage is undisturbed, however in Standby the high voltage is also removed from the TWT.

Some comments on thermal control pertinent to the overall design are appropriate here. The satellite contractor was responsible for the thermal control of the electronics package and to some extent the antennas. The satellite thermal design included heaters on the back of the scatterometer baseplate and adsorptive/reflective louvers attached to the edges of the baseplate, both aimed at maintaining the temperature between $0^{\circ}C$ and $35^{\circ}C$. The antennas were conductively isolated from the spacecraft. The locations of the 24 electronics package temperatures are listed in Appendix A.

A summary of the SASS data is given below.

Data Stream Summary	
DATA TYPE	ALLOCATION
SYNC	31 bits
STATUS	56 bits
HOUSEKEEPING	280 bits (28 WORDS)
SCIENCE	300 bits (30 WORDS)
SPARES	153 bits
TOTAL	820 bits

Both bi-level and 10 bit analog words are formatted serially in a data stream containing 820 total bits per frame which is updated once every 1.89 sec. Appendix A is a complete list of all parameters in the scatterometer data stream along with the identification number for each and its location in a given frame. The 24 electronics package and 40 antenna assembly temperature monitors are subcommutated such that 3 and 5 temperature values respectively are reported in each data frame, thereby requiring 8 frames of data for a complete set of temperature measurements.

SIGNIFICANT EVENTS

The purpose of this section is to document and discuss the significant events for the entire mission that concern the scatterometer. Therefore, its scope will not be limited to engineering assessment. Table 2 lists the events considered to be the most significant and Figure 10 summarizes descriptively the event sequence.

Engineering Assessment Operations

Table 2 shows the scatterometer antennas being deployed during the second orbit. They were deployed in pairs with the second pair following the first by only 25 seconds. Each deployment took approximately 15 seconds to complete. This close timing was not satisfactory from the scatterometer viewpoint since it would not have allowed time to postpone the second command for problem and work around considerations had the first deployment been unsuccessful. The requirement for rapid deployment of all antennas for the sake of satellite orbit and attitude stabilization was favored over the aforementioned risk. It is not the point here to criticize the final plan but just to reiterate that scheduling the SASS antenna deployments only 25 seconds apart was considered a risk to the scatterometer experiment.

The scatterometer was turned on in the following sequence with respect to the other sensors approximately 10 days after launch. This sequence allowed an evaluation of the scatterometer in the low voltage condition for 2 orbits prior to turning the high voltage and transmitter on. It also provided for RFI data to be taken as other sensors came on sequentially.

Sensor Turn-On Sequence			
Event	SASS Command	Rev#	Time
SASS On	SASS Off (Initialize)	139	187/1819:20
	SASS Enable	139	1819:50
	HVPS Enable	141	2144:04
	Operate Mode 4	141	2147:24
SMMR On		143	188/0057:00
VIRR On		144	0244:00
ALT On		145	0409:00
SAR On		150	1220:00

The first 30 days of scatterometer operation were designated the engineering assessment period. Figure 11 shows the basic mode sequencing plan followed with the orbit numbers noted at the beginning and end of each major period. A prime consideration in arriving at this plan was to limit instrument mode changes in the beginning. Therefore, it was left in the prime data taking mode (i.e. Mode 4) making dual polarization measurements for the first 6 days. Next, Modes 1 and 6 were used for 6 days each making full swath and double integration time or enhanced resolution measurements respectively, thus demonstrating the main instrument capabilities. The next 6 day period was used to exercise the other 5 data modes. Finally, engineering assessment was completed by running a "6 Day Orbit Normal" sequence, including Continuous Calibrate and Standby, that was to be the standard scatterometer operating procedure, repeating every 6 days, for the mission duration. The rationale used in defining this mode sequence was developed based on science requirements, was not pertinent to engineering assessment, and need not be discussed here. On July 15, JASIN operations began where the instrument was switched to either Mode 3 or Mode 4 for 20 minutes when the satellite passed over the JASIN experiment site in the North Atlantic, always returning to the mode planned for engineering assessment. The objective here was to generate data for comparison with JASIN in situ measurements and aircraft underflight data. Appendix B is a complete list of all modes used and time tagged as executed except where data gaps prevented verification. In such cases, the Command Request Profile (CRP) times are listed. Execution of a mode command generally came 4-5 seconds after the CRP time. The entire "6 Day Orbit Normal" is not listed but the sequences shown are typical for all orbits. The flight operations for engineering assessment were completed on August 6.

Thermostat Failure

Thermal Control of the scatterometer was to be maintained by the satellite. Heaters with thermostats were used for automatic thermal control of the scatterometer baseplate. Power was provided to both the SASS heaters and a similar altimeter heater circuit through a common switch so that both were either powered or unpowered. This sets the stage for a temperature or heater circuit problem that lasted from July 24 through most of the rest of the mission. The scatterometer was designed to operate within specification with the baseplate temperature between 0°C and 35°C. A failure of the altimeter control thermostat resulted in operation of the scatterometer at marginally low temperatures for approximately 82% of the mission. The details of instrument performance, including low temperature effects, are contained in the Hardware Evaluation section.

The thermostats used here were the Texas Instruments M2 type rated at 2.0 A. The scatterometer heater circuit drew 6.5 A and the altimeter 4.7 A. Consequently, the altimeter thermostat failed closed on about July 24, and the scatterometer thermostat appeared to be intermittently sticking in the closed position. Both instruments required heat but at less than a 100% duty factor at this point in the mission, thus the altimeter began to overheat. The operational solution required switching the heater circuit power to maintain an acceptable heating duty factor for both sensors. This allowed the altimeter to operate continuously. It turned out that the only compatible thermal condition kept the altimeter near its maximum allowable temperature and the scatterometer just below its minimum allowable temperature for most of the rest of the mission. The heater duty factor required was approximately 30% on July 24 and decreased to 0% as the angle with respect to the Sun changed.

When the thermostat failure was recognized, the altimeter had overheated and the heater circuit power was turned off. During this period of preliminary failure analysis and operational "work around" definition, one monitor point on the scatterometer baseplate reached -6.6°C which turned out to be the minimum for the mission. The scatterometer was designed to survive baseplate temperatures as low as -10°C and no damage was suffered during these heater circuit failure exercises.

Orbit Adjust Maneuvers

Each maneuver operation is listed in Table 3 along with the time that the thruster burn actually occurred. There were 5 individual maneuvers with the thrusters actually firing for approximately 30 seconds to 7 minutes. Maneuvers are worth noting because the satellite attitude and sensor pointing are disturbed and because the plan included turning the sensors off during thruster firings. The scatterometer off times, which total approximately 21 hours, are listed below. The SASS was left on during Cal Burn #2 due to a lack of understanding of the requirement by Mission Planning Team personnel.

	SCATTEROMETER OFF TIMES	
Maneuver	SASS Off	SASS On
Cal Burn #1	227/0110:30	227/1029:02
Orbit Adjust #1	230/0108:30	230/0938:32
Cal Burn #2	SASS Left On	
Orbit Adjust #2	238/0817:14	238/1102:59
Orbit Trim	253/0108:00	253/0119:10

A note of caution is due here. The requirement to turn the scatterometer off during a maneuver was derived from the fear that local pressure changes due to thruster emissions might cause RF arcing at the antennas or even high voltage arcing in the electronics package. Exhaust plume characteristics were defined by the satellite contractor in other studies and existing information did not indicate that a thruster firing would affect the SASS environment. Also, electromechanical relays were switched in the process of turning the scatterometer off and on, and this was considered to be a relatively high risk operation that should be avoided, particularly early in the mission. In the early mission planning just prior to launch, maneuvers were scheduled within days of turning the scatterometer on. In light of the exhaust plume information that existed, the planned maneuver schedule, and the risks involved in switching relays, the issue of sensor operations during maneuvers was poorly resolved.

Low Bus Voltage Problem

On August 28, overloading of the spacecraft power system on successive orbits caused the spacecraft bus voltage to continually decline until on Rev 891 the Altimeter tripped off just prior to reaching a minimum bus voltage of 21.8 VDC. With the Altimeter off, the loading condition was relieved and eventually operations and mission planning personnel realized what had occurred and corrective action was taken.

Figure 12 is a plot of bus voltage as a function of time from the ascending node on Rev 891 and is useful in describing the basic problem. At this point in time, the satellite was in occultation for the longest period during each orbit and in the minimum available power period expected for the entire mission. Figure 12 shows occultation on Rev 891 lasting 27 minutes. The satellite contractor's power model used for mission planning purposes operated on an orbit average basis and predictable transient effects, such as occultation, could be taken into account. The events following occultation in Figure 12 were evidently not taken into account properly. The solar collector panels are designed to sense their angle with respect to the sun and if less than some minimum value to rotate 180°. The heaters were being operated at 12 - 1/2% duty factor at this point. After occultation, plus a battery charging time of less than 5 minutes, the solar panels rotated and the heaters came on further discharging the batteries for another 20 minutes. On each successive Rev leading up to the Altimeter going off, the minimum bus voltage dropped. By the time of the next station pass at Hawaii, the bus voltage had recovered so that the problem was not apparent to the operations personnel.

The only low voltage effects on the scatterometer were a proportionate increase in HVPS input current from 2.30 A to approximately 3.0 A and an HVPS temperature increase of approximately 1°C. The regulated bus voltage did not begin to drop. No scatterometer damage was sustained and performance was not affected.

Aircraft Underflights

The mission for the SASS was to infer, through empirical models, surface wind speed and direction by sensing the normalized radar cross section or scattering coefficient, σ^o, of the roughened ocean surface. Consequently, the satellite instrument must be calibrated in terms of σ^o. This is being done by comparing satellite data to data taken simultaneously with a calibrated aircraft scatterometer. The aircraft scatterometer was calibrated to an accuracy better than 0.5 dB and it was installed on the Johnson Space Center C-130 (NASA-929) for a series of underflights which were conducted from August 23 through September 30 in conjunction with the JASIN and GOASEX experiments in the North Atlantic and Gulf of Alaska respectively. Table 3 outlines the JASIN and GOASEX data sets. Nine underflights covering 11 satellite Revs were conducted, including 3 in the Atlantic off the eastern coast of the U.S., in winds from 7-35 knots. GOASEX and the last 2 east coast flights are considered the prime data sets due to the high wind conditions, which should give high signal-to-noise measurements in the outer cells. The underflight program was considered successful, and an excellent calibration of the satellite instrument is expected.

Satellite Failure

On October 10 the satellite power system failed at approximately 0312 GMT over the Oakhanger (OAK) ground station in Farnsborough, England, and the last contact with the satellite was on Rev 1503 at 0408:28 GMT. The cause of the failure was determined to be short circuiting of slip ring contacts in the solar array assembly. This short circuited both the batteries and the charging system and drained the batteries to the point where the satellite was lost in approximately 1/2 orbit. The data in Figure 13, taken real time at the Oakhanger, Santiago (AGO), and Orroral (ORR) gound stations, shows piecewise from acquisition of signal (AOS) to loss of signal (LOS) the decay in the unregulated bus voltage and the corresponding effects on the SASS regulated bus voltage and the SASS current drawn from the unregulated bus. The interesting features here are the sudden 3-1/2 volt drop when the short circuit occurred, the last available data before losing the satellite of 19.0 volts unregulated, and the SASS undervoltage trip at 25.4 volts regulated. The undervoltage trip occurred on day 283 at 0406:30 turning the scatterometer transmitter off as designed and at precisely the same value of regulated bus voltage as determined in subsystem tests. As signal was lost at the Orroral station the scatterometer receiver continued to operate with no apparent damage to the instrument but with most parameters reacting to the low input voltages.

Figures 13-16 demonstrate the scatterometer behavior as the satellite failed. The HVPS input current increased proportionately for the most part as the unregulated bus voltage decreased until the sudden drop to 0.6 A when the undervoltage trip turned the transmitter off. The transmitter output power began to drop before the cathode voltage started losing regulation probably as a result of a drop in drive power, filament current, etc. in response to the lower bus voltages. The cathode voltage begins to drop at 21.1 volts unregulated and this was the prime cause for the power drop. As the cathode voltage decreases, the beam begins to defocus and the tube body current increases sharply. Figure 16 shows the response of the SASS internal power supplies as the regulated bus voltage drops below 28 volts. Most of these supplies appear to go out of specification in the neighborhood of 26.25 volts.

The scatterometer gathered data almost continuously for 95.5 days prior to the satellite failure.

SOFTWARE EVALUATION

The following software packages have been evaluated.

a. Sensor Data Record (SDR)

b. Sensor Performance Summary (SPS)

c. Project Operations Control Center (POCC)

Items a. and b. were developed at the Jet Propulsion Laboratory and c. was developed at the Goddard Space Flight Center. The validation of SDR processing was required in order to guarantee that correct data products were available for geophysical processing, and it was necessary to evaluate the SPS software to define the utility and limitations of SPS listings in routine sensor monitoring and health assessment. Even though cell location processing is done at the SDR level it will not be discussed in this report. The POCC processing system was designed to accommodate sensor assessment to the degree required for operations only. With the severe data availability time lag created by the projects inability to deliver data tapes to JPL, the POCC system became critical to the scatterometer team for engineering assessment in general. Even though POCC operations terminated when the satellite failed, a summary of the processing validation is appropriate here.

SDR Validation

SDR processing validation consisted of verifying that all scatterometer status parameters, which are mostly bi-level, are interpreted properly and used properly in SDR processing, and verifying that engineering unit conversion of all analog parameters was done correctly. All data discrepancies identified in the engineering assessment activity were determined to be ground data system rather than SASS hardware problems and consequently will be discussed in this section along with a general data quality analysis.

Continuous frame by frame listings of the 12 data sets, one in each instrument operating mode, given in Table 4 were reviewed in detail and no errors in the handling of either status or analog parameters were found. Analog parameter EU conversions were evaluated by a direct counts-to-EU comparison for all parameters in a single frame of data. The frame chosen was at 2325:00 GMT on day 187, and the results are in Appendix C.

The temperature interpolations on transmit power and TWT filament current are being done correctly at JPL. The 2 values 2 dB apart for L.O. power exist because JPL was not discriminating between the high and low frequency L.O. calibration curves based on the value of parameter SS715 (High Frequency Select) as planned. The low frequency L.O. curve is being used for all data, but this was not considered a major problem and the software was not modified. The remaining electrical parameters, including science voltages from 0.1564-4.975 volts, are being converted correctly.

Figures C.1 and C.2 compare the Lockheed calibration data used in the JPL software with the calibration data specified by Langley. Figures C.1 and C.2 deal with electronics package temperature words 43, 44 and 45. All LMSC data used in converting word 43 and data for certain parameters on words 44 and 45 were updated at one point in the LMSC calibration book. Some parameters on words 44 and 45 were not changed. It is clear that all updated calibrations are quite accurate while those not updated may be as much as 1.5°C low. Originally LMSC did not use all of the data supplied by LaRC in their curve fitting routine and lost accuracy. In any case, this was considered acceptable for the electronics package temperatures. The ASM temperature was the lowest point monitored during the mission, is measured on word 43, and is accurate. The conversion processing itself using the LMSC calibration data is correct.

The antenna temperatures are converted to $^{\circ}C$ in the Langley Antenna Squint Angle Determination Algorithm rather than using the LMSC calibration curves. In this algorithm, temperature is a function of the Thermistor Reference Voltage. A comparison of computations made at Langley with values produced with the JPL software is included in Appendix C. There are discrepancies approaching $2^{\circ}C$ caused by taking the reference voltage from the data frame immediately preceding the frame for which temperature is being computed. In the short term the reference volt e is stable to $<\pm 2$ counts and the worst case sensitivity to reference voltage appears to be,

$$\frac{\Delta \text{ Ant Temp}}{\Delta \text{ Ref Volt}} < 1 \ ^{\circ}\text{C/COUNT}$$

for antenna temperatures around $-70^{\circ}C$. Antenna temperatures are reported by the instrument in groups of 5 per frame, and all temperature pairs used for differential computations in the algorithm lie in the same 5 word group. Therefore, reference voltage errors would not significantly affect squint estimates based on temperature differentials. The algorithm's sensitivity to bulk temperature error is $.0022^{\circ}$ in squint per $^{\circ}C$. Clearly a $2^{\circ}C$ temperature error translates to an insignificant squint error of $<.005^{\circ}$. The antenna temperature processing accuracy was considered acceptable and no software corrections were requested.

SRD processing of all SASS parameters, excluding cell location, is considered acceptable for the 4.8 C version software.

Once SASS data began flowing in large quantities through the JPL system, it became apparent that the quality was poor. For this reason, an error analysis was undertaken using a limit test on 3 static SASS 10 bit words (SYNC words), SS873-875. These parameters have fixed bit patterns and decimal equivalent values. Out of a population of 1.45×10^6 samples, 273 errors were detected for a probability of an error occurring in a given 10 bit SASS parameter approximately equal to 1 in 5×10^3 frames of data. For the scatterometer, this must be translated to the probability of error in a σ^o measurement to judge data quality in terms of the geophysical measurement. SASS parameters that couple to the σ^o computation contribute to the probability of error in a science measurement as follows:

$$P(\sigma^o \text{ ERROR}) = \frac{1}{5 \times 10^3} \times \Sigma \text{ Multipliers}$$

where the multipliers* are given below,

Contributing Parameter	Multipliers
Antenna Beam I.D.	3
Antenna Temperature	75
Ant. Temp. Ref. Voltage	60
Directional Detector Temp.	30
ASM Temperature	116
Transmit Power	15
Receiver Gain State	0.2
Science Voltages	2
TOTAL	301.2

*e.g., a single Transmit Power error causes 15 σ^o errors, one in each measurement cell.

and the likelihood of a science measurement error is equal to the probability of a σ^o error. For the scatterometer, P(σ^o Error) = 1/16. However, filtering tests have been included in the SASS σ^o algorithm designed to eliminate unreasonable data. For example, the limit test 96 watts $< P_T <$ 101 watts is performed on each value of transmit power, and if the test is failed then the value from a latest available data (LAD) table is substituted. If all values rejected are truly bad data, and if the LAD value is considered accurate, then P(σ^o Error) reduces to 1 in 2.3×10^3 measurements. This is considered acceptable even though the error rate on the raw data is surprisingly high.

SPS listings were used to identify data discrepancies during engineering assessment, and continuous C-TAB listings were used to resolve each one. Because of the data quality problem just discussed, a discrepancy was considered legitimate only if it lasted more than 1 frame and correlated properly with other parameters. Eighteen of these were identified and all proved to be either multiple single frame errors or caused by data gaps. Therefore all data discrepancies are considered resolved and none were related to the SASS hardware.

SPS Evaluation

The basic SPS report types are as follows:

a. Standard Reports

Type 1 - Statistics

Type 2 - Event marking

Type 3 - Limit checking

b. Special Reports

1. Continuous instrument status verification

2. High voltage and TWT filament timers

The following table identifies each SASS standard report, gives the processing type (i.e., 1, 2, or 3) for each, and describes the content of each.

SPS CONTENTS		
LIST #	REPORT TYPE	DESCRIPTION
1	2	Operating Mode
2	1 and 2	HVPS/TWT
3	1 and 2	Housekeeping
4	1	SEP Temperatures
5,6,7,8	1	Ant. Temperatures
9	1	Sat. Parameters
10	1 and 3	Spares
11	1	S+N Cal
12	1	N ONLY Cal
13	1	CH-15 Noise
-	Special	Status
-	Special	HVPS/TWT Timers

Appendix D is a complete SPS for Day 188 covering a standard 6 hour period, in this case 1759:59 - 2352:33, which includes examples of each report type. SPS processing was evaluated primarily using a continuous listing (C-TAB) from day 187/2323:50-2326:02. The SPS evaluation identified a number of processing problems, all of which have been corrected except for the following,

a. List 10 - Wrong units for grounded spares.

b. List 13 - Ocean zone filtering incorrect.

c. Special Status Report - Was not thoroughly validated.

d. The Max/Min test in all Type 1 Standard Reports is useless due to data quality.

Items a. and b. were not pursued because these lists were not being used. The special status report (item C) was expected to be one of the most useful SASS reports but the poor quality of SeaSat data rendered it useless. Therefore its validation was dropped. Likewise regarding item d. this test was intended for intermittent failure screening and for dynamic temperature information but was useless because of poor data quality.

SPS evaluation is complete and the software as of 4.8C is considered acceptable for the given quality of SeaSat data. However, the poor data quality significantly limits the usefulness of SPS listings.

POCC Validation

The operation at POCC was designed to provide data in the following forms primarily in real time during ground station passes.

a. CRT display

b. CRT page hard copy

c. All parameter hard copy

Appendix E is a complete set of scatterometer pages that could be displayed on the CRT. All SASS parameters could not be included on a single CRT page so provisions were made to provide a hard copy listing that included a complete frame of data. In addition, data gathered during station passes could be played back non-real time at selected speeds. The POCC processing evaluation included status parameter handling and EU conversions in CRT pages and the all data listings.

A number of problems existed at launch and were corrected. The results of this evaluation, as listed in Appendix C, are based on the final software.

All status parameters were checked using CRT pages and are handled correctly. No temperature corrections were planned for transmit power and filament current and they differ in comparison to the JPL products accordingly. The high frequency rather than low frequency L.O. curve was used for L.O. power and a switch was planned, but the satellite failed. The other electrical parameters are straightforward except for the science voltages that were not available for comparison due to an all data listing problem that will be discussed shortly.

All temperatures were converted correctly. The calibration curves for a reference voltage of 5.0 volts were in the POCC system and the voltage was actually 5.1 volts; consequently, errors as a function of temperature itself as great as $10^{\circ}C$ with the antennas at $-70^{\circ}C$ existed. This effect has been taken into account in Appendix C. Figure C.3 shows that the LMSC calibration data is correct and the tabulated values compare well.

A deficiency existed with the all data listing that became a major problem as a result of the 3 month time lag in data availability at JPL. All data "snapshots", which were intended to produce frame-by-frame lists of all SASS data, were required as the prime tool for engineering assessment, even though this was counter to the original intent for the POCC system. It was determined that the data was not buffered at the printer resulting in the mixing of data from many SASS frames in each "snapshot". This problem was being resolved when the satellite failed.

Within a few days after launch the POCC processing was considered acceptable except for the data buffering problem at the printer.

HARDWARE EVALUATION

The scatterometer was turned on and began transmitting at 2147:19 GMT on July 6 and ceased transmitting due to the undervoltage trip on October 10 at 0406:30 GMT. After subtracting the total time off for maneuvers this yields a total operating time of 2,290 hours or 95.5 days. The hardware validation for engineering assessment is based on data available from the antenna deployment events just after launch and the first 30 days of operation. This was restrictive only in determining electronics package and antenna temperature behavior versus sun angle over the planned 1 year mission duration, but the short satellite life makes this indeterminant. The data sets in Table 4 were used along with SPS listings from Days 187-218 to conduct the validation tests outlined in Table 5. Item 1 is a detailed verification that all status and engineering parameters are correct and self consistent on a frame-by-frame basis in all 10 operating modes. In addition, mode switching, fault circuit status, and engineering housekeeping data were reviewed using SPS listings. Items 2-5 are selected receiver performance tests that could be conducted using SDR products only. The exception is the RFI test where results from the P_R algorithm were available and were required for a legitimate RFI conclusion to be drawn. The transmitter can only be evaluated up to the TWT output, using SDR products, and then only in terms of an average power measurement. The pulse shape and radiated power cannot be verified. Tasks 6 and 7 are attempts to define the usefulness of the S+N voltages on the SDR for monitoring the end-to-end performance of the scatterometer.

Antenna Deployments

The SASS antenna assemblies had independent deployment mechanisms and were deployed in pairs. The deployment angle with respect to the spacecraft axis was specified to be $91.6 \pm 0.2^{\circ}$. Deployment tests on the mechanisms alone were successfully run at LMSC during satellite component testing and the antennas were fully deployed during the RFI test at LMSC. Therefore, the accuracy and repeatability of the deployment mechanisms themselves was established and a single, end-to-end calibration was made. But, the end-to-end ability to verify correct deployment through the deployment sensor (a potentiometer) and satellite data system was not planned. The repeatability of the sensor was expected to be on the order of 1° at best, and the data system resolution was $\pm 0.5^{\circ}$. Clearly the deployment monitoring system was not designed to verify in orbit deployment angle and was not tested sufficiently to even define its own capability. With this in mind, the following data were reported at POCC after full deployment of the antenna assemblies in orbit.

Antenna Assembly	Deployment Angle
1	92.0°
2	90.6°
3	90.7°
4	92.5°

It is left for the aircraft underflights to account for antenna gain versus incidence angle at the earth's surface in the end-to-end scatterometer calibration.

Engineering and Status

The data sets in Table 4, each greater than 4 minutes long, were used to verify the following status items in all 10 modes by frame-by-frame inspection using C-TABs.

a. Antenna sequence

b. L.O. selection

c. Temperature subcommutation

d. Calibration cycle

e. Noise diode switching

f. Science voltage gain state identification

A frame-by-frame correlation of particular engineering parameters such as TWT cathode voltage and transmit power with status indicators such as mode number and calibrate status was required.

SPS listings over the first 30 days were the prime data source for the instrument functional validation. Eighty eight percent of the engineering data gathered during this period was delivered by JPL to Langley as SPS listings. Approximately 43% of this data was processed on software after 4.8C. The main deficiency, with respect to the scatterometer, in SPS listings generated before 4.8C, was an incorrect standard deviation computation in all Standard Report 1's. Therefore, a virtually continuous record of the mean value, averaged over 6 hour periods, of each analog parameter plus the standard deviation for approximately half of the records was reviewed. The results of this are listed in the Key Parameter Matrix, Table 6. All electrical parameters were stable throughout the assessment period except for slight temperature effects on a few, none of which affected system level quantities such as transmit power or receiver Noise Figure. Table 6 demonstrates that the instrument met all goals and specifications and duplicated its pre-launch behavior. The in orbit receiver Noise Figure is slightly lower than the other values since the temperature of the instrument was lower than the nominal condition (25°C) for the pre-launch tests. The 5.2 dB does agree with thermal vacuum data at comparable temperatures from satellite system tests. Maximum and minimum temperature averages are given for the electronics package since absolute max and min data from the Standard Reports 1's was not reliable. These minimum values were reached on Day 205 during the Altimeter heating circuit thermostat failure and subsequent heater cycling exercises and returned to -2° minimum on the baseplate for the rest of the mission. The lowest temperature reached by any subsystem was -10.7°C on the ASM during this same period. The antenna temperatures were lower at times than the predicted value of -67°C but never below the -90°C qualification test value. SPS listings were also used to verify that the instrument switched modes properly and that no faults occurred (e.g. body current trip, etc.).

Since the electronics and antenna thermal environments were less predictable prior to launch than the electrical characteristics, thermal data is particularly interesting. Figure 17 shows the temporal behavior of the max and min baseplate temperatures and typical antenna temperature extremes over the first 30 days. The upper pair of curves are taken from the 6 electronics baseplate temperature monitors. On day 187 the SASS was turned on and warmed up from approximately 3°C to 22°C after all other sensors began operating. All temperatures are stable with a spread of about 4°C between the 6 monitor points, most of which is variation with time over the 6 hour SPS period. The excursions around Day 205 are results of the Altimeter thermostat failure and subsequent heater bus cycling exercises. After a heater duty cycle was determined the baseplate temperatures again settled down around a median value of $0^{\circ}C$ and a spread of approximately $7^{\circ}C$. This spread consists of a variation over the baseplate of about $4^{\circ}C$, and the other $3^{\circ}C$ is due to the time variation. As the sun angle changed, the satellite continued to warm up to the point where the median baseplate temperature over any 6 hour period was $>0^{\circ}C$ by the end of engineering assessment and through the rest of the mission.

The lower curves on Figure 17 show time histories of the temperature extremes on antenna assemblies 1 and 4. These two are representative of all four assemblies since 1 and 2 are situated outboard on the satellite and 3 and 4 are inboard. Thus 3 and 4 were somewhat shaded from the sun by the satellite structure and antenna assemblies 1 and 2 during the mission. The characteristics in Figure 17 demonstrate the magnitude of this shadowing effect. A collection of 10 temperature measurements are made on each antenna assembly that vary with location on the back and sides of the assembly and vary with time. The total variation of temperature from max to min is greater for antenna assembly 1, and the median temperature on number 4 was generally cooler, at times by as much as 25-$30^{\circ}C$.

The temperature spread between the max and min value over the entire antenna that occurs in any 6 hour period, as in Figure 17, is broken down in Figure 18. The fluctuation extremes versus time and the distribution over the length of antenna assembly 1 on Day 191 are given for one complete orbit. The same general behavior would repeat orbit by orbit until significant changes in sun angle occur. In this case, the feed end of the antenna (T1, 2, 3) is cooler than the outer end due to spacecraft shadowing and the maximum temperature difference along the entire length is 15°C, which is about 4° greater than the maximum variation in the temperature at any one point over the orbit. One reason that shadowing has this great an effect is because the antenna assemblies are extremely well isolated thermally from the satellite.

Receiver Characteristics

The scatterometer science data at the SDR level, except for the value of transmitted power, was restricted to a set of receiver output voltages that were proportional to input power plus a set of gain scale factors. A single frame of data included 15 measurements with returned signal present (S+N), 15 measurements with no returned signal present (N ONLY), and the 15 gain factors whose values are set by the magnitude of the returned signal. An algorithm in the IGDR software is used to compute P_R for each of the 15 channels. The SDR outputs are clearly "raw data", which are difficult to interpret and manipulate to a meaningful engineering unit, such as P_R, and any receiver performance evaluation based solely on SDR products will be limited.

Figure 19 shows the gain switching technique used to achieve the required 45 dB receiver dynamic range. Return pulses are sampled at the beginning of each measurement integration period with the receiver in Gain Step 1, and if the received power is sufficiently high for the integrator output voltage to exceed the switching threshold of 4.786 volts the receiver switches to Gain Step 2, and the same test is repeated on the next two return pulses. By inspection of Figure 19 all gain curves are separated by approximately 10 dB. After applying this test 3 times, the receiver will be operating in a gain state that will prohibit saturation during the measurement. The gain state is independently set in each of the 15 channels, and they determine the 15 gain factors applied to each frame of science data.

It can be shown that for a fixed receiver input power, the ratio of the standard deviation on the estimate of received power to the true value is approximately equal to the ratio of the standard deviation on the output voltage to the mean value of the voltage and is given by

$$\frac{\sigma_V}{\mu_V} \simeq \frac{1}{\sqrt{BT}}$$

where B and T are the bandwidth and integration time respectively. As the record length or the number of data points averaged increases this relationship approaches an equality. Under constant input conditions for the length of the record, either S+N voltages or N ONLY voltages for fixed gain state, local oscillator frequency, and signal path can be used to evaluate the receiver in terms of

a. Channel bandwidth and bandwidth stability

b. Range gate width and stability

c. Accumulator (i.e. integrator) stability

d. Local oscillator stability

e. Overall gain stability

where stability is judged with respect to time periods greater than 1 measurement frame but less than the record length. Table 7 shows a typical set of data taken at the end of the engineering assessment period with the instrument in Mode 10 (Standby), in order to evaluate the receiver with the transmitter off. The computed values of $1/\sqrt{BT}$ for the S+N range gate width and the N ONLY range gate width in all 15 channels are listed with the values of σ_V/μ_V averaging over 20 measurements. Experience from test data before launch indicated that a reasonable criterion for acceptable performance was that all data points be within 3% of their estimated mean value; therefore, no anomalies are indicated.

Noise Figure is a standard figure of merit for any receiver and is a measure of the noise added by the receiver itself to any measurement. The SASS Noise Figure can be computed from either the S+N or N ONLY voltages during a calibrate cycle using the Y-Factor method where

$$\text{Noise Figure} = 10 \, \text{Log}_{10} \frac{\text{ENR}}{Y - 1}$$

with,

$$Y = \frac{V_{High}}{V_{Low}} \times \frac{G_{Low}}{G_{High}}$$

and

ENR = Excess Noise Ratio

V_{High} = Output voltage with high input signal (noise diode on).

V_{Low} = Output voltage with low input signal (noise diode off).

G_{High} = Gain with high input signal.

G_{Low} = Gain with low input signal.

For our purposes

$$\text{Noise Figure} \simeq 10 \operatorname{Log}_{10} \frac{100}{(\frac{V_{High}}{V_{Low}} \times 100) - 1}$$

This gives a Noise Figure approximation to a precision limited by the stability of the voltage measurements themselves. A more accurate computation of Noise Figure, typically 5.5 dB, is routinely done in the σ^o algorithm. Table 8 list Noise Figure computed in each operating mode from Channel 1 S+N voltages and averaging the high and low frequency L.O. results. The Mode 9 (Continuous Calibrate) computation was done using S+N voltages averaged over a 4 minute record. These values are comparable to those observed during satellite system thermal vacuum tests under similar, cool conditions.

The same data in Mode 9 was convenient for determining the stability of the noise diode and noise injection circuit. Using Channel 1, N ONLY voltages the stability of the High CAL (noise diode on) values on a 32 point record are compared in Table 9 to the computed ideal case.

RFI

An RFI investigation using only SDR Products would be limited to an assessment of short term receiver input noise stability with gain and temperature effects normalized out. This could be done by operating on the N ONLY voltages in the conventional way to compute the normalized standard deviation on the receiver noise when all sensors are operating. Attempting to sense perturbations to the return signal itself due to RFI, is not within the scope of this effort since the computation of σ^o would be required. However, to at least assure that there was no effect on the average receiver noise level as well as its standard deviation, the P_R software, which is beyond SDR processing, was used to convert the N ONLY voltages to receiver antenna temperature, T_A. This is an exception to the engineering assessment guidelines but it is considered a minimum requirement for a worthwhile RFI study.

Three RFI test cases were chosen for time periods when all sensors were operating and include SASS operation using all 8 antennas. These are listed below.

Day	Rev	Start Time	Stop Time	SASS Mode
188	150	1211:00	1331:00	4
195	251	1330:00	1350:00	1
208	430	0215:00	0235:00	3

Table 10 shows the comparison of the normalized standard deviation over 20 N ONLY measurements to the ideal as a function of bandwidth and integration time for Channels 1, 12, and 15. This would indicate the presence of interference whose contribution might vary on a period >1.89 seconds but <20 × 1.89 seconds. No RFI of this type was noted above the normal estimate of inherent receiver noise.

As pointed out in the Engineering Assessment Plan the scatterometer can be used to make a rough measurement of surface brightness temperature to a resolution of approximately 12-30 K in the near nadir cells to Cell #12 respectively according to the following equation,

$$\Delta T = \frac{(F - L)T_o + T_A}{B_N T}$$

where,

F = Total receiver Noise Figure, 7 dB

T_o = Receiver ambient temperature, 290K

T_A = Antenna noise temperature, 150 K

B_N = Receiver noise bandwidth

T = Signal integration time

For purposes here, there is no point in removing atmospheric effects in an effort to isolate surface brightness temperature. It will suffice to work in terms of antenna noise temperature, T_A, which can be computed from each scatterometer noise measurement by the following,

$$T_A = T_E - (L - 1)T_{ASM} - LT_R$$

where

T_E = Effective measured input noise temperature

T_{ASM}=ASM temperature

T_R = Receiver noise temperature (TDA Noise Figure ≃ 5.5 dB)

L = ASM path loss

The quantity T_A is routinely computed for the N ONLY measurement in each channel for each frame of data. Since the signal here is broad band noise, there is no spatial discrimination by filtering and the target is defined by the entire antenna footprint. Therefore, T_A in each receiver channel varies as the bandwidth and integration time only and is a function of the surface radiation properties over a wide range of incidence angles. The values for T_A reported here are averaged over all 15 cells. The objective is to determine the RFI effects of the other sensors on the average noise level into the scatterometer, and the approach taken will be to establish baseline characteristics in terms of T_A with only the SASS on and then draw comparisons with all sensors on.

The scatterometer transmitter was turned on during Rev 141 as the satellite, travelling from north to south, crossed over the northern end of South America. The instrument was operating with antennas 3V and 4V in a Mode 5 sequence until it began transmitting in Mode 4 with antennas 1V, 1H, 2V, and 2H. No other sensors were on. Averaging over 20 data points, all taken over water, first with only the receiver on and then after sending the HVPS ENABLE command produced the following results.

Electronics	Antenna	Mean $T_A \pm 1\sigma$, K
Receiver Only	3V	183.6 ± 3.9
Receiver Only	4V	173.7 ± 3.6
HVPS Enabled	3V	183.4 ± 2.7
HVPS Enabled	4V	174.5 ± 3.8

As expected, turning on the high voltage power supply had no effect on the receiver characteristics since the high voltage and transmitter were not yet on. The difference between T_A for the 3V and 4V antennas is due to the difference in ASM path loss for each (0.1 dB). This is the only data available with the transmitter and all other sensors off but these values of T_A are typical for all antennas where the entire footprint is viewing water.

Approximately 3 minutes after turning the power supply on a Mode 4 command was given and the instrument began transmitting as it approached land. Figure 20 shows the T_A profiles for antennas 1V and 2V with the transitions from water to land. The forward looking antenna, 1V, is the first to level off at approximately 270 K with a land filled footprint, and the aft looking antenna, 2V, follows. After approximately 5 minutes, the forward footprint is again over water and T_A is returning to the neighborhood of 170-180 K. Figure 21 shows the effect of polarization on the measurement of T_A. Since the antenna beam 3 dB points correspond to a nominal range on incidence angle at the surface of 25^o-55^o, and since a noise measurement effectively integrates over incidence angle, the vertically polarized measurement is typically 10-20K higher than the horizontally polarized measurement over water. There is apparently a polarization dependence over land also but the effect is less than that over water.

Baseline performance and RFI test criteria are now established in terms of T_A. Measured values of T_A over water with the transmitter on and off are in the 170 K neighborhood with an estimated 40 K dependence on ASM path loss differences and antenna polarization. The average value on T_A over land is estimated to be less than 280 K.

Figure 22 shows the results from the 3 RFI test cases. The data was sampled once every 60 seconds and the bars represent a band on T_A which includes values for each antenna at a particular sample time. The Rev 251 data was taken entirely over water, and the mean values on T_A are in the 180-185 K range with a spread at each time point due to statistical noise on each estimate of T_A, but dominated by the ASM path loss differences and polarization differences. There is no visible RFI effect. On Rev 430 the instrument was in Mode 3, switching between a forward and aft antenna and alternating polarizations, and moving from land to water during the RFI test period. Consequently, there is a large spread in the 4 values of T_A at any sample time, however the data band is generally within the expected range for land and then water indicating no RFI effects. Likewise on Rev 150, the data spread at each sample time reflects the fact that path loss and polarization effects are included. Further, the transition from water to land with fore and aft looking antenna measurements mixed at each sample time enhances the spread. The band of data is in the expected range for both water and land, which indicates no effects from RFI.

From the data available, it appears that the SASS transmitter and the other SeaSat sensors have no EMI or RFI effects on the SASS receiver. However, these results are limited since interference effects on the return signal itself were not investigated in terms of σ^o. Also, an operating plan that would have provided a more thorough RFI baseline data set could have been used. The instrument was operated in Standby using only antennas 3V and 4V prior to turning the transmitter on and in Mode 4 only prior to turning the other sensors on in an effort to minimize SASS commands and changes of state early in the mission. The instrument could have been operated in Modes 1 and 2 both before and after the transmitter was turned on in order to gather data using all 8 antennas. The risk involved would be minimal since the only difference between any of Modes 1-8 is the ASM and logic switching. If interference effects had been indicated in the available data, having a limited set could have been regrettable.

End-to-End Evaluation Techniques

Any end-to-end instrument performance exercise must be done in terms of σ^o. However, since the use of SDR products only was a guideline for the IDPS and engineering assessment, the use of the S+N voltage with standard processing for instrument evaluation and routine monitoring will be explored. The most likely measurements for doing this type of thing are V_{S+N} in Channel 13, where the 8° angle of incidence measurement of σ° is wind speed independent, and V_{S+N} in Channel 15, where the Nadir measurement of σ° is polarization independent.

The value of σ° is directly proportional to P_R/P_T if all of the other terms in the radar range equation are considered constant. The relationship between P_R and V_{S+N} may be computed from the receiver transfer function, and P_T is independently monitored. The following equation may be written for P_R,

$$P_R = P_{S+N} - P_N$$

where P_{S+N} and P_N are the average powers derived from the V_{S+N} and V_N voltages respectively. It can be shown that,

$$P_R = \left[\frac{1}{T_S} V_{S+N} - \frac{T_G}{T_S T_N} V_N \right] \frac{1}{GL_{ASM}}$$

where,

T_S = Signal Integration Time

T_G = S+N Integration Time

T_N = N ONLY Integration Time

G = Gain Value Computed from Internal Calibration Measurements

L_{ASM} = ASM Path Loss

The ability to utilize V_{S+N} in evaluating the instrument depends upon the resolution with which changes in P_R can be determined or the precision with which a constant P_R can be monitored. The latter can be shown to be equal to $1/\sqrt{BT}$ for a single measurement in each channel (as given in Table 9) for high signal-to-noise ratio (SNR) and the precision may be increased by using more measurements in estimating P_R. The sensitivity of the V_{S+N} parameter to changes in P_R for Channels 13 and 15 is given by

$$\frac{\Delta V_{S+N}}{V_{S+N}} \simeq \frac{\Delta P_R}{P_R} \left[\frac{1}{1 + 1.2/SNR}\right]$$

and is plotted below.

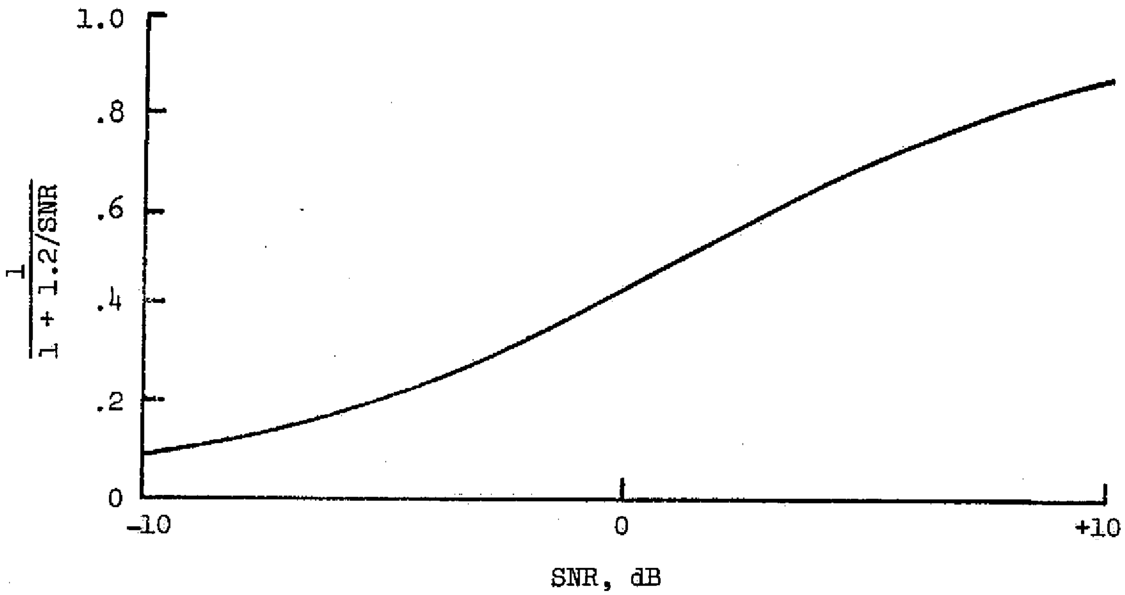

For high SNR changes in P_R transfer directly to V_{S+N}, for unity SNR a given change in P_R will result in a change in V_{S+N} 2.6 dB smaller in magnitude, and as SNR approaches zero V_{S+N} is less sensitive to changes in P_R.

Profiles of σ^o vs time for the 8^o and Nadir channels taken from Rev 142 when the satellite was over the Gulf of Mexico are plotted in Figure 23. The surface winds were low and variable producing a surface that varies from specular to slightly rough. It has been demonstrated experimentally that σ^o for 8^o incidence angle is insensitive to wind speed for winds > 3 m/sec. However, for a smooth surface σ^o is a strong function of incidence angle and for very low wind speeds the 8^o measurement is extremely sensitive to surface conditions as in Figure 23. On the other hand, the signatures in Figures 24 and 25 demonstrate that for moderate wind conditions the 8^o measurement is quite stable. The problem is that the 8^o measurement would be used to indicate instrument stability, but a priori knowledge of the instability due to surface conditions for low wind speeds is required. Therefore the test cannot be implemented for routine monitoring.

Profiles of the Nadir (Cell 15) measurement for both horizontal and vertical polarization on Antenna 4 for smooth and moderate surface conditions are given in Figures 23, 24, and 25. The objective here is to determine the estimated difference between the H-POL and V-POL measurements by subtracting their mean values. The following table was developed from 2 sets of data on Rev 142 (smooth conditions) and Rev 430 (rough conditions). On Rev 142, the estimated mean value is 1.32 dB higher for H-POL than for V-POL, and on Rev 430 the figure is 1.24 dB. There is good agreement between the estimated mean value differences for both data sets, with 20 points averaged on Rev 430 but only 9 points available on Rev 142. One set includes data that is stable to within ±0.5 dB of the estimated mean and the other set is relatively unstable, yet the estimated mean value differences are similar.

Cell 15 HH/VV σ^{o} Comparison

Data Set	Pol	Mean Value, dB	Std. Dev., dB
Rev 142	H	15.848	±1.70
Smooth Surface	V	14.530	±3.09
Rev 430	H	11.429	±0.48
Rough Surface	V	10.194	±0.47

The next table shows the results of the same comparison in terms of signal plus noise voltages. On Rev 142 the estimated mean value for H-POL is 2.60 dB higher than for V-POL, and on Rev 430 the difference is 2.31 dB.

Cell 15 HH/VV V_{S+N} Comparison

Data Set	Pol	Mean Value, Volts	Norm. Std. Dev., %
Rev 142	H	4.8119	47.13
Smooth Surface	V	.8629	51.96
Rev 430	H	3.0601	9.56
Rough Surface	V	.9086	6.53

The magnitude of these differences is not the same as the correct value determined from σ^{o} data due to the biasing influence of the noise power, however the results from the two data sets compare fairly well. In both cases the SNR is sufficiently high (>0 dB) to expect good resolution on each measurement.

This technique should produce good results for a wide variety of surface conditions with the repeatability primarily dependent upon the number of points averaged for the given variance on the data being used. Specific criteria could be developed and expected repeatability established for all 8 antennas from a large number of test cases by following this same procedure, and routine monitoring could be implemented in standard SPS type processing. The desirability of implementing such a test in terms of V_{S+N} is questionable, given the effort required to establish test criteria. Periodically checking the polarization difference in terms of σ^o, if the software is available, seems more efficient and sensible.

SUMMARY

Support to the MPT, ADWG and SPAT activities were supplied both prior to launch and during the course of the mission as required, and both the SASS hardware and SDR software have been validated so that SASS SDRs are acceptable for use in geophysical processing.

It has been determined that SDR processing of all SASS parameters, excluding cell location, is acceptable in the 4.8C software version and is expected to be maintained correct in subsequent versions. The IDPS input data quality is extremely poor; however, with data quality checks that have been implemented in the geophysical processing the probability of an error in σ^{o} is less than 1 in 2.3×10^{3} measurements. This is considered acceptable since the magnitude of the error rate is comparable to that from other error sources.

The 4.8C version SPS software was also determined to be acceptable for the given data quality. However, the frequency of data errors makes the Standard Report 1 Max/Min test for analog parameters useless for flagging intermittent hardware anomalies and the Special Status Report useless for flagging instrument status anomalies.

The POCC processing met all of the initial requirements for the system. However, the lack of availability of data through the JPL system created a requirement for continuous, all data records from the POCC for preliminary engineering assessment. It turned out that SASS all data "snapshots" were not buffered at the printer and therefore were not useful for frame-by-frame evaluations. This deficiency was only minor from an engineering assessment standpoint.

Through 2,290 hours of operation the SASS operated flawlessly meeting all of its electrical design goals and specifications. A satellite heater circuit failure caused the instrument to operate marginally close to its minimum temperature, $0^{\circ}C$, for most of the mission, and the antenna temperatures went below the estimated $-67^{\circ}C$ lower limit but never reached the qualification test limits. These low temperature excursions on the electronics package and the antennas are not believed to have affected instrument performance. All available evaluation methods in terms of SDR products indicate that the transmitted power was correct and stable and that the receiver gain and noise characteristics were identical with pre-launch test experience throughout the entire mission.

An RFI analysis was performed, primarily using P_R software to compute T_A, which went beyond initial engineering assessment guidelines. It was determined that neither the SASS transmitter nor any of the other sensors had any detectable EMI or RFI effect on the SASS receiver.

Two techniques for end-to-end performance evaluation or monitoring in terms of SDR products alone were investigated. It turns out that monitoring the stability of the signal-plus-noise voltage in the 8° cell is particularly useless since σ^{o} at 8° is unstable for low wind speeds ($<$ 1.5 m/sec or so). On the other hand, the difference between the V-POL and H-POL signal-plus-noise measurements in the nadir cell are potentially useful since no a priori knowledge of surface conditions is required. For example, a test for data stability could be made prior to comparing the average values of H-POL and V-POL measurements. There may be other techniques as well. In any case, it is clear that as a general rule the end-to-end evaluation and performance monitoring of the SASS should be done at the σ^{o} level and not using SDR products.

ACKNOWLEDGEMENTS

This is a note of appreciation for the support given by many others to the scatterometer operation during integration and system testing at LMSC, in the development of software and operations planning at JPL and GSFC, and in operations and data processing during and after the mission. A large number of people from JPL, LMSC and GSFC as well as the scatterometer contractors, General Electric (GE), Aerojet, and Hughes contributed to the effort. Particular thanks are due Art Heath and Attie Salamon of GE for their assistance throughout, especially during satellite system tests. Special thanks also to John Schlue and Carl Kloss of JPL and Vince Moughan of LMSC.

APPENDIX A

SASS DATA CATALOG

SASS Data Catalog

Parameter I.D.	Word No.	Bit No.	Parameter Description
SS 700	9	3	Mode 1
701	9	4	Mode 2
702	9	5	Mode 3
703	9	6	Mode 4
704	9	7	Mode 5
705	9	8	Mode 6
706	9	9	Mode 7
707	9	10	Mode 8
708	10	1	Mode 9
709	10	2	Mode 10
710	8	4	Cal. Status
711	8	6	Polarization
712	8	7	L/R Antenna
713	8	8	F/A Antenna
714	4	10	LO Frequency Select
715	10	4	HI Frequency Select
716	5	1,2	Gain Channel No. 1
717	5	3,4	Gain Channel No. 2
718	5	5,6	Gain Channel No. 3
719	5	7,8	Gain Channel No. 4
720	5	9,10	Gain Channel No. 5
721	6	1,2	Gain Channel No. 6
722	6	3,4	Gain Channel No. 7
723	6	5,6	Gain Channel No. 8
724	6	7,8	Gain Channel No. 9
725	6	9,10	Gain Channel No. 10
726	7	1,2	Gain Channel No. 11
727	7	3,4	Gain Channel No. 12
728	7	5,6	Gain Channel No. 13
729	7	7,8	Gain Channel No. 14
730	7	9,10	Gain Channel No. 15
731	13	1-10	Signal & Noise Channel No. 1
732	14	1-10	Signal & Noise Channel No. 2
733	15	1-10	Signal & Noise Channel No. 3
734	16	1-10	Signal & Noise Channel No. 4
735	17	1-10	Signal & Noise Channel No. 5
736	18	1-10	Signal & Noise Channel No. 6
737	19	1-10	Signal & Noise Channel No. 7
738	20	1-10	Signal & Noise Channel No. 8
739	21	1-10	Signal & Noise Channel No. 9
740	22	1-10	Signal & Noise Channel No. 10
SS 741	23	1-10	Signal & Noise Channel No. 11

Parameter I.D.	Word No.	Bit No.	Parameter Description
SS 742	24	1-10	Signal & Noise Channel No. 12
743	25	1-10	Signal & Noise Channel No. 13
744	26	1-10	Signal & Noise Channel No. 14
745	27	1-10	Signal & Noise Channel No. 15
746	28	1-10	Noise Only Channel No. 1
747	29	1-10	Noise Only Channel No. 2
748	30	1-10	Noise Only Channel No. 3
749	31	1-10	Noise Only Channel No. 4
750	32	1-10	Noise Only Channel No. 5
751	33	1-10	Noise Only Channel No. 6
752	34	1-10	Noise Only Channel No. 7
753	35	1-10	Noise Only Channel No. 8
754	36	1-10	Noise Only Channel No. 9
755	37	1-10	Noise Only Channel No. 10
756	38	1-10	Noise Only Channel No. 11
757	39	1-10	Noise Only Channel No. 12
758	40	1-10	Noise Only Channel No. 13
759	41	1-10	Noise Only Channel No. 14
760	42	1-10	Noise Only Channel No. 15
761	61	1-10	Transmit Power
762	8	5	Input Current Trip
763	8	10	Undervoltage Trip
764	9	1	Body Current Trip
765	56	1-10	TWT Cathode Voltage
766	57	1-10	TWT Cathode Current
767	58	1-10	TWT Body Current
768	59	1-10	Ion Pump Current
769	60	1-10	HVPS Input Current
770	10	5	LO Looplock Status
771	10	6	Transmit Looplock Status
772	54	1-10	LO Power
773	55	1-10	Modulator Power
774	64	1-10	Transmit Channel Power
775	75	1-10	Upconverter Bias
776	76	1-10	TDA Stage 1 Bias
777	77	1-10	TDA Stage 2 Bias
778	78	1-10	TDA Stage 3 Bias
779	8	9	Rec. Protet Circuit Status
780	9	2	Noise Diode Status
781	51	1-10	DC/DC Conv. Volt. +5V
782	52	1-10	DC/DC Conv. Volt +15V
783	53	1-10	DC/DC Conv. Volt -15V
784	65	1-10	Low Gain GND
SS 785	67	1-10	DC/DC Conv. Volt -6V

Parameter I.D.	Word No.	Bit No.	Parameter Description	Subcom. I.D.		
SS 786	68	1-10	DC/DC Conv. Volt +6V			
787	69	1-10	Thermistor Ref. No. 1			
788	70	1-10	Thermistor Ref. No. 2			
789	44	1-10	Baseplate RT 3 (SSS/LO)	0	0	0
790	43	1-10	Baseplate RT 5 (TWT GUN)	0	1	0
791	44	1-10	Baseplate RT 14 (TWT COLL)	0	1	0
792	45	1-10	Baseplate RT 7 (TDA)	0	1	1
793	43	1-10	Baseplate RT 17 (HVPS)	1	0	0
794	44	1-10	Baseplate RT 18 (IEA)	1	1	0
795	43	1-10	TWT RT 6	0	0	1
796	44	1-10	TWT RT 10	0	0	1
797	45	1-10	TWT RT 16	0	0	1
798	45	1-10	Output ISO RT 13	0	1	0
799	44	1-10	HVPS RT 9	1	0	0
800	43	1-10	ASM RT 12	0	1	1
801	43	1-10	SSS/LO RT 1	0	0	0
803	45	1-10	Up Conv. RT 2	0	0	0
804	43	1-10	A/D Conv.	1	1	0
805	45	1-10	Noise Source RT 15	1	1	0
806	43	1-10	Dir. Dector RT 11	1	1	1
807	44	1-10	1st Mixer RT 4	1	1	1
808	45	1-10	2nd Mixer	1	1	1
809	44	1-10	TDA RT 8	0	1	1
810	45	1-10	Crystal Filter P6	1	0	0
811	43	1-10	Crystal Filter P1-	1	0	1
812	44	1-10	Crystal Filter P10	1	0	1
813	45	1-10	Crystal Filter P12	1	0	1
814	46	1-10	Ant. No. 1 Temp. No. 1	0	0	0
815	47	1-10	Ant. No. 1 Temp. No. 2	0	0	0
816	48	1-10	Ant. No. 1 Temp. No.3	0	0	0
817	49	1-10	Ant. No. 1 Temp. No. 4	0	0	0
818	50	1-10	Ant. No. 1 Temp. No. 5	0	0	0
819	46	1-10	Ant. No. 1 Temp. No. 6	0	0	1
820	47	1-10	Ant. No. 1 Temp No. 7	0	0	1
821	48	1-10	Ant. No. 1 Temp No. 8	0	0	1
822	49	1-10	Ant. No. 1 Temp No. 9	0	0	1
823	50	1-10	Ant. No. 1 Temp No. 10	0	0	1
824	46	1-10	Ant. No. 2 Temp. No. 1	1	0	0
825	47	1-10	Ant. No. 2 Temp. No. 2	1	0	0
826	48	1-10	Ant. No. 2 Temp. No. 3	1	0	0
827	49	1-10	Ant. No. 2 Temp. No. 4	1	0	0
828	50	1-10	Ant. No. 2 Temp. No. 5	1	0	0
829	46	1-10	Ant. No. 2 Temp. No. 6	1	0	1
SS 830	47	1-10	Ant. No. 2 Temp. No. 7	1	0	1

Parameter I.D.	Word No.	Bit No.	Parameter Description	Subcom I.D.		
SS 831	48	1-10	Ant. No. 2 Temp. No. 8	1	0	1
832	49	1-10	Ant. No. 2 Temp. No. 9	1	0	1
833	50	1-10	Ant. No. 2 Temp. No. 10	1	0	1
834	46	1-10	Ant. No. 3 Temp No. 1	0	1	0
835	47	1-10	Ant. No. 3 Temp. No. 2	0	1	0
836	48	1-10	Ant. No. 3 Temp. No. 3	0	1	0
837	49	1-10	Ant. No. 3 Temp. No. 4	0	1	0
838	50	1-10	Ant. No. 3 Temp. No. 5	0	1	0
839	46	1-10	Ant. No. 3 Temp. No. 6	0	1	1
840	47	1-10	Ant. No. 3 Temp. No. 7	0	1	1
841	48	1-10	Ant. No. 3 Temp. No. 8	0	1	1
842	49	1-10	Ant. No. 3 Temp. No. 9	0	1	1
843	50	1-10	Ant. No. 3 Temp. No. 10	0	1	1
844	46	1-10	Ant. No. 4 Temp. No.1	1	1	0
845	47	1-10	Ant. No. 4 Temp. No. 2	1	1	0
846	48	1-10	Ant. No. 4 Temp. No. 3	1	1	0
847	49	1-10	Ant. No. 4 Temp. No. 4	1	1	0
848	50	1-10	Ant. No. 4 Temp. No. 5	1	1	0
849	46	1-10	Ant. No. 4 Temp. No. 6	1	1	1
850	47	1-10	Ant. No. 4 Temp. No. 7	1	1	1
851	48	1-10	Ant. No. 4 Temp. No. 8	1	1	1
852	49	1-10	Ant. No. 4 Temp. No. 9	1	1	1
853	50	1-10	Ant. No. 4 Temp. No. 10	1	1	1
854	8	1-3	Sub Com Counter			
855	4	1-9	Spares (0)			
856	10	3	Spares (0)			
857	10	7-10	Spares (1)			
858	11	1-4	Spares (1)			
859	11	5-10	Spares (0)			
860	12	1,2	Spares (0)			
861	12	3-10	Spares (1)			
862	62	1-10	Low Gain GND Red.			
863	63	1-10	Low Gain GND Red.			
864	66	1-10	Low Gain GND Red.			
865	71	1-10	Transmit Power Red.			
866	72	1-10	Transmit Power Red			
867	73	1-10	Transmit Power Red			
868	74	1-10	Transmit Power Red.			
869	79	1-10	High Gain GND			
870	80	1-10	High Gain GND Red.			
871	81	1-10	High Gain GND Red.			
872	82	1-10	High Gain GND Red.			
873	1	1-10	Sync			
874	2	1-10	Sync			
875	3	1-10	Sync			
SS 876	4	1-10	Sync			

APPENDIX B

ENGINEERING ASSESSMENT OPERATING MODE LIST

Engineering Assessment Operating Mode List

Date	Day/Time, GMT	Rev #	Mode
7/6/78	187/1819:50	139	SASS ENABLE
	2147:24	141	MODE 4
7/12/78	193/1501:05	223	MODE 1
7/15/78	196/0301:44 0321:44	259	MODE 3 MODE 1
	0440:21 0500:21	260	MODE 4 MODE 1
	2006:01 2026:01	269	MODE 4 MODE 1
	2147:39 2207:38	270	MODE 3 MODE 1
7/16/78	197/0231:32 0251:32	273	MODE 3 MODE 1
	0410:08 0430:09	274	MODE 4 MODE 1
	1934:43 1954:43	283	MODE 4* MODE 1*
	2117:27 2137:27	284	MODE 3 MODE 1
7/17/78	198/0339:56 0359:55	288	MODE 3 MODE 1
	0518:33 0538:34	289	MODE 4 MODE 1
	198/2047:13 2107:17	298	MODE 4 MODE 1
	2224:51 2244:50	299	MODE 3 MODE 1

Date	Day/Time, GMT	Rev #	Mode
7/18/78	199/0309:44 0329:40	302	MODE 3 MODE 1*
	0447:18 0507:18	303	MODE 4* MODE 1*
	1507:37	309	MODE 6
	2013:00 2033:01	312	MODE 4 MODE 6
	2154:39 2214:39	313	MODE 3 MODE 6
7/19/78	200/0417:05 0437:05	317	MODE 3* MODE 6*
	2124:23 2144:23	327	MODE 3* MODE 6*
7/20/78	201/0346:56 0406:56	331	MODE 3 MODE 6
	0525:31 0545:35	332	MODE 4* MODE 6
	2054:12 2114:13	341	MODE 4 MODE 6
	2232:51 2252:52	342	MODE 3 MODE 6
7/21/78	202/0316:44 0336:44	345	MODE 3 MODE 6
	0454:22 0514:23	346	MODE 4 MODE 6
	2024:02 2044:01	355	MODE 4 MODE 6
	2201:39 2221:39	356	MODE 3 MODE 6

Date	Day/Time, GMT	Rev #	Mode
7/22/78	203/0424:10 0444:10	360	MODE 3 MODE 6
	2131:24 2151:24	370	MODE 3* MODE 6*
7/23/78	204/0353:54 0413:54	374	MODE 3* MODE 6*
	0532:32 0552:32	375	MODE 4 MODE 6
	2101:14 2121:15	384	MODE 4 MODE 6
	2239:53 2259:52	385	MODE 3 MODE 6
7/24/78	205/0323:51 0343:50	388	MODE 3 MODE 6
	0501:28 0521:28	389	MODE 4 MODE 6
	1521:57	395	MODE 2
	2031:04 2051:04	398	MODE 4* MODE 2*
	2209:45 2229:45	399	MODE 3 MODE 2
7/25/78	206/0431:17 0451:16	403	MODE 3 MODE 2
	2138:30 2158:30	413	MODE 3* MODE 2*
	2243:43	413	MODE 3
7/26/78	207/0539:42 0559:42	418	MODE 4 MODE 3
	2108:21 2128:22	427	MODE 4 MODE 3
7/27/78	208/0350:53	431	MODE 5

Date	Day/Time, GMT	Rev #	Mode
	0508:31 0528:30	432	MODE 4 MODE 5
	2038:06 2058:06	441	MODE 4* MODE 5*
	2216:44 2236:47	442	MODE 3* MODE 5*
7/28/78	209/0438:17 0458:17	446	MODE 3 MODE 5
	1002:41	449	MODE 7
	2146:34 2206:34	456	MODE 3 MODE 7
7/29/78	210/0408:05 0428:05	460	MODE 3 MODE 7
	0546:41 0606:44	461	MODE 4 MODE 7
	1606:43	467	MODE 8*
	2115:23 2135:22	470	MODE 4 MODE 8
	2233:01 2253:00	471	MODE 3 MODE 8
7/30/78	211/0337:50 0357:50	474	MODE 3* MODE 8*
	0515:28 0535:28	475	MODE 4* MODE 8*
	2044:07 2104:11	484	MODE 4* MODE 8
	2223:45 2243:45	485	MODE 3 MODE 8

Date	Day/Time, GMT	Rev #	Mode
7/31/78	212/0140:32	487	MODE 3
	0145:32		MODE 6
	0159:03		MODE 3
	0204:02		MODE 1
	0224:21		MODE 5
	0246:21		MODE 1
	0318:40	488	MODE 6
	0332:43		MODE 1
	0404:59		MODE 5
	0426:59		MODE 1
	0457:19	489	MODE 3
	0505:19		MODE 6
	0514:48		MODE 3
	0523:19		MODE 1
	0545:37		MODE 5
	0607:36		MODE 1
	0635:26	490	MODE 4
	0641:55		MODE 6
	0652:25		MODE 3
	0655:54		MODE 1
	0726:13		MODE 5
	0748:12		MODE 1
	etc. ⋮		
8/6/78	218/0119:44	572	Continuous Cal
	0129:45	572	Standby
	0139:05	572	MODE 2
	0332:42	573	Engineering Assessment Operation Complete

*Denotes Mode Changes Not Verified Due to Data Gaps. The Times Listed Are From CRP.

APPENDIX C

SDR AND POCC EU CONVERSION VALIDATION

EU Conversion Validation

Data Source - Day 187 Rev 142 t = 2325:00

Electrical

Parameter	Counts	LaRC Data	LMSC Data	JPL	POCC
Trans. Power, W	338	100.3	99.9	99.9	100.7
Cathode V, kV	260	-8.023	-8.023	-8.022	-8.023
Cathode I, mA	165	56.4	56.42	56.42	56.42
Body I, mA	70	5.83	5.80	5.80	5.80
Ion Pump I, µA	1	-.06	-.06	-.06	-.06
HVPS Input I, A	274	2.28	2.28	2.28	2.28
Filament I, A	377	1.505	1.506	1.504	1.50
L.O. Power, dBm	358/427	11.59/13.50	11.57/13.47	11.57/13.47	11.91/12.19
Mod. Power, dBm	403	21.3	21.2	21.2	21.2
Trans. Drive Power, dBm	388	17.19	17.18	17.18	17.2
Upcnv. Bias, V	216	.1013	.1014	.1013	.1013
TDA 1 Bias, V	305	.1431	.1431	.1431	.143
TDA 2 Bias, V	339	.1591	.1590	.1589	.159
TDA 3 Bias, V	358	.1680	.1680	.1680	.168
+5V, V	521	5.093	5.078	5.078	5.078
+15V, V	512	15.02	14.97	14.97	14.91
-15V, V	291	-15.05	-15.05	-15.05	-15.05
-6V, V	253	-6.031	-6.032	-6.032	-6.032
+6V, V	510	5.982	5.965	5.965	5.965
Therm. Ref. 1, V	521	5.093	5.098	5.097	5.097
Therm. Ref. 2, V	522	5.103	5.107	5.107	5.107
Satellite Parameters					
Baseplate T1, °F	176	NA	45.83	45.83	
(Rev 223)	158	↓	62.21		62.21
Baseplate T2, °F	169		52.56	52.56	
(Rev 223)	149		69.70		69.70
Unreg. 28V, V	177		30.01	30.01	30.01
Reg. 28V, V	151		28.25	28.25	28.11
(Rev 223)	149		28.11		
Total SASS I, A	89		7.12	7.12	
(Rev 223)	33		2.64		2.64

Science Voltages   t = 2325:00

Parameter	Counts	LaRC Data	JPL	POCC
S+N 1, V	58	.5670	.5664	.5670
2	84	.8211	.8203	NA
3	169	1.652	1.651	
4	221	2.160	2.160	
5	206	2.014	2.014	
6	145	1.417	1.417	
7	85	.8309	.8301	
8	50	.4888	.4883	
9	293	2.864	.2863	
10	188	1.838	1.837	
11	147	1.437	1.437	
12	107	1.046	1.046	1.046
13	382	3.734	3.733	NA
14	389	3.802	3.802	NA
15	450	4.399	4.398	4.399
N Only 1	55	.5376	.5371	.5376
2	45	.4399	.4395	NA
3	40	.3910	.3906	
4	37	.3617	.3613	
5	31	.3030	.3027	
6	24	.2346	.2344	
7	18	.1760	.1758	
8	16	.1564	.1563	
9	121	1.183	1.183	
10	92	.8993	.8984	
11	83	.8113	.8105	
12	69	.6744	.6738	.6745
13	498	4.868	4.867	NA
14	486	4.751	4.750	NA
15	509	4.975	4.975	4.976

NA ≜ Not Available.

SEP Temperatures   t = 2325:00 - 2325:04

Parameter	Counts	LMSC Data	JPL	POCC
BP RT3, °C	677	9.953	9.953	9.855
BP RT5	653	9.372	9.371	9.380
BP RT14	688	8.856	8.855	8.858
BP RT7	655	12.11	12.11	12.11
BP RT17	662	8.443	8.441	8.452
BP RT18	679	9.755	9.754	9.756
TWT RT6	649	9.784	9.781	9.791
TWT RT10	655	10.57	10.77	10.77
TWT RT16	633	12.95	12.95	12.95
Out ISO	680	9.656	9.652	9.656
HVPS	667	10.94	10.94	10.94
ASM	704	3.990	3.988	3.999
SSS/LO	653	9.372	9.371	9.380
Upcnv.	689	8.755	8.754	8.756
A/D Cnv.	501	24.48	24.48	24.49
Noise Source	725	5.054	5.055	5.055
Dir. Det.	673	7.296	7.293	7.305
1st Mixer	663	11.33	11.33	11.33
2nd Mixer	541	21.77	21.77	21.77
TDA	416	35.60	35.59	35.60
XTAL. Fil. P6	502	25.50	25.50	25.50
XTAL Fil. P1	449	29.74	29.74	29.74
XTAL Fil. P10	451	30.55	30.55	30.54
XTAL Fil. P12	470	28.64	28.64	28.64

Antenna Temperatures   t ≃ 2325:00

Parameter	Counts	LaRC Algorithm	JPL	POCC
Ant 1 T1	877	-33.85	-34.06	-34
2	880	-34.24	-34.47	-34
3	880	-34.24	-34.47	-34
4	848	-30.24	-30.42	-30
5	848	-30.24	-30.42	-30
6	851	-30.59	-30.59	-30
7	851	-30.59	-30.59	-30
8	838	-29.08	-29.08	-29
9	837	-28.97	-28.97	-29
10	841	-29.43	-29.42	-29
Ant 2 T1	930	-41.86	-41.86	-42
2	929	-41.69	-41.67	-42
3	928	-41.51	-41.50	-41
4	873	-33.29	-33.28	-32
5	874	-33.42	-33.41	-33
6	872	-33.38	-33.37	-32
7	871	-33.25	-33.23	-32
8	857	-31.48	-31.47	-30
9	860	-31.85	-31.84	-31
10	860	-31.85	-31.84	-31
Ant 3 T1	993	-57.60	-56.87	-58
2	993	-57.60	-56.87	-58
3	996	-58.79	-58.02	-59
4	987	-55.44	-54.80	-55
5	987	-55.44	-54.80	-55
6	990	-55.82	-56.48	-57
7	990	-55.82	-56.48	-56
8	988	-55.14	-55.78	-56
9	992	-56.53	-57.22	-58
10	992	-56.53	-57.22	-57
Ant 4 T1	1003	-62.93	-61.05	-62
2	1002	-62.42	-60.59	-62
3	1001	-61.93	-60.14	-62
4	994	-58.81	-57.31	-57
5	995	-59.22	-57.69	-58
6	992	-56.58	-57.28	-57
7	992	-56.58	-57.28	-57
8	994	-57.32	-57.05	-58
9	992	-56.58	-57.28	-57
10	992	-56.58	-57.28	-57

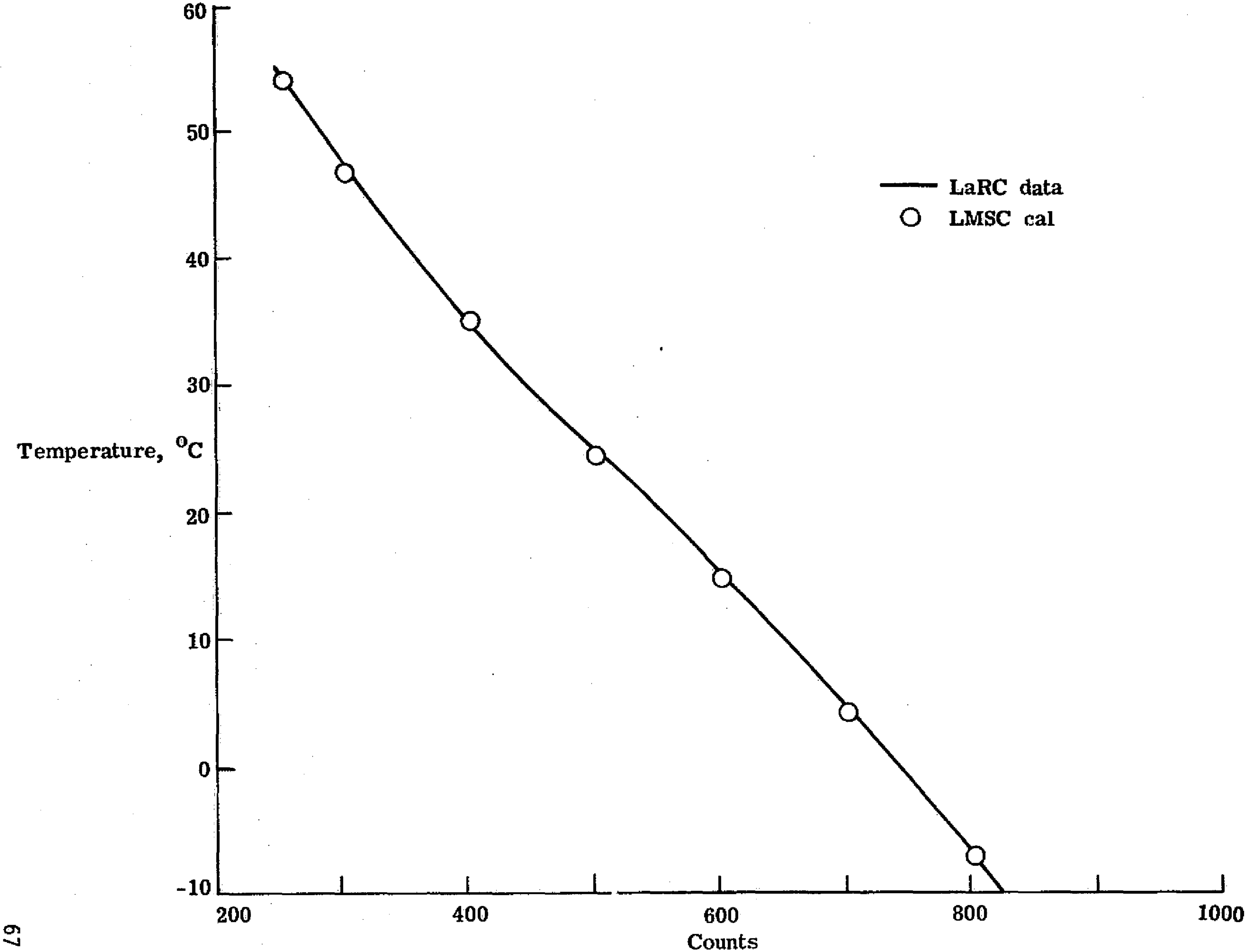

Figure C.1.- Electronics package temperature calibration comparison for word 43.

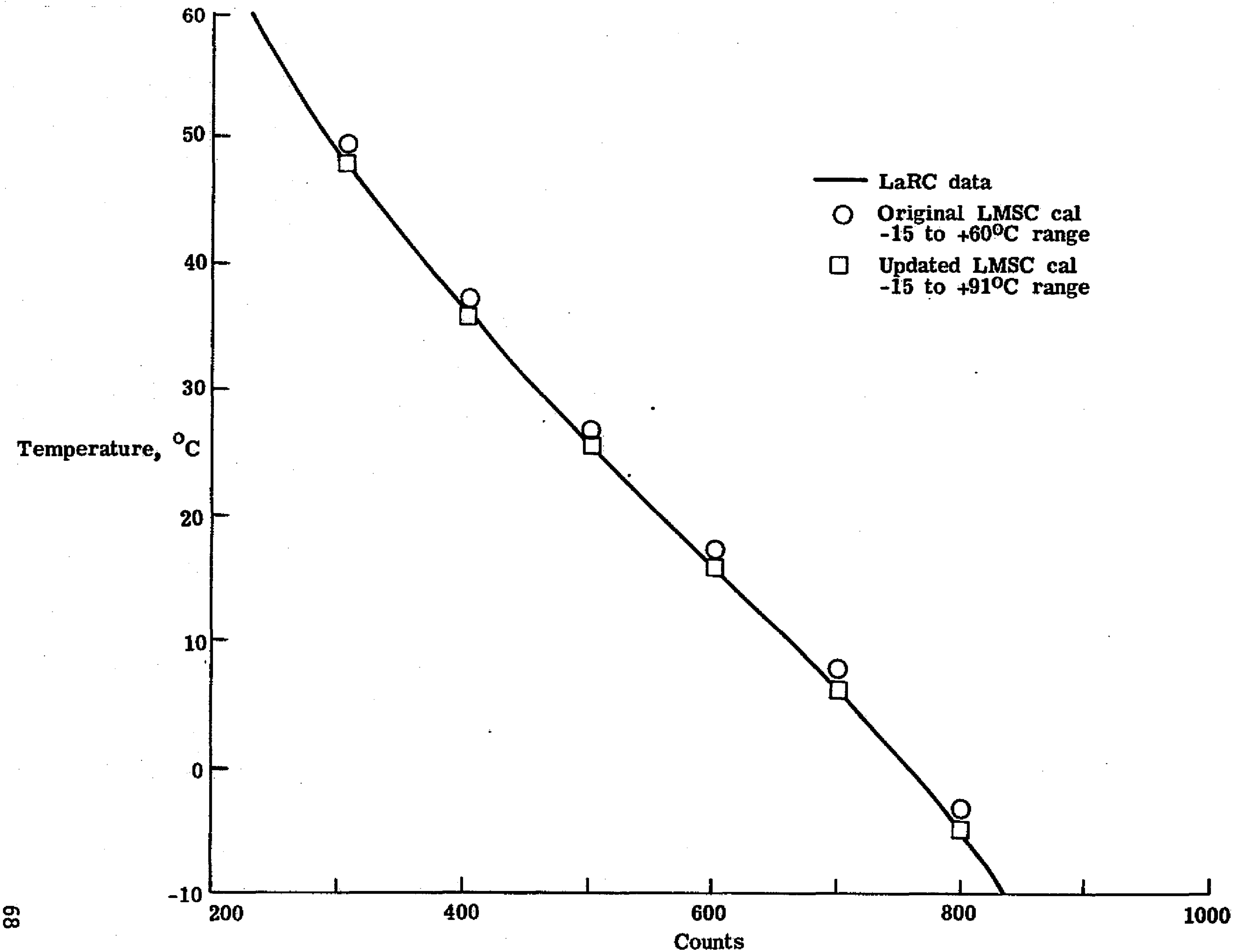

Figure C.2.- Electronics package temperature calibration comparison for words 44 and 45.

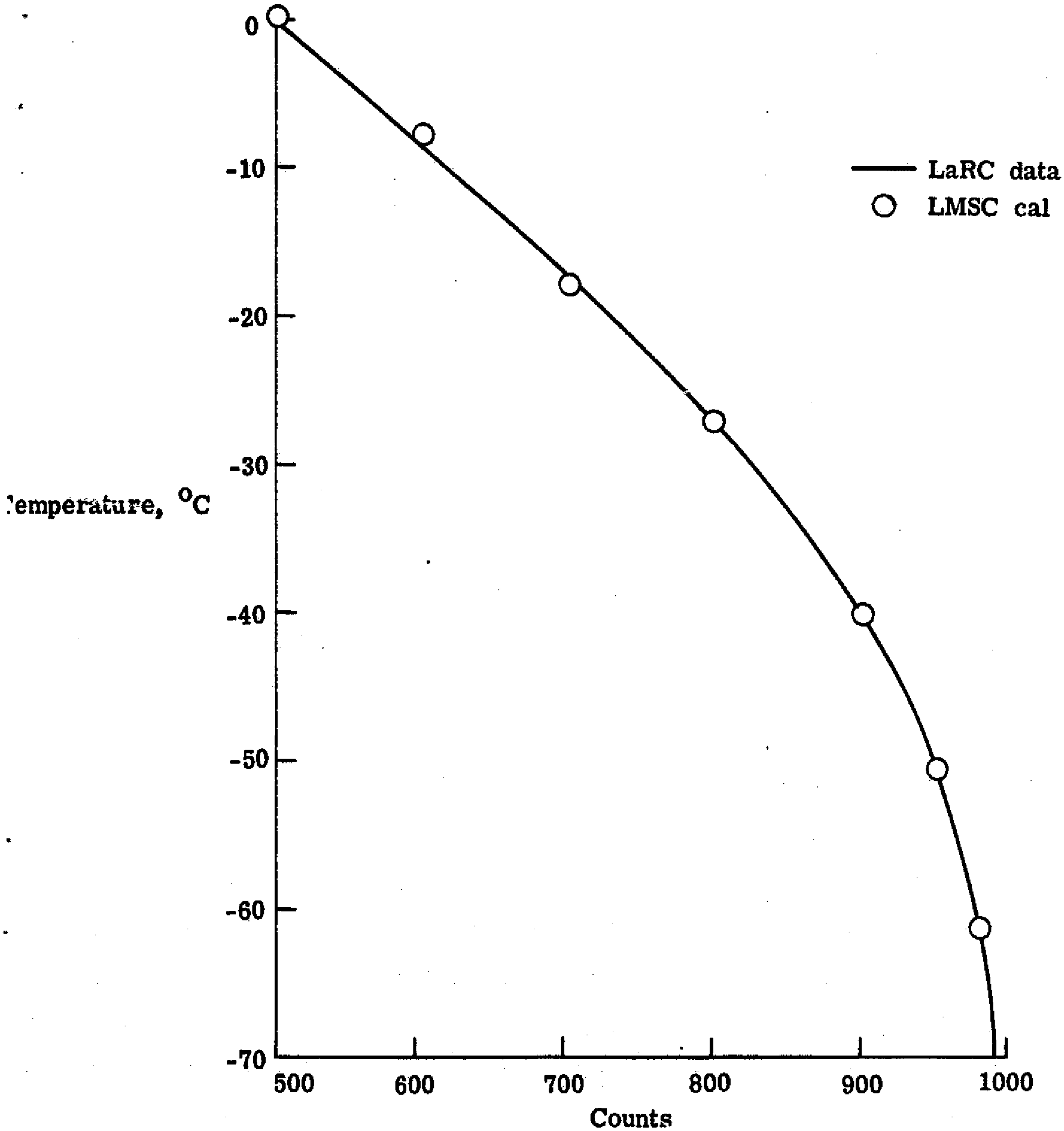

Figure C.3.- Antenna temperature calibration comparison at 5.0 volts reference.

APPENDIX D

SPS FOR 188/1759:59 - 2352:33 GMT

188 78 4.8D


```
 SSSSSSSSSS    AAAAAAAAAA    SSSSSSSSSS    SSSSSSSSSS
SSSSSSSSSSSS  AAAAAAAAAAAA  SSSSSSSSSSSS  SSSSSSSSSSSS
SS        SS  AA        AA  SS        SS  SS        SS
SS            AA        AA  SS            SS
SSS           AA        AA  SSS           SSS
 SSSSSSSSS    AAAAAAAAAAAA   SSSSSSSSS     SSSSSSSSS
  SSSSSSSSS   AAAAAAAAAAAA    SSSSSSSSS     SSSSSSSSS
         SSS  AA        AA           SSS           SSS
          SS  AA        AA            SS            SS
SS        SS  AA        AA  SS        SS  SS        SS
SSSSSSSSSSSS  AA        AA  SSSSSSSSSSSS  SSSSSSSSSSSS
 SSSSSSSSSS   AA        AA   SSSSSSSSSS    SSSSSSSSSS
```

RMPF TAPE NOS. 781987 731888
STANDARD REPORT 1   LIST 2 1978 188

SYSTEM ID 4.00   SASS   PAGE 1
JOB: JDL8188D   78-329/ 02:10:01

TIME-1ST	TIME-LST	CHAN	MEAN VALUE	STD DEVN	MAX VALUE	MIN VALUE	TIME-MAX	TIME-MIN	NMAX	NMIN	LAT	LONG	POINTS	UNITS	REV#
17:59:59	23:52:33	SS761A	9.8278 1	4.9494-1	9.9844 1	9.4578 1	22:20:37	19:58:42	1	1			10820	WATTS	157
17:59:59	23:52:33	SS765A	-8.0224 0	7.9101-4	-8.0205 0	-8.0254 0	18:23:20	18:26:05	29	14			11165	KV	157
17:59:59	23:52:33	SS766A	5.5855 1	5.0164 0	5.7133 1	1.2773 0	23:38:52	18:01:55	1	87			10820	MA	157
17:59:59	23:52:33	SS767A	5.7187 0	4.6089-1	5.8838 0	4.9609-1	18:00:03	19:05:57	1026	2			10820	VA	157
17:59:59	23:52:33	SS768A	-5.6817-2	2.4302-2	[illegible]	[illegible]	17:59:59	[illegible]	2522	1795			11165	MICROAMP	157
17:59:59	23:52:33	SS769A	2.2358 0	1.2254-1	2.4412 0	1.0420 0	20:57:09	18:46:16	7	3			10820	AMPS	157
18:01:47	23:49:42	SS769C	1.2134 0	5.5548-1	2.2500 0	3.7085-1	21:33:16	19:26:05	1	9			345	AMPS	157
17:59:59	23:52:33	SS862A	1.5189 0	3.0576-3	1.5310 0	1.5107 0	23:40:38	19:56:04	1	175			11165	AMPS	157

PMDF TAPE NOS. 781887 781988 SYSTEM ID 4.80 SASS PAGE 2
STANDARD REPORT 1 1 IST 3 1979 138 JCE: JDL8188D 78-329/ 02:10:01

TIME-1ST	TIME-LST	CHAN	MEAN VALUE	STD DEVN	MAX VALUE	MIN VALUE	TIME-MAX	TIME-MIN	NMAX	NMIN	LAT	LONG	POINTS	UNITS	REV#
18:00:01	23:52:32	SS772A	1.3353 1	2.7794-2	1.3419 1	1.3308 1	18:00:03	18:[illegible]:16	125	641			5583	DBM	157
17:59:59	23:52:29	SS772B	1.1471 1	2.0305-2	1.1520 1	1.1437 1	18:01:26	18:01:13	21	1024			5582	DBM	157
17:59:59	23:52:33	SS773A	2.1185 1	1.3689-2	2.1219 1	2.1145 1	18:19:35	22:15:57	44	3			11165	DBM	157
17:59:59	23:52:33	SS774A	1.7031 1	1.2579-2	1.7065 1	1.7019 1	18:04:47	17:59:59	14	1875			11165	DBM	157
17:59:59	23:52:33	SS775A	1.6203-1	3.3163-4	1.6498-1	1.5563-1	18:01:09	18:07:35	274	509			11165	VOLTS DC	157
17:59:59	23:52:33	SS776A	1.3849-1	3.1291-4	1.4253-1	1.3550-1	18:02:55	20:18:56	7	2			11165	VOLTS DC	157
17:59:59	23:52:33	SS777A	1.5932-1	9.2976-4	1.6138-1	1.5698-1	18:01:32	18:02:59	587	322			11165	VOLTS DC	157
17:59:59	23:52:33	SS778A	1.6766-1	8.7577-4	1.7251-1	1.6455-1	18:[illegible]:51	18:12:47	10	26			11165	VOLTS DC	157
17:59:59	23:52:33	SS781A	5.0353 0	7.9363-3	5.1072 0	5.0583 0	[illegible]	18:00:39	3	80			11165	VOLTS DC	157
17:59:59	23:52:33	SS782A	1.4972 1	.0000 0	1.4970 1	1.4970 1	[illegible]	17:59:59	11165	1			11165	VOLTS DC	157
17:59:59	23:52:33	SS783A	-1.5031 1	1.4670-2	-1.4975 1	-1.5048 1	[illegible]	17:59:59	[illegible]	4482			11165	VOLTS DC	157
17:59:59	23:52:33	SS785A	-6.0410 0	9.8738-3	-6.0156 0	-6.0645 0	[illegible]	18:00:37	53	537			11165	VOLTS DC	157
17:59:59	23:52:33	SS786A	5.9627 0	9.9255-3	5.9883 0	5.9297 0	18:0[illegible]:54	18:12:02	897	13			11165	VOLTS DC	157
17:59:59	23:52:33	SS787A	5.1032 0	5.6508-3	5.1169 0	5.0779 0	18:05:25	18:03:50	193	58			11165	VOLTS DC	157
17:59:59	23:52:33	SS788A	5.1028 0	6.5655-3	5.1169 0	5.0779 0	18:03:37	18:04:20	53	110			11165	VOLTS DC	157

PMDF TAPE NOS. 781687 781888
STANDARD REPORT I   LIST 4 1978 188

SYSTEM ID 4.8D   SASS   PAGE 3
JOE: JDL8188D   78-329/ 02:10:01

TIME-FST	TIME-LST	CHAN	MEAN VALUE	STD DEVN	MAX VALUE	MIN VALUE	TIME-MAX	TIME-MIN	NMAX	NMIN	LAT	LONG	POINTS	UNITS	REV#
18:00:09	23:52:31	SS789A	1.8350 1	2.8755-1	1.8797 1	1.7473 1	20:20:32	18:00:54	48	4	.68	347.58	1398	DEG. C	157
18:00:13	23:52:35	SS790A	1.8499 1	2.8194-1	1.9062 1	1.7586 1	23:42:45	18:01:43	2	6	.47	347.50	1393	DEG. C	157
18:00:13	23:52:35	SS791A	1.8361 1	2.9482-1	1.8891 1	1.7473 1	23:37:27	18:00:28	3	4	.47	347.50	1393	DEG. C	157
17:59:59	23:52:22	SS792A	2.0954 1	2.7358-1	2.1445 1	2.0023 1	23:41:31	18:03:46	9	1	1.22	347.80	1396	DEG. C	157
18:00:01	23:52:23	SS793A	1.8123 1	3.0053-1	1.8668 1	1.7094 1	23:45:55	18:00:32	1	2	1.11	347.75	1396	DEG. C	157
18:00:05	23:52:27	SS794A	1.7857 1	2.7064-1	1.8227 1	1.6996 1	20:26:01	18:01:36	10	4	.90	347.67	1395	DEG. C	157
18:00:11	23:52:33	SS795A	1.9122 1	2.9583-1	1.9551 1	1.8277 1	20:35:27	18:00:26	22	30	.57	347.54	1395	DEG. C	157
18:00:11	23:52:33	SS796A	2.0691 1	2.9056-1	2.1199 1	1.9777 1	22:12:29	18:02:42	6	1	.57	347.54	1395	DEG. C	157
18:00:11	23:52:33	SS797A	2.2319 1	2.7023-1	2.3293 1	2.7055 1	23:44:44	18:00:26	4	25	.57	347.54	1395	DEG. C	157
18:00:13	23:52:35	SS798A	1.9028 1	2.6028-1	1.9457 1	1.8133 1	22:12:01	18:00:58	19	5	.47	347.50	1393	DEG. C	157
18:00:21	23:52:43	SS799A	2.0579 1	3.1045-1	2.1066 1	1.9645 1	23:39:32	18:00:01	7	30	1.11	347.75	1396	DEG. C	157
17:59:59	23:52:22	SS800A	1.3334 1	2.7613-1	1.3824 1	1.2523 1	23:46:19	18:00:14	2	7	1.22	347.80	1396	DEG. C	157
18:00:09	23:52:31	SS801A	1.7718 1	2.9447-1	1.8176 1	1.6598 1	21:56:49	18:00:24	41	9	.68	347.58	1398	DEG. C	157
18:00:09	23:52:31	SS803A	1.7525 1	2.9008-1	1.8039 1	1.6617 1	23:49:33	18:07:12	1	3	.68	347.58	1398	DEG. C	157
18:00:05	23:52:27	SS804A	3.2163 1	2.8571-1	3.2574 1	3.1410 1	22:09:07	18:07:54	12	1	.90	347.67	1395	DEG. C	157
18:00:05	23:52:27	SS805A	1.3924 1	2.9340-1	1.4430 1	1.3187 1	23:38:20	18:00:05	3	13	.90	347.67	1395	DEG. C	157
18:00:07	23:52:29	SS806A	1.6399 1	2.7780-1	1.7191 1	1.5910 1	23:35:06	18:07:38	1	1	.79	347.62	1398	DEG. C	157
18:00:07	23:52:29	SS807A	1.9088 1	2.8311-1	2.0215 1	1.8891 1	23:45:41	18:00:07	2	23	.79	347.62	1398	DEG. C	157
18:00:07	23:52:29	SS808A	3.0514 1	3.1286-1	3.0852 1	2.9840 1	20:47:25	18:00:52	219	57	.79	347.62	1398	DEG. C	157
17:59:59	23:52:22	SS809A	3.5749 1	3.1448-1	3.5922 1	3.5594 1	18:07:03	18:01:00	201	394	1.22	347.80	1398	DEG. C	157
18:00:01	23:52:23	SS810A	3.3773 1	3.0160-1	3.4191 1	3.3027 1	22:58:02	18:11:21	33	2	1.11	347.75	1396	DEG. C	157
18:00:03	23:52:25	SS811A	3.7859 1	3.0235-1	3.8316 1	3.7176 1	22:27:19	18:00:03	4	71	1.01	347.71	1394	DEG. C	157
18:00:03	23:52:25	SS812A	3.8700 1	3.0715-1	3.9172 1	3.8031 1	21:46:24	18:00:03	5	42	1.01	347.71	1394	DEG. C	157
18:00:03	23:52:25	SS813A	3.6572 1	3.0344-1	3.7023 1	3.5922 1	23:49:54	18:00:03	1	107	1.01	347.71	1394	DEG. C	157

PMDF TAPE NOS. 781887 781888
STANDARD REPORT 1 LIST 5 1978 188

SYSTEM ID 4.80 SASS PAGE 4
JOE: JCL8166D 78-329/ 02:10:01

TIME-1ST	TIME-LST	CHAN	MEAN VALUE	STD DEVN	MAX VALUE	MIN VALUE	TIME-MAX	TIME-MIN	NMAX	NMIN	LAT	LONG	POINTS	UNITS	REV#
18:00:09	23:52:31	SS814A	-3.6681 1	2.8237 0	-3.2344 1	-4.3516 1	18:00:57	23:36:23	4	1	.68	347.58	1398	DEG. C	157
18:00:09	23:52:31	SS815A	-3.6895 1	2.6339 0	-3.2469 1	-4.3359 1	18:07:58	23:37:09	4	1	.68	347.58	1398	DEG. C	157
18:00:09	23:52:31	SS816A	-3.6546 1	2.7471 0	-3.1719 1	-4.2766 1	18:56:36	23:36:23	1	1	.68	347.58	1398	DEG. C	157
18:00:09	23:52:31	SS817A	-3.2278 1	2.6643 0	-2.7016 1	-3.9109 1	18:58:22	23:31:51	1	1	.68	347.58	1398	DEG. C	157
18:00:09	23:52:31	SS818A	-3.2529 1	2.7071 0	-2.7453 1	-3.9266 1	18:58:37	23:31:51	2	1	.68	347.58	1398	DEG. C	157
18:00:11	23:52:33	SS819A	-3.2417 1	2.6036 0	-2.6906 1	-3.8359 1	19:00:10	23:34:54	1	1	.57	347.54	1395	DEG. C	157
18:00:11	23:52:33	SS820A	-3.2437 1	2.6040 0	-2.7016 1	-3.8516 1	18:58:54	23:34:54	2	1	.57	347.54	1395	DEG. C	157
18:00:11	23:52:33	SS821A	-3.1114 1	2.6832 0	-2.5437 1	-3.7641 1	19:00:40	23:30:07	1	1	.57	347.54	1395	DEG. C	157
18:00:11	23:52:33	SS822A	-3.0926 1	2.6722 0	-2.4922 1	-3.7047 1	19:01:11	23:31:38	1	1	.57	347.54	1395	DEG. C	157
18:00:11	23:52:33	SS823A	-3.1262 1	2.6025 0	-2.5344 1	-3.7453 1	19:01:56	23:29:52	1	1	.57	347.54	[illegible]	DEG. C	157

PMDF TAPE NOS. 781887 781888 SYSTEM ID 4.8D SASS PAGE 5
STANDARD REPORT 1 LIST 6 1978 188 JOE: JDL81880 78-329/ 02:10:01

TIME-1ST	TIME-LST	CHAN	MEAN VALUE		STD DEVN		MAX VALUE		MIN VALUE		TIME-MAX	TIME-MIN	NMAX	NMIN	LAT	LONG	POINTS	UNITS	REV#
18:00:01	23:52:23	SS824A	-1.9322	1	2.4290	0	-3.3234	1	-4.3859	1	18:53:43	23:34:45	1	1	1.11	347.75	1396	DEG. C	157
19:00:01	23:58:23	SS825A	-3.9536	1	2.4007	0	-3.3359	1	-4.4062	1	18:53:43	23:34:45	1	1	1.11	347.75	1396	DEG. C	157
18:00:01	23:52:23	SS826A	-3.9550	1	2.4232	C	-3.4109	1	-4.4500	1	13:51:11	23:36:16	1	1	1.11	347.75	1396	DEG. C	157
19:00:01	23:52:23	SS827A	-3.1486	1	2.4578	C	-2.5719	1	-3.6672	1	18:57:44	23:30:43	2	2	1.11	347.75	1396	DEG. C	157
18:00:01	23:52:23	SS828A	-3.1769	1	2.4830	0	-2.6141	1	-3.6612	1	18:57:44	23:32:44	3	1	1.11	347.75	1396	DEG. C	157
18:00:03	23:52:25	SS829A	-3.1891	1	2.4846	C	-2.6453	1	-3.7672	1	18:56:01	23:33:31	3	1	1.01	347.71	1394	DEG. C	157
18:00:03	23:52:25	SS830A	-3.1523	1	2.5253	0	-2.5922	1	-3.7219	1	18:57:31	23:33:31	1	1	1.01	347.71	1394	DEG. C	157
18:00:03	23:52:25	SS831A	-2.9346	1	2.5330	0	-2.3594	1	-3.4328	1	19:00:33	23:29:29	1	2	1.01	347.71	1394	DEG. C	157
18:00:03	23:52:25	SS832A	-2.9884	1	2.4441	C	-2.4328	1	-3.5422	1	18:59:47	23:30:30	1	1	1.01	347.71	1394	DEG. C	157
18:00:03	23:52:25	SS833A	-3.0041	1	2.4140	0	-2.4641	1	-3.5297	1	18:59:47	21:50:11	1	4	1.01	347.71	1394	DEG. C	157

PMDF TAPE NOS. 781887 781888 SYSTEM ID 4.80 SASS PAGE 6
STANDARD REPORT 1 LIST 7 1978 188 JOB: JDL8188D 78-329/ 02:10:01

TIME-1ST	TIME-LST	CHAN	MEAN VALUE	STD DEVN	MAX VALUE	MIN VALUE	TIME-MAX	TIME-MIN	NMAX	NMIN	LAT	LONG	POINTS	UNITS	REV#
18:00:13	23:52:22	SS834A	-5.8213 1	1.6022 C	-5.4156 1	-6.2828 1	18:02:59	23:34:56	5	1	.47	347.50	1393	DEG. C	157
18:00:13	23:52:20	SS835A	-5.8215 1	1.6157 C	-5.4156 1	-6.3344 1	18:05:15	23:34:56	3	1	.47	347.50	1393	DEG. C	157
18:00:13	23:52:20	SS836A	-5.8952 1	1.5574 0	-5.4797 1	-6.3891 1	18:08:47	23:34:56	2	1	.47	347.50	1393	DEG. C	157
18:00:13	23:52:20	SS837A	-5.5373 1	1.7419 C	-5.1484 1	-5.9578 1	18:06:00	22:39:59	10	1	.47	347.50	1393	DEG. C	157
18:00:13	23:52:20	SS838A	-5.5519 1	1.7356 0	-5.1484 1	-5.9578 1	18:03:29	22:31:40	10	3	.47	347.50	1393	DEG. C	157
17:59:59	23:52:22	SS839A	-5.6168 1	1.7478 0	-5.1766 1	-6.0875 1	18:09:19	2 :33:58	2	1	1.22	347.80	1396	DEG. C	157
17:59:59	23:52:22	SS840A	-5.6172 1	1.7445 C	-5.2047 1	-6.0422 1	18:09:04	22:33:58	7	1	1.22	347.80	1396	DEG. C	157
17:59:59	23:52:22	SS841A	-5.5787 1	1.5211 0	-5.2297 1	-6.0422 1	18:10:04	22:33:58	1	1	1.22	347.80	1396	DEG. C	157
17:59:59	23:52:22	SS842A	-5.6665 1	1.5335 C	-5.2625 1	-6.0875 1	18:09:19	22:33:58	2	1	1.22	347.80	1396	DEG. C	157
17:59:59	23:52:22	SS843A	-5.6670 1	1.5352 C	-5.2625 1	-6.1344 1	18:10:35	22:33:58	1	1	1.22	347.80	1396	DEG. C	157

PMDF TAPE NOS. 761887 781888
STANDARD REPORT 1 LIST 8 1978 188

SYSTEM ID 4.8C SASS PAGE 7
JCE: JDL8188D 78-329/ 02:10:01

TIME-1ST	TIME-LST	CHAN	MEAN VALUE	STD DEVN	MAX VALUE	MIN VALUE	TIME-MAX	TIME-MIN	NMAX	NMIN	LAT	LONG	POINTS	UNITS	REV#
18:00:05	23:52:27	SS844A	-6.0963 I	1.3147 0	-5.7344 I	-6.5125 I	19:47:43	23:38:35	1	1	.50	347.67	1395	DEG. C	157
18:00:05	23:52:27	SS845A	-6.0914 I	1.3428 0	-5.7687 I	-6.4547 I	18:04:52	23:33:48	8	3	.50	347.67	1395	DEG. C	157
18:00:05	23:52:27	SS846A	-6.0189 I	1.2667 0	-5.6937 I	-6.3984 I	18:05:53	23:32:48	4	1	.50	347.67	1395	DEG. C	157
18:00:05	23:52:27	SS847A	-5.7495 I	1.5926 0	-5.3578 I	-6.1437 I	18:08:05	22:42:08	6	2	.50	347.67	1395	DEG. C	157
18:00:05	23:52:27	SS848A	-5.7559 I	1.6125 0	-5.3312 I	-6.1437 I	19:47:43	23:33:35	1	1	.50	347.67	1395	DEG. C	157
18:00:07	23:52:29	SS849A	-5.6024 I	1.5305 0	-5.2687 I	-6.0109 I	18:04:54	22:36:07	2	1	.79	347.62	1398	DEG. C	157
18:00:07	23:52:29	SS850A	-5.6574 I	1.5115 0	-5.2687 I	-6.0484 I	18:06:25	19:18:00	1	1	.79	347.62	1398	DEG. C	157
18:00:07	23:52:29	SS851A	-5.7671 I	1.4800 0	-5.3891 I	-6.0969 I	18:06:40	22:32:50	8	3	.79	347.62	1398	DEG. C	157
18:00:07	23:52:29	SS852A	-5.6863 I	1.4103 0	-5.3781 I	-6.0484 I	18:03:39	19:18:00	5	1	.79	347.62	1398	DEG. C	157
18:00:07	23:52:29	SS853A	-5.6895 I	1.4365 0	-5.2984 I	-6.2516 I	18:04:24	22:32:50	3	1	.79	347.62	1398	DEG. C	157

TIME-1ST	TIME-LST	CHAN	MEAN VALUE	STD DEVN	MAX VALUE	MIN VALUE	TIME-MAX	TIME-MIN	NMAX	NMIN	LAT	LONG	POINTS	UNITS	REV#
18:00:00	23:57:33	LC101D	2.9829 1	7.2015-1	3.1090 1	2.8383 1	19:52:38	22:32:19	69	1227			447247	VOLTS DC	157
18:00:00	23:52:33	LC117A	2.8165 1	7.2885-2	2.8383 1	2.8113 1	18:01:11	18:00:00	255	11733			20651	VOLTS DC	157
18:00:00	23:52:33	LC135A	4.0732 0	1.8694 0	8.7998 0	2.5596 0	20:49:12	18:03:44	43	1029			20651	AMPS	157

PMDF TAPE NOS. 781887 781888
STANDARD REPORT 1   LIST 10   1978 188

SYSTEM ID 4.8D   SASS   PAGE 9
JOE: JDL8188D   78-329/   02:10:01

TIME-1ST	TIME-LST	CHAN	MEAN VALUE	STD DEVN	MAX VALUE	MIN VALUE	TIME-MAX	TIME-MIN	NMAX	NMIN	LAT	LONG	POINTS	UNITS	REV#
17:59:59	22:52:33	SS865A	9.6182 1	4.6179-1	9.9719 1	9.4562 1	18:02:02	18:29:59	2	3			10820	WATTS	157
17:59:59	22:52:33	SS866A	9.6383 1	4.5882-1	9.7734 1	9.2500 1	22:24:24	19:42:35	1	1			10820	WATTS	157
17:59:59	22:52:33	SS867A	9.6315 1	4.5760-1	9.7734 1	9.3031 1	20:39:47	23:16:19	2	1			10820	WATTS	157
17:59:59	22:52:33	SS868A	9.6243 1	4.5313-1	9.7578 1	9.2500 1	18:02:04	19:58:42	1	1			10820	WATTS	157

PMDF TAPE NOS. 781887 781888
STANDARD REPORT 1   LIST 11 1978 188

SYSTEM ID 4.8C   SASS   PAGE 10
JOE: JCL8188D   78-329/   02:10:01

TIME-IST	TIME-LST	CHAN	MEAN VALUE	STD DEVN	MAX VALUE	MIN VALUE	TIME-MAX	TIME-MIN	NMAX	NMIN	LAT	LONG	POINTS	UNITS		REV#
18:01:47	23:48:40	SS731A	3.3275 0	8.0893-2	3.4393 0	3.1670 0	19:00:22	22:19:53	1	1			173	VOLTS	DC	157
18:05:51	23:48:42	SS731C	1.0153 0	8.8340-2	1.0752 0	9.6680-1	20:10:56	23:00:15	1	3			172	VOLTS	DC	157
18:01:47	23:48:40	SS732A	2.9395 0	8.3840-2	3.0693 0	2.7852 0	18:09:55	22:03:45	5	1			173	VOLTS	DC	157
18:05:51	23:48:42	SS732C	8.7666-1	2.5102-2	9.2773-1	8.3008-1	18:05:55	21:51:41	1	2			172	VOLTS	DC	157
18:01:47	23:48:40	SS733A	2.7201 0	8.2087-2	2.8437 0	2.5605 0	18:22:01	23:32:29	2	1			173	VOLTS	DC	157
18:05:51	23:48:42	SS733C	8.0021-1	2.5529-2	8.4961-1	7.6172-1	19:30:36	18:54:15	1	7			172	VOLTS	DC	157
18:01:47	23:48:40	SS734A	2.5756 0	8.2814-2	2.7363 0	2.4336 0	18:05:53	23:00:13	2	1			173	VOLTS	DC	157
18:05:51	23:48:42	SS734C	7.4756-1	2.4725-2	7.9102-1	7.0313-1	19:26:34	21:07:20	5	4			172	VOLTS	DC	157
18:01:47	23:48:40	SS735A	2.2644 0	7.5147-2	2.4238 0	2.1406 0	19:42:40	20:51:10	1	3			173	VOLTS	DC	157
18:05:51	23:48:42	SS735C	6.5810-1	2.1949-2	7.0313-1	6.1523-1	18:30:07	23:20:25	1	1			172	VOLTS	DC	157
18:01:47	23:48:40	SS736A	1.8875 0	6.2998-2	1.9932 0	1.7881 0	18:09:55	20:18:54	3	2			173	VOLTS	DC	157
18:05:51	23:48:42	SS736C	5.7048-1	1.9551-2	6.0547-1	5.3711-1	18:05:55	19:02:19	3	3			170	VOLTS	DC	157
20:27:04	22:56:13	SS736D	5.2539 0	1.4100-1	5.3955 0	5.1123 0	20:27:04	22:56:13	1	1			2	VOLTS	DC	157
18:01:47	23:48:40	SS737A	1.5922 0	5.4574-2	1.6709 0	1.4854 0	18:05:53	20:39:04	3	3			173	VOLTS	DC	157
18:05:55	23:48:42	SS737C	4.7036-1	1.6567-2	4.9805-1	4.3945-1	18:18:01	20:43:08	5	5			109	VOLTS	DC	157
18:05:51	23:48:39	SS737D	4.3712 0	1.4113-1	4.6621 0	4.1738 0	19:38:40	23:44:27	1	1			63	VOLTS	DC	157
18:01:47	23:48:40	SS738A	1.4976 0	5.2523-2	1.6123 0	1.3877 0	21:15:26	20:51:10	1	1			173	VOLTS	DC	157
19:13:55	23:48:42	SS738C	4.5022-1	1.5916-2	4.6875-1	4.1992-1	18:18:01	18:54:15	5	5			39	VOLTS	DC	157
18:05:51	23:44:40	SS738D	4.1123 0	1.3180-1	4.3789 0	3.8799 0	19:50:46	23:28:29	2	1			133	VOLTS	DC	157
18:01:47	23:48:40	SS739A	1.3347 0	4.9940-2	1.4268 0	1.2314 0	18:46:13	19:46:38	1	1			173	VOLTS	DC	157
19:46:44	23:40:38	SS739C	3.8086-1	.0000 0	3.8086-1	3.8086-1	19:46:44	19:46:44	5	1			5	VOLTS	DC	157
18:05:51	23:48:42	SS739D	3.5557 0	1.2917-1	3.8213 0	3.3135 0	19:10:26	21:55:43	1	1			167	VOLTS	DC	157
18:01:47	23:48:40	SS740A	1.1653 0	4.3905-2	1.2510 0	1.0752 0	19:02:20	23:00:13	2	1			173	VOLTS	DC	157
18:05:51	23:48:42	SS740D	3.3247 0	1.2410-1	3.5771 0	3.1084 0	18:46:14	22:56:13	1	2			172	VOLTS	DC	157
18:01:47	23:48:40	SS741A	1.0432 0	3.7794-2	1.1240 0	9.6680-1	18:17:59	23:00:13	1	1			173	VOLTS	DC	157
18:05:51	23:48:42	SS741D	2.9182 0	1.0226-1	3.1182 0	2.6973 0	21:43:41	20:1?:52	1	1			172	VOLTS	DC	157
18:01:47	23:48:40	SS742A	8.5661-1	3.4340-2	9.2773-1	7.9102-1	23:12:23	18:33:05	1	3			173	VOLTS	DC	157
18:05:51	23:48:42	SS742D	2.4633 0	9.4069-2	2.6387 0	2.2969 0	20:10:53	21:43:37	2	2			172	VOLTS	DC	157
18:01:47	23:48:40	SS743A	3.1472 0	5.5187-2	3.2939 0	3.0205 0	18:30:05	20:51:10	1	2			173	VOLTS	DC	157
18:05:51	23:48:42	SS743C	9.3239-1	1.5917-2	9.7656-1	8.9844-1	18:09:57	20:43:08	1	2			172	VOLTS	DC	157
18:01:47	23:48:40	SS744A	2.9626 0	3.7287-2	3.0596 0	2.8823 0	18:38:09	22:15:51	2	2			173	VOLTS	DC	157
18:05:51	23:48:42	SS744C	9.3171-1	1.1762-2	9.5703-1	8.9844-1	18:05:55	22:56:13	6	1			172	VOLTS	DC	157
18:01:47	23:48:40	SS745A	3.1555 0	3.4852-2	3.2549 0	3.0693 0	19:02:20	22:15:51	1	1			173	VOLTS	DC	157
18:05:51	23:48:42	SS745C	9.6811-1	1.0602-2	1.0968 0	9.4727-1	19:14:28	19:02:19	1	12			172	VOLTS	DC	157

PMDF TAPE NOS. 781887 781888
STANDARD REPORT 1 LIST 12 1978 188

SYSTEM ID 4.8D SASS PAGE 11
JOB: JDL8188D 78-329/ 02:10:01

TIME-1ST	TIME-LST	CHAN	MEAN VALUE	STD DEVN	MAX VALUE	MIN VALUE	TIME-MAX	TIME-MIN	NMAX	NMIN	LAT	LONG	POINTS	UNITS	REV#
18:01:47	23:48:40	SS746A	4.2577 0	1.0222-1	4.4375 0	4.0762 0	18:30:05	22:36:01	3	1			173	VOLTS DC	157
18:05:51	23:48:42	SS746C	1.2987 0	3.4796-2	1.3584 0	1.2314 0	18:22:03	21:47:39	4	1			172	VOLTS DC	157
18:01:47	23:48:40	SS747A	3.6395 0	1.0086-1	3.8115 0	3.4795 0	23:24:29	20:39:04	1	2			173	VOLTS DC	157
18:05:51	23:48:42	SS747C	1.0856 0	3.3717-2	1.1436 0	1.0264 0	18:05:55	19:50:42	2	5			172	VOLTS DC	157
18:01:47	23:48:40	SS748A	3.2153 0	1.0061-1	3.3916 0	3.0400 0	18:46:13	21:23:26	1	2			173	VOLTS DC	157
18:05:51	23:48:42	SS749C	9.5534-1	3.0662-2	1.0068 0	8.9844-1	19:30:36	23:20:25	3	1			172	VOLTS DC	157
18:01:47	23:48:40	SS749A	2.9342 0	9.2481-2	3.1182 0	2.7754 0	18:58:19	19:46:38	1	1			173	VOLTS DC	157
18:05:51	23:48:42	SS749C	8.5671-1	2.7280-2	9.0920-1	8.0078-1	18:38:11	22:52:11	2	1			172	VOLTS DC	157
18:01:47	23:48:40	SS750A	2.4529 0	7.8019-2	2.6094 0	2.3164 0	18:05:53	19:14:25	1	3			173	VOLTS DC	157
18:05:51	23:48:42	SS750B	7.1158-1	2.4356-2	7.6172-1	6.6406-1	18:13:59	21:55:43	2	1			172	VOLTS DC	157
18:01:47	23:48:40	SS751A	1.9162 0	6.2229-2	2.0332 0	1.8076 0	18:17:59	20:02:46	2	3			173	VOLTS DC	157
18:05:51	23:48:42	SS751C	5.7945-1	2.0592-2	6.2500-1	5.4688-1	19:38:40	20:18:56	1	7			170	VOLTS DC	157
20:27:04	22:56:13	SS751D	5.2393 0	1.4702-1	5.4053 0	5.0732 0	20:27:04	22:56:13	1	1			2	VOLTS DC	157
18:01:47	23:48:40	SS752A	1.4901 0	5.2014-2	1.5928 0	1.3975 0	21:19:27	23:35:02	1	2			173	VOLTS DC	157
18:05:55	23:48:42	SS752C	4.4196-1	1.5393-2	4.7852-1	4.1016-1	18:05:55	18:54:15	1	2			109	VOLTS DC	157
18:05:51	23:48:39	SS752D	4.1218 0	1.3480-1	4.3984 0	3.9092 0	18:34:09	20:10:52	2	1			63	VOLTS DC	157
18:01:47	23:48:40	SS753A	1.2966 0	4.9025-2	1.4170 0	1.2119 0	18:05:55	21:19:24	1	2			173	VOLTS DC	157
18:13:55	23:48:42	SS753C	3.8867-1	1.3245-2	4.1016-1	3.6133-1	18:30:07	21:35:37	2	3			39	VOLTS DC	157
18:05:51	23:44:40	SS753D	3.5631 0	1.1260-1	3.7432 0	3.3330 0	21:19:29	23:36:33	2	1			133	VOLTS DC	157
18:01:47	23:48:40	SS754A	1.0522 0	3.9640-2	1.1338 0	9.7656-1	18:38:09	20:55:12	3	3			173	VOLTS DC	157
19:46:44	23:40:38	SS754C	2.9639-1	4.7842-3	3.0273-1	2.9297-1	19:46:44	21:19:29	2	3			5	VOLTS DC	157
18:05:51	23:48:42	SS754D	2.8071 0	1.0408-1	3.0303 0	2.6289 0	19:02:22	21:43:37	1	3			167	VOLTS DC	157
18:01:47	23:48:40	SS755A	8.1410-1	3.0523-2	8.7891-1	7.5195-1	20:39:08	20:56:48	2	3			173	VOLTS DC	157
18:05:51	23:48:42	SS755D	2.3332 0	8.5819-2	2.5215 0	2.1406 0	19:14:28	20:31:02	1	1			172	VOLTS DC	157
18:01:47	23:48:40	SS756A	7.2993-1	2.8503-2	8.1055-1	6.7383-1	20:35:06	21:59:43	1	2			173	VOLTS DC	157
18:05:51	23:48:42	SS756D	2.0483 0	7.6157-2	2.2285 0	1.9150 0	18:09:57	22:40:05	3	1			172	VOLTS DC	157
18:01:47	23:48:40	SS757A	6.0575-1	2.5836-2	6.6406-1	5.4688-1	18:05:53	22:44:05	1	1			173	VOLTS DC	157
18:05:51	23:48:42	SS757D	1.7403 0	6.6343-2	1.8857 0	1.6123 0	19:54:48	19:10:23	1	2			172	VOLTS DC	157
18:01:47	23:48:40	SS758A	4.4229 0	7.0002-2	4.5937 0	4.2812 0	21:11:24	21:31:30	1	1			173	VOLTS DC	157
18:05:51	23:48:42	SS758C	1.2904 0	1.9884-2	1.3389 0	1.2510 0	18:46:14	23:08:19	3	1			172	VOLTS DC	157
18:01:47	23:48:40	SS759A	4.2263 0	4.9922-2	4.3301 0	4.1152 0	18:46:13	21:47:38	1	1			173	VOLTS DC	157
18:05:51	23:48:42	SS759C	1.3124 0	1.6058-2	1.3486 0	1.2803 0	18:18:01	20:39:06	2	10			172	VOLTS DC	157
18:01:47	23:48:40	SS760A	4.5209 0	4.5083-2	4.6816 0	4.4180 0	18:13:53	23:27:27	1	1			173	VOLTS DC	157
18:05:51	23:48:42	SS760C	1.3753 0	1.3521-2	1.4072 0	1.3486 0	18:13:59	20:55:14	6	5			172	VOLTS DC	157

PMDF TAPE NOS. 781887 791888 SYSTEM ID 4.8D SASS PAGE 12
STANDARD REPORT 1 LIST 13 1978 188 JOB: JOL8188D 78-329/ 02:10:01

TIME-1ST	TIME-LST	CHAN	MEAN VALUE	STD DEVN.	MAX VALUE	MIN VALUE	TIME-MAX	TIME-MIN	NMAX	NMIN	LAT	LONG	POINTS	UNITS	REV#
18:00:24	18:00:32	SS760D	4.2178 0	4.8828-3	4.2227 0	4.2129 0	18:00:32	18:00:24	1	1	-.17	347.24	2	VOLTS DC	157
18:00:26	18:00:33	SS760E	4.4434-1	4.8828-3	4.4922-1	4.3945-1	18:00:33	18:00:26	1	1	-.28	347.20	2	VOLTS DC	157
18:00:28	18:00:35	SS760H	4.2373 0	4.8828-3	4.2422 0	4.2324 0	18:00:35	18:00:28	1	1	-.29	347.15	2	VOLTS DC	157
18:00:22	18:00:30	SS760I	4.3457-1	4.8828-3	4.3945-1	4.2969-1	18:00:22	18:00:30	1	1	.06	347.28	2	VOLTS DC	157

TIME TAG	LAT	LONG	CHAN	TITLE	BINARY VALUE	REV#
188:17:59:59	1.22	347.80	SS700A	OPER MODE	0000000000000001	153
188:17:59:59	1.22	347.80	SS701A	OPER MODE	0000000000000001	153
188:17:59:59	1.22	347.80	SS702A	OPER MODE	0000000000000001	153
188:17:59:59	1.22	347.80	SS703A	OPER MODE	0000000000000000	153
188:17:59:59	1.22	347.80	SS704A	OPER MODE	0000000000000001	153
188:17:59:59	1.22	347.80	SS705A	OPER MODE	0000000000000001	153
188:17:59:59	1.22	347.80	SS706A	OPER MODE	0000000000000001	153
188:17:59:59	1.22	347.80	SS707A	OPER MODE	0000000000000001	153
188:17:59:59	1.22	347.80	SS708A	OPER MODE	0000000000000001	153
188:17:59:59	1.22	347.80	SS709A	OPER MODE	0000000000000001	153

PMDF TAPE NOS. 781887 781888
STANDARD REPORT 2 LIST 2 1978 188

SYSTEM ID 4.80 SASS PAGE 14
JOB: JDL8188D 78-329/ 02:10:01

TIME TAG	LAT	LONG	CHAN	TITLE	BINARY VALUE	REV#
188:17:55:59			SS762A	TWT PARAMS	0000000000000000	153
188:17:55:59			SS763A	TWT PARAMS	0000000000000000	153
188:17:55:59			SS764A	TWT PARAMS	0000000000000000	153

TIME TAG	LAT	LONG	CHAN	TITLE	BINARY VALUE	REV#
188:17:55:59			SS770A	ENGN HSKPG	0000000000000000	153
188:17:55:59			SS771A	ENGN HSKPG	0000000000000000	153
188:17:55:59			SS779A	ENGN HSKPG	0000000000000000	153

PMDF TAPE NOS. 781887 781888
STANDARD REPORT 3   LIST 10   1978 188

SYSTEM ID 4.8D   SASS   PAGE 16
JOE: JDL81880   78-329/   02:10:01

SAMPLE 1 TIME	VALUE	CHAN	TITLE	CROSS TIME	MIN VALUE	MAX VALUE	LIMIT	DATA VALUE	UP/DOWN	UNITS	LAT	LONG	REV#
17:59:59	.0000 0	SS764A	SPARES	00:00:00	.0000 0	9.7656-3	.0000 0	.0000 0	NEITHER	VOLTS DC			157
17:59:59	.0000 0	SS863A	SPARES	00:00:00	.0000 0	9.7656-3	.0000 0	.0000 0	NEITHER	VOLTS DC			157
17:59:59	.0000 0	SS864A	SPARES	00:00:00	.0000 0	9.7656-3	.0000 0	.0000 0	NEITHER	VOLTS DC			157
17:59:59	1.7090-3	SS869A	SPARES	00:00:00	.0000 0	3.6621-3	.0000 0	.0000 0	NEITHER	VOLTS DC			157
17:59:59	.0000 0	SS870A	SPARES	00:00:00	.0000 0	3.6621-3	.0000 0	.0000 0	NEITHER	VOLTS DC			157
17:59:59	2.4414-4	SS871A	SPARES	00:00:00	.0000 0	3.6621-3	.0000 0	.0000 0	NEITHER	VOLTS DC			157
17:59:59	1.2207-3	SS872A	SPARES	00:00:00	.0000 0	3.6621-3	.0000 0	.0000 0	NEITHER	VOLTS DC			157
17:59:59	3.4600 2	SS873A	SPARES	00:00:00	3.4600 2	3.4600 2	.0000 0	.0000 0	NEITHER	COUNTS			157
17:59:59	6.0200 2	SS874A	SPARES	00:00:00	6.0200 2	6.0200 2	.0000 0	.0000 0	NEITHER	COUNTS			157
17:59:59	4.2700 2	SS875A	SPARES	00:00:00	4.2700 2	4.2700 2	.0000 0	.0000 0	NEITHER	COUNTS			157

TIME TAG	CHAN	CH.VALUE	SS730-SS709	SEQ
168:23:52:23	SS710	00000000	1110111111	NO ANOMALY 157=REV#

88

TIME TAG	CHAN	CH.VALUE	SS700-SS709	SEQ
188:23:52:33	SS711	00000000	1110111111	NO ANOMALY 157=REV#

TIME TAG	CHAN	CH.VALUE	SS700-SS709	SEQ
188:23:52:33	SS712	10000001	1111111111	NO ANOMALY ·157=REV#

90

TIME TAG	CHAN	CH.VALUE	SS700-SS709	SEQ	
188:23:52:33	SS713	00000001	1110111111		NO ANOMALY 157=REV#

TIME TAG	CHAN	CH.VALUE	SS713	SEQ
188:23:52:33	SS714	000C0000	000000000	NO ANOMALY IS7=REV#

TIME TAG	CHAN	CH.VALUE	SS713	SEQ
188:23:52:33	SS715	00000001	000000000	NO ANOMALY 157=REV#

TIME TAG	CHAN	CH.VALUE	SS730-SS709	SEG	
188:23:52:33	SS785	00000000	1111111111		NO ANOMALY 157=REV#

TIME TAG	CHAN	CH.VALUE	SS700-SS709		SEQ
188:23:52:33	SS854	00000001	1110111111	,	NO ANOMALY, 157=REV# .

TIME TAG CHAN
188:17:55:59 SS765 7.1154 4 =ELAPSED TIME 157=REV#

PMDF TAPE NOS. 781887 781888
SASS SPECIAL REPORT LIST 0 1978 188

SYSTEM ID 4.8D SASS PAGE 26
JOB: JDL8188D 78-329/ 02:10:01

TIME TAG CHAN
188:17:59:59 SS862 2.1154 4 =ELAPSED TIME 157=REV#

97

APPENDIX E

SASS CRT PAGES

ORB;00142 SYS; C06 PTCH;-.02000 SUN;YES CMD ACC:251 GMT=187:23:21:08
PRI; MIL QUAL;GOOD ROLL;.337558 BUS VLT;29.80 CMD EXC:016 SCT=187:23:21:07
SRCE;R/T YAW; -2.5331 PTE; 007 009 MEM;COMPARE FRAME LOCK:08733
PAGE 14 QUICKLOOK PAGE 2 SCATTEROMETER SYSTEM STATUS

INPUT CURRENT	3.5998	AMPS	00045	MODE 8	NSEL		00239
+28 VOLTS REG PS	28.116	VOLT	00149	MODE 9	NSEL		00783
TWT CATHODE VOLT	-8.028	KV	00260	STANDBY	NSEL		00783
TWT CATHODE CURR	56.418	MAMP	00165	DC/DC CON#3 STAT	ON		00216
TWT BODY CURRENT	5.7157	MAMP	00069	DC/DC CON#4 STAT	OFF		00216
ION PUMP CURRENT	4.0208	UAMP	00002	DC/DC +5V CONV	5.0780	VOLT	00521
HVPS INPUT CURR	2.3003	AMPS	00276	DC/DC +15V CONV	14.911	VOLT	00512
TWT FIL CURRENT	1.4945	AMPS	00376	DC/DC -15V CONV	-15.02	VOLT	00292
MODE 1	NSEL		00239	DC/DC -6V CONV	-6.032	VOLT	00253
MODE 2	NSEL		00239	DC/DC +6V CONV	5.9765	VOLT	00511
MODE 3	NSEL		00239	TRANSMIT POWER	100.72	WATT	00338
MODE 4	SEL		00239	RCVR PROT CKT ST	PROT		00392
MODE 5	NSEL		00239	INPUT CURR TRIP	NTRP		00392
MODE 6	NSEL		00239	UNDERVOLT TRIP	NTRP		00392
MODE 7	NSEL		00239	BODY CURENT TRIP	NTRP		00238

ORB:00000 SYS: C07 PTCH:-.95200 SUN:NO CMD ACC:178 GMT-122:16:29:06
PRI: PB QUAL:GOOD ROLL:.969997 BUS-VLT:27.50 CMD EXC:138 SCT-001:01:33:19
SRCE:TAPE YAW: N.A. PTE:N.A. N.A. MEM:ENABLE FRAME LOCK:00736
PAGE ~~24~~ 25 SASS PAGE 1 STATUS DATA

MODE 1	SEL	00127	POLARIZATION	VV	00660
MODE 2	NSEL	00127	LEFT/RIGHT ANT	LEFT	00660
MODE 3	NSEL	00127	FORE/AFT ANT	FWD	00660
MODE 4	NSEL	00127	LO PHASE LOCK LP	LOCK	00000
MODE 5	NSEL	00127	XMIT PHASE LOCK	LOCK	00000
MODE 6	NSEL	00127	BODY CURR TRIP	NTRP	00127
MODE 7	NSEL	00127	INPUT CURR TRIP	NTRP	00660
MODE 8	NSEL	00127	UNDERVOLT TRIP	NTRP	00660
MODE 9	SEL	00000	RCVR PROT CKT ST	PROT	00660
MODE 10	STBY	00000			
CALIBRATE STATUS	NCAL	00660			
NOISE DIODE STAT	OFF	00127			
HIGH FREQ SELECT	HIGH	00000			
LOW FREQ SELECT	LOW	00512			

100

ORB:00141	SYS: C06	PTCH:=.10000	SUN:YES	CMD ACC:198	GMT=187:21:59:02
PRI: AGO	QUAL:GOOD	ROLL:=.25220	BUS VLT:30.28	CMD EXC:011	SCT=187:21:59:01
SRCE:R/T		YAW: 1.69017	PTE: 007 008	MEM:ENABLE	FRAME LOCK:09787

PAGE 26 SASS-PAGE 2 ANALOG ENGINEERING

CALIBRATE STATUS	NCAL		00652	DC/DC +5V CONV	5.0682	VOLT	00520
STANDBY	NSEL		00847	DC/DC +15V CONV	14.911	VOLT	00512
TWT CATHODE VOLT	=8.022	KV	00259	DC/DC =15V CONV	=15.02	VOLT	00292
TWT CATHODE CURR	56.060	MAMP	00164	DC/DC =6V CONV	=6.032	VOLT	00253
TWT BODY CURRENT	5.8841	MAMP	00071	DC/DC +6V CONV	5.9649	VOLT	00510
ION PUMP CURRENT	=.0987	UAMP	00000	UP CONV BIAS	.10228	VOLT	00218
HVPS INPUT CURR	2.2701	AMPS	00273	TDA STAGE 1 BIAS	.14357	VOLT	00306
TWT FIL CURRENT	1.4844	AMPS	00374	TDA STAGE 2 BIAS	.15812	VOLT	00337
TRANSMIT POWER	100.20	WATT	00337	TDA STAGE 3 BIAS	.16844	VOLT	00359
LOCAL OSC POWER	12.182	DBM	00429	THERMISTOR REF 1	5.1073	VOLT	00522
MODULATOR POWER	21.182	DBM	00402	THERMISTOR REF 2	5.0976	VOLT	00521
XMIT DRIVE	17.195	DBM	00389				

ORB:00142 SVS: C06 PTCH:-.02000 SUN:YES CMD ACC:251 GMT:187:23:21:48
PRI: MIL QUAL:GOOD ROLL:.376358 BUS VLT:30.07 CMD EXC:016 SCT:187:23:21:47
SRCE:R/T YAW: -2.6121 RTE: 097 009 MEM:COMPARE FRAME LOCK:09713
PAGE 27 SASS PAGE 3 TEMPERATURES

CALIBRATE STATUS	NCAL		00028	FIRST MIXER	11.236	DEGC	00666
STANDBY	NSEL		00847	SECOND MIXER	21.863	DEGC	00540
TWT 1	9.9963	DEGC	00647	TDA	35.593	DEGC	00416
TWT 2	10.673	DEGC	00656	XTAL FILTER P1	29.743	DEGC	00449
TWT 3	12.855	DEGC	00634	XTAL FILTER P6	25.408	DEGC	00503
OUTPUT ISO	9.6560	DEGC	00680	XTAL FILTER P10	30.547	DEGC	00451
HVPS	10.843	DEGC	00668	XTAL FILTER P12	28.539	DEGC	00471
ASM	3.9986	DEGC	00704	BASEPLATE 1	9.8543	DEGC	00678
SSG/LO	9.3803	DEGC	00653	BASEPLATE 2	9.4837	DEGC	00658
UP-CONVERTER	8.8563	DEGC	00688	BASEPLATE 3	8.7578	DEGC	00688
A/D CONVERTER	26.386	DEGC	00502	BASEPLATE 4	11.920	DEGC	00657
NOISE SOURCE	4.8448	DEGC	00727	BASEPLATE 5	8.2436	DEGC	00666
DIR DETECTOR	7.1996	DEGC	00674	BASEPLATE 6	9.6560	DEGC	00680
SASS BP TEMP#1	48.833	DEGF	00176	SASS BP TEMP#2	52.568	DEGF	00168

ORB:00139 SYS: C06 PTCH:.131598 SUN:YES CMD ACC:188 GMT=187:19:12:23
PRI: ORR QUAL:GOOD ROLL:-.22116 BUS VLT:30.34 CMD EXC:254 SCT=187:19:12:21
SRCE:R/T YAW: 1.63750 PTE:-001 001 MEM:ENABLE FRAME LOCK:10031
PAGE 28 SASS PAGE 4 SCIENCE DATA

MODE 1	NSEL	01023	POLARIZATION	VV		00497
MODE 2	NSEL	01023	LEFT/RIGHT ANT	LEFT		00497
MODE 3	NSEL	01023	FORE/AFT ANT	AFT		00497
MODE 4	NSEL	01023	GAIN CHANNEL #1	G3		00341
MODE 5	NSEL	01023	GAIN CHANNEL #12	G2		00661
MODE 6	NSEL	01023	GAIN CHANNEL #15	G3		00661
MODE 7	NSEL	01023	SIG+NOISE CH #1	1.2512	VOLT	00128
MODE 8	NSEL	01023	SIG+NOISE CH #12	3.0596	VOLT	00313
MODE 9	NSEL	00783	SIG+NOISE CH #15	1.1827	VOLT	00121
MODE 10	NSTB	00783	NOISE ONLY CH#1	1.6031	VOLT	00164
CALIBRATE STATUS	CAL	00497	NOISE ONLY CH#12	2.1798	VOLT	00223
NOISE DIODE STAT	ON	01023	NOISE ONLY CH#15	[illegible].7008	VOLT	00174
HIGH FREQ SELECT	HIGH	00783				
LOW FREQ SELECT	HIGH	00513				

```
ORB:00140  SYS: C06   PTCH:.051598  SUN:YES         CMD ACC:194  GMT=187:20:54:02
PRI: ORR   QUAL:GOOD  ROLL:-.32204  BUS VLT:29.46   CMD EXC:007  SCT=187:20:54:01
SRCE:R/T              YAW: 3.55960  PTE: 004  006   MEM:ENABLE   FRAME LOCK:22380
PAGE 29               SAGS-PAGE 5  ALARM PARAMETERS
    ION PUMP CURRENT  -.0598  UAMP 00001
    HVPS INPUT CURR   -.4776  AMPS 00000
    DC/DC +15V CONV   14.911  VOLT 00512
    DC/DC -15V CONV   -15.04  VOLT 00291
    RCVR PROT CKT ST  PROT         00817
    BASEPLATE 4       9.3569  DEGC 00683
```

Table 1. Electrical Behavior In All Modes

<table>
<tr><th rowspan="2">PARAMETER</th><th colspan="3">NOMINAL VALUE</th></tr>
<tr><th>MODES 1-8</th><th>CONTINUOUS CALIBRATE MODE 9</th><th>STANDBY MODE 10</th></tr>
<tr><td>+5 v</td><td>+5 v</td><td colspan="2" rowspan="14">Same as Modes 1-8</td></tr>
<tr><td>+15 v</td><td>+15 v</td></tr>
<tr><td>-15 v</td><td>-15 v</td></tr>
<tr><td>-6 v</td><td>-6 v</td></tr>
<tr><td>+6 v</td><td>+6 v</td></tr>
<tr><td>Therm. Ref. 1</td><td>+5 v</td></tr>
<tr><td>Therm. Ref. 2</td><td>+5 v</td></tr>
<tr><td>L.O. Power</td><td>11.5/13.5 dBm</td></tr>
<tr><td>Mod. Power</td><td>21 dBm</td></tr>
<tr><td>Xmit Drive</td><td>16.5 dBm</td></tr>
<tr><td>Upcnv. Bias</td><td>0.1 v</td></tr>
<tr><td>TDA Stage 1 Bias</td><td>.135 v</td></tr>
<tr><td>TDA Stage 2 Bias</td><td>.155 v</td></tr>
<tr><td>TDA Stage 3 Bias</td><td>.165 v</td></tr>
<tr><td>TWT Cathode Voltage</td><td>8.02 kv</td><td>8.02 kv</td><td>0 kv</td></tr>
<tr><td>TWT Cathode Current</td><td>57 ma</td><td>0 ma</td><td>0 ma</td></tr>
<tr><td>TWT Body Current</td><td>5.8 ma</td><td>0 ma</td><td>0 ma</td></tr>
<tr><td>Ion Pump Current</td><td>0μA</td><td>0μA</td><td>0μA</td></tr>
<tr><td>HVPS Input Current</td><td>2.57 A</td><td>0.9 A</td><td>0.7 A</td></tr>
<tr><td>TWT Filament Current</td><td>1.53 A</td><td>1.53 A</td><td>1.53 A</td></tr>
<tr><td>SASS Input Current</td><td>9.2 A Peak</td><td>2.7 A</td><td>1.8 A</td></tr>
<tr><td>Transmit Power</td><td>100 Watts</td><td>0 Watts</td><td>0 Watts</td></tr>
</table>

Table 2. Significant Events.

Event	Day #	Date*	Time*	Rev #
Launch	178	June 27	1012:00	-
Deploy Ant. 1,3	178	June 27	0236:15	2
Deploy Ant. 2,4	178	June 27	0236:40	2
SASS Turn-On	187	July 6	1819:50	139
Start JASIN Ops	196	July 15	0301:44	259
Heater Ckt. Failure	205	July 24	1200:00	-
End Engn. Assess. Ops.	218	Aug. 6	0332:42	573
Cal Burn #1 Maneuver	227	Aug. 15	0741:08	705
OA #1 Maneuver	230	Aug. 18	0746:58	748
Cal Burn #2 Maneuver	235	Aug. 23	0920:36	820
Start JASIN Underflts.	235	Aug. 23	1313:00	823
OA #2 Maneuver	238	Aug. 26	0922:22	863
Sat. Power Problem	240	Aug. 28	0816:21	892
Stop JASIN Underflts.	247	Sept. 4	0844:00	992
Orbit Trim Maneuver	253	Sept. 10	0110:22	1073
Start GOASEX Underflts.	257	Sept. 14	1723:00	1140
Stop GOASEX Underflts.	273	Sept. 30	1432:00	1367
Sat. Failure	283	Oct. 10	0312:01	1503
SASS XMTR. Off	283	Oct. 10	0406:28	1503
Loss of Sat.	283	Oct. 10	0408:28	1503

*GMT

Table 3. Aircraft Underflights

Area	Date	Rev #	Antenna/Measurement Cells		Polarization	Wind Speed, kts
EAST COAST OF U.S.	8/23/78	823	1/5-7	2/7-12	V and H	10
JASIN ↓	8/25/78	848	4/1,2,4	3/1,2,4	V and H	>10
	8/29/78	905	4/4-8	3/3-7	V and H	7
		906	1/2-10	2/3-12	V and H	7
	9/4/78	991	4/3-11	3/2-9	V or H	8
		992	1/1-10	2/2-11	V or H	10-20
GOASEX ↓	9/14/78	1140	4/1-6,13,15	3/1-5,13,15	V and H	30-35
	9/17/78	1183	4/1-6,13,15	3/1-5,13,15	V and H	30
	9/19/78	1212	1/1-9,13,15	2/1-9,13,15	V and H	30
EAST COAST OF U.S.	9/28/78	1339	1/1-8,13,15	2/2-8,13,15	V and H	8-14
	9/30/78	1367	4/3-12	3/2-12	V and H	15-30

Table 4. Primary Data Sets for Engineering Assessment

DAY	REV	LOCATION	MODE	START*	STOP*
187	141	Land, Water	Turn-On	2148.00	2200:30
187	142	Gulf of Mexico	4	2323:00	2330:30
188	150	Land	4	1211:00	1217:30
191	187-189	NA	NA	0256:02	0555:34
195	251	FICO	1	1334:30	1339:00
201	331	FICO	6	0425:00	0429:30
206	400	South Atlantic	2	0005:00	0009:30
208	430	Water	3	0226:00	0234:00
208	432	Gulf of Alaska	5	0538:00	0542:30
210	461	Gulf of Alaska	7	0615:30	0620:00
211	475	Gulf of Alaska	8	0545:30	0550:00
218	572, 573	Water	9, 10	0125:00	0134:30

*GMT in hours, mins.:secs.

Table 5. Hardware Validation Tests

TEST #	DESCRIPTION	MODES	WINDS	CELLS	PURPOSE
1	Engn. & Status Using C-TABs & SPSs	1-10	Any	NA	Complete Functional Validation
2	S+N and N ONLY Stats.	10	Any	1-15	Receiver Stability
3	N ONLY Stats.	1,3,4	Any	1,12,15	RFI
4	High Cal Stats.	9	Any	NA	Cal Stability
5	Cal Y-Factor	1-10	Any	1	Noise Figures
6	HH & VV S+N @ Nadir	3,4	Any	15	Antenna Gain
7	S+N @ 8°	Any	Low & High	13	Transmitter Stability

Table 6. Key parameter matrix

PARAMETER	DESIGN	SASS SYSTEM	SAT. SYSTEM	IN ORBIT	
ELECTRICAL					
TRANSMIT POWER	110 $^{+23}_{-23}$ WATTS PEAK	99 WATTS	100 WATTS	99 ± 1 WATTS	
TWT CATH. VOLT.	-8.0 ± 0.5 kV	-8.02 kV	-8.02 kV	-8.02 kV	
TWT CATH. CURR.	58 mA NOMINAL	57 mA	57 mA	55.5 mA	
TWT BODY CURR.	6 ± 3 mA	5.7 mA	5.8 mA	5.7 mA	
ION PUMP CURR.	< 5 μA	0 μA	0 μA	0 μA	
HVPS INPUT CURR.	< 3.54 A	2.48 A	2.57 A	2.3 A	
TWT FILAMENT CURR.	1.55 A NOMINAL	1.53 A	1.53 A	1.50 A	
LO POWER	> + 10 dBm	13.8/12.2 dBm	13.6/12.0 dBm	13.3/11.4 dBm	
MODULATOR POWER	> + 20 dBm	21.3 dBm	21.1 dBm	21.1 dBm	
TRANS. CHAN. POWER	> + 16 dBm	16.7 dBm	16.4 dBm	17.0 dBm	
UPCONV. BIAS	NA	.104 vdc	.105 vdc	.10 vdc	
TDA STAGE 1 BIAS	NA	.135 vdc	.135 vdc	.14 vdc	
TDA STAGE 2 BIAS	NA	.158 vdc	.160 vdc	.16 vdc	
TDA STAGE 3 BIAS	NA	.167 vdc	.170 vdc	.17 vdc	
DC/DC CONV. VOLT., +5	+5 ± 7% vdc	5.17 vdc	5.11 vdc	5.08 vdc	
DC/DC CONV. VOLT., +15	+15 ± 1% vdc	15.02 vdc	15.05 vdc	14.97 vdc	
DC/DC CONV. VOLT., -15	-15 ± 1% vdc	-15.09 vdc	-15.09 vdc	-15.03 vdc	
DC/DC CONV. VOLT., -6	-6 ± 1 % vdc	-6.05 vdc	-6.04 vdc	-6.04 vdc	
DC/DC CONV. VOLT., +6	+6 ± 1% vdc	5.98 vdc	5.96 vdc	5.96 vdc	
THERMISTOR REF. NO. 1	+5 ± 7% vdc	5.10 vdc	5.10 vdc	5.10 vdc	
THERMISTOR REF. NO. 2	+5 ± 7% vdc	5.09 vdc	5.11 vdc	5.10 vdc	
REG. BUS VOLTAGE	28 ± .28 v	NA	28.1 v	28.1 vdc	
TOTAL INPUT CURR.	< 10 A	NA	8.96 A PEAK	< 9.0 A PEAK	
UNREG. BUS VOLTAGE	28 ± 4 v	NA	27.50 v	27.5-30 vdc	
RECEIVER NF	5.6 dB NOMINAL	5.61 dB	5.70 dB	5.2 dB	
THERMAL				MIN	MAX
BASEPLATE T1	0 - 36.5°C	28.6°C	33.3°C	-4.1	19.1°C
BASEPLATE T2	0 - 37.1°C	27.9°C	31.9°C	-4.1	19.2°C
BASEPLATE T3	0 - 37.1°C	25.4°C	32.7°C	-4.1	18.9°C
BASEPLATE T4	0 - 37.0°C	27.5°C	33.9°C	-0.8	21.6°C
BASEPLATE T5	0 - 37.7°C	27.0°C	32.1°C	-4.6	18.7°C
BASEPLATE T6	0 - 37.6°C	29.0°C	33.9°C	-3.7	18.5°C

PARAMETER	DESIGN	SASS SYSTEM	SAT. SYSTEM	IN ORBIT	
THERMAL CONTD.				MIN	MAX
TWT NO. 1	0 - 48.0°C	28.0°C	32.6°C	-3.1	19.7°C
TWT NO. 2		26.2°C	32.7°C	-1.3	21.3°C
TWT NO. 3		26.2°C	33.3°C	1.5	23.4°C
OUTPUT ISO		25.4°C	32.9°C	-2.8	19.5°C
HVPS		26.8°C	34.2°C	-2.5	21.2°C
ASM		26.2°C	30.7°C	-8.5	13.8°C
SSS/LO		30.8°C	32.9°C	-4.4	18.4°C
UPCONV.		26.5°C	33.0°C	-4.2	18.2°C
A/D CONV.		40.7°C	42.8°C	12.1	32.8°C
NOISE SOURCE		24.7°C	32.0°C	-7.3	14.4°C
DIR. DET.		27.1°C	31.7°C	-5.2	17.3°C
1st MIXER		29.5°C	34.7°C	-2.2	20.4°C
2nd MIXER		34.8°C	39.6°C	9.3	31.2°C
TDA		35.3°C	36.3°C	31.8	35.7°C
CRYS. FIL. P6		35.4°C	40.7°C	13.7	34.5°C
CRYS. FIL. P1		37.7°C	42.3°C	18.1	38.6°C
CRYS. FIL. P10		37.4°C	42.8°C	19.2	38.4°C
CRYS. FIL. P12		37.3°C	42.2°C	16.9	37.3°C
ANT. 1 TEMP. 1	-67 - +55°C	NA	NA	-78.8	-21.1°C
ANT. 1 TEMP. 2					
ANT. 1 TEMP. 3					
ANT. 1 TEMP. 4					
ANT. 1 TEMP. 5					
ANT. 1 TEMP. 6					
ANT. 1 TEMP. 7					
ANT. 1 TEMP. 8					
ANT. 1 TEMP. 9					
ANT. 1 TEMP. 10					
ANT. 2 TEMP. 1				-74.3	-18.2
ANT. 2 TEMP. 2					
ANT. 2 TEMP. 3					
ANT. 2 TEMP. 4					
ANT. 2 TEMP. 5					
ANT. 2 TEMP. 6					
ANT. 2 TEMP. 7					
ANT. 2 TEMP. 8					
ANT. 2 TEMP. 9					
ANT. 2 TEMP. 10					

PARAMETER	DESIGN	SASS SYSTEM	SAT. SYSTEM	IN ORBIT	
THERMAL CONTD.				MIN	MAX
ANT. 3 TEMP. 1	-67 - +55^{0}C	NA	NA	-80.7	-49.1^{0}C
ANT. 3 TEMP. 2					
ANT. 3 TEMP. 3					
ANT. 3 TEMP. 4					
ANT. 3 TEMP. 5					
ANT. 3 TEMP. 6					
ANT. 3 TEMP. 7					
ANT. 3 TEMP. 8					
ANT. 3 TEMP. 9					
ANT. 3 TEMP. 10					
ANT. 4 TEMP. 1				-82.5	-49.9^{0}C
ANT. 4 TEMP. 2					
ANT. 4 TEMP. 3					
ANT. 4 TEMP. 4					
ANT. 4 TEMP. 5					
ANT. 4 TEMP. 6					
ANT. 4 TEMP. 7					
ANT. 4 TEMP. 8					
ANT. 4 TEMP. 9					
ANT. 4 TEMP. 10					
MOUNT SUR. T1	32 - 95^0 F	32 - 95^{0}F	89.7^{0}F	NA	
MOUNT SUR. T2	32 - 95^{0}F	32 - 95^{0}F	93.1^{0}F	NA	

Table 7. Receiver stability

$$\frac{\sigma_V}{\mu_V} = \frac{1}{\sqrt{BT}} \quad , \%$$

CHANNEL	σ_V/μ_V (S +N)		σ_V/μ_V (N ONLY)	
	COMPUTED	MEASURED	COMPUTED	MEASURED
1	0.99	1.02	0.87	0.83
2	1.02	0.83	0.92	0.81
3	1.07	1.16	0.99	1.25
4	1.11	0.99	1.04	0.91
5	1.21	1.10	1.16	1.03
6	1.29	1.33	1.28	1.02
7	1.40	1.46	1.44	1.65
8	1.48	1.36	1.59	1.33
9	1.59	1.45	1.79	1.54
10	1.65	1.36	1.98	2.21
11	1.80	1.25	2.15	2.23
12	1.95	1.60	2.32	2.09
13	1.01	0.91	0.86	0.53
14	1.02	0.97	0.86	0.80
15	1.02	0.81	0.86	0.81

DATA TAKEN FROM MODE 10 ON DAY 218
20 DATA POINTS AVERAGED

Table 8. Channel 1 Noise Figure

DAY	MODE	TDA TEMPERATURE, °C	NOISE FIGURE*, dB
195	1	35.7	5.3
206	2	30.3	5.2
208	3	35.2	5.0
188	4	35.6	5.4
208	5	35.4	5.0
201	6	35.8	5.3
210	7	34.1	5.1
211	8	34.8	5.0
218	9	35.5	5.1 **
218	10	35.5	5.1

* USING V_{S+N} VOLTAGE AND AVERAGING VALUES FOR BOTH HIGH AND LOW FREQUENCY L.O.'s FREQUENCY

** AVERAGED OVER 4 MINUTES OF DATA (64 POINTS)

Table 9. Short term calibration stability

$$\frac{\sigma_{v_N}}{\mu_{v_N}} = \frac{1}{\sqrt{BT_N}} \quad , \%$$

COMPUTED	MEASURED			
	LOW CAL LOW FREQ	HIGH CAL LOW FREQ	LOW CAL HIGH FREQ	HIGH CAL HIGH FREQ
0.87	0.84	1.07	0.80	0.94

DATA TAKEN IN MODE 9 ON DAY 218

32 DATA POINTS AVERAGED

Table 10. Receiver noise level stability test for RFI

$$\frac{\sigma_{v_N}}{\mu_{v_N}^{*}} = \frac{1}{\sqrt{BT_N}}, \%$$

		CHANNEL 1	CHANNEL 12	CHANNEL 15
COMPUTED		0.87	2.32	0.86
MEASURED	ANT 1V	1.12	2.99	1.40
	ANT 2V	0.83	2.30	0.97
	ANT 3V	0.76	1.66	0.65
	ANT 4V	1.00	2.54	0.72
	ANT 1H	0.97	2.04	1.12
	ANT 2H	0.78	1.53	0.86
	ANT 3H	0.81	1.71	0.93
	ANT 4H	1.08	1.93	1.04

* 20 DATA POINTS AVERAGED

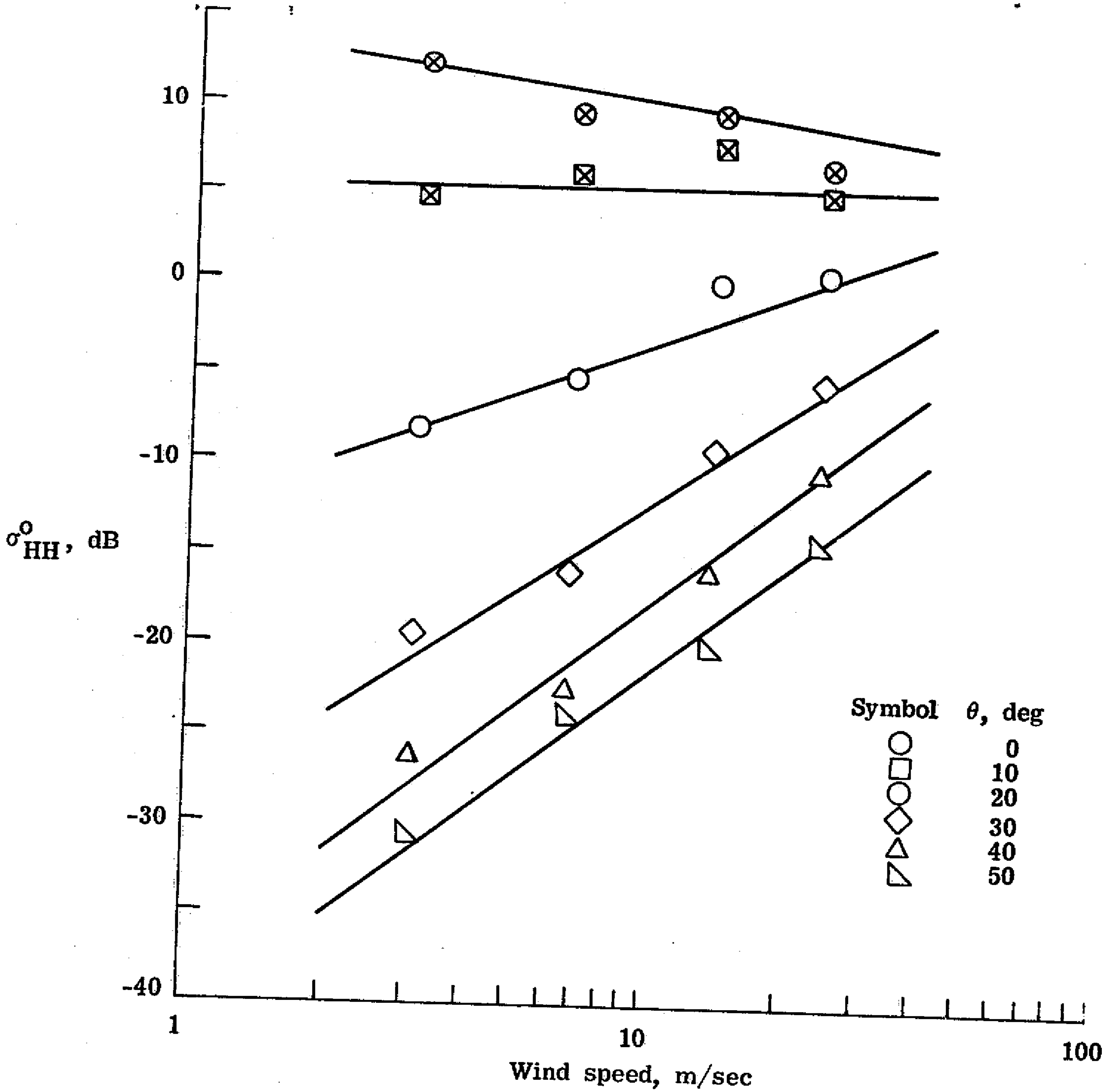

Figure 1.- Aircraft scatterometer data, downwind.

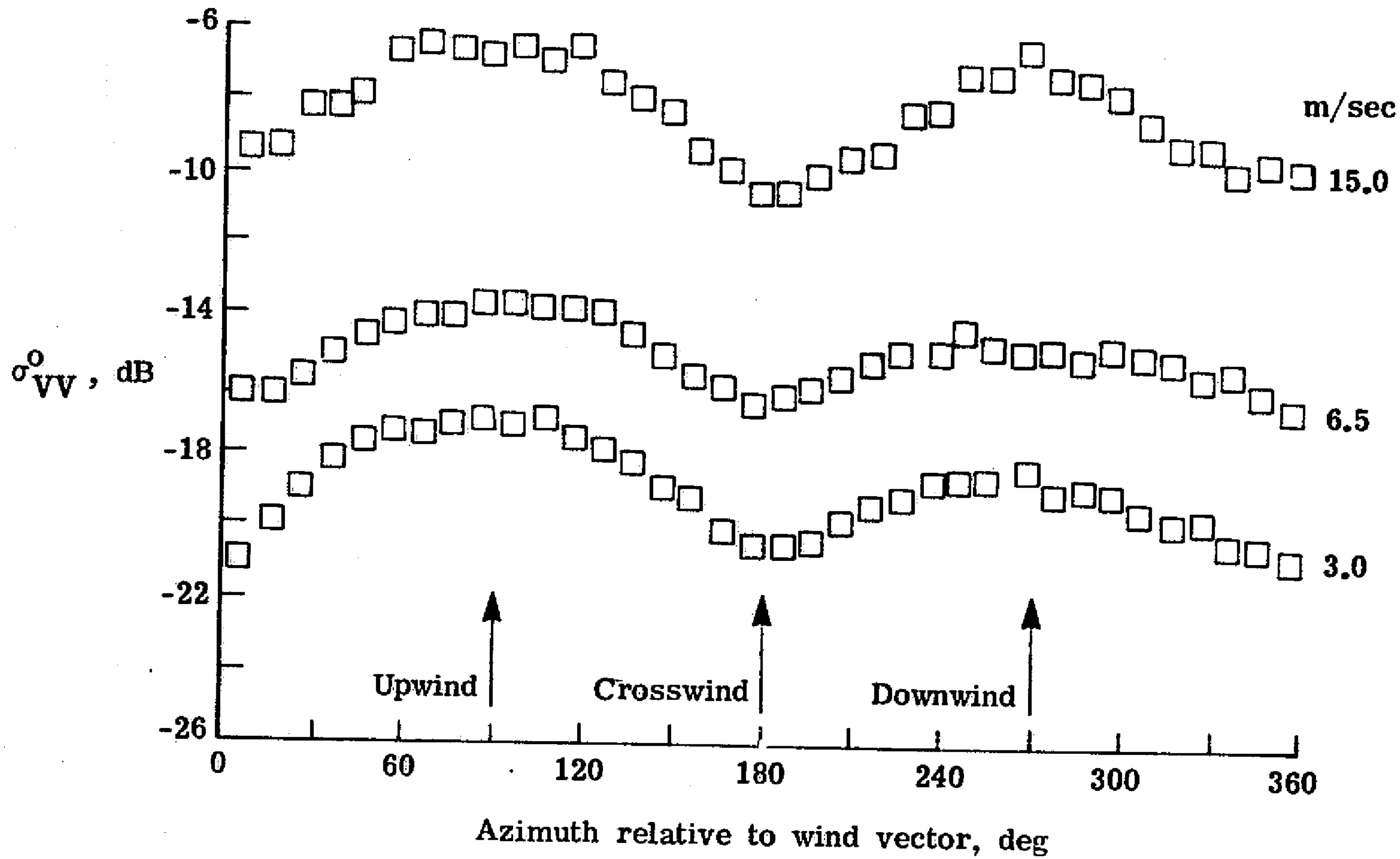

Figure 2.- Aircraft scatterometer circle data.

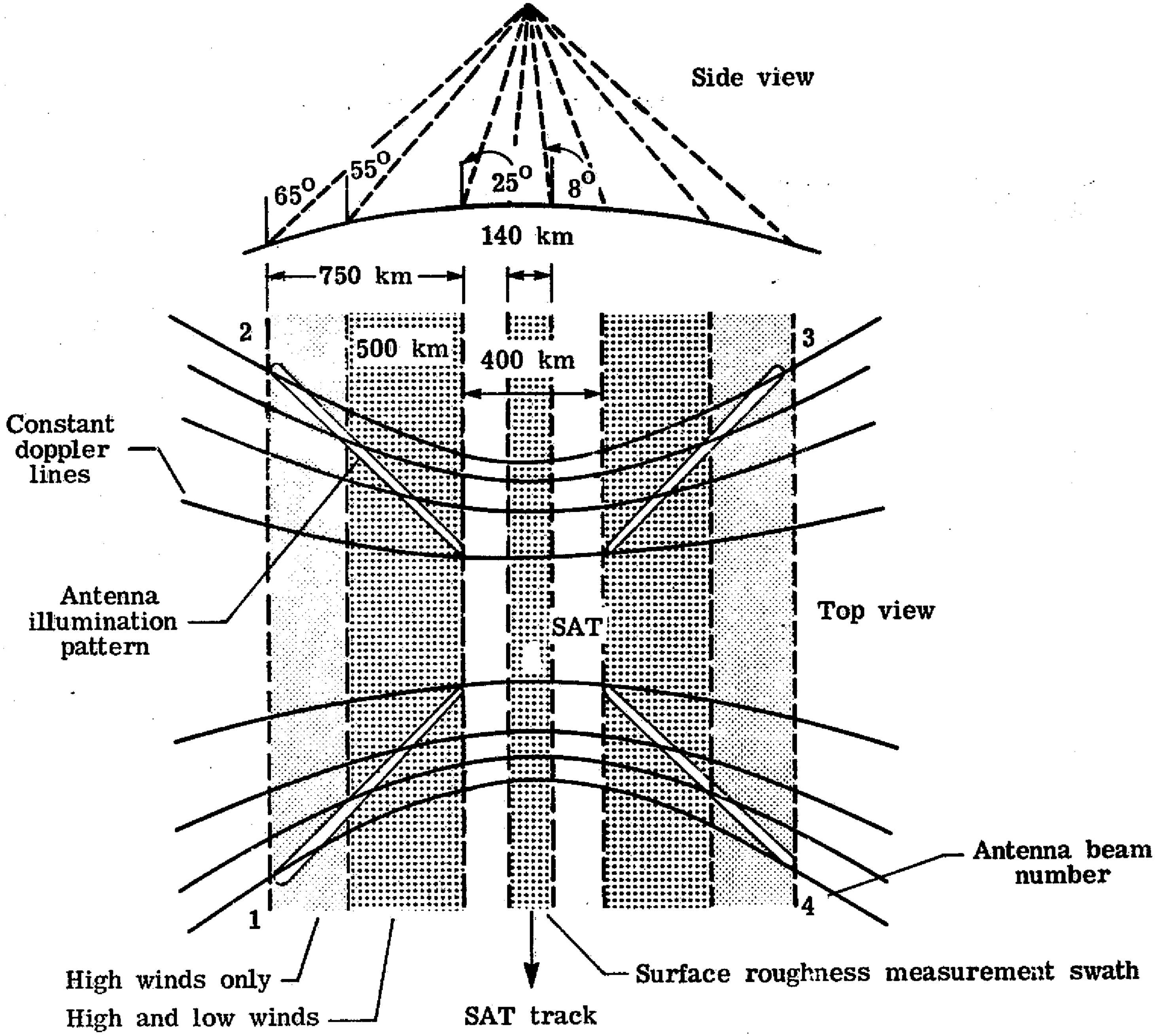

Figure 3.- SeaSat scatterometer measurement characteristics.

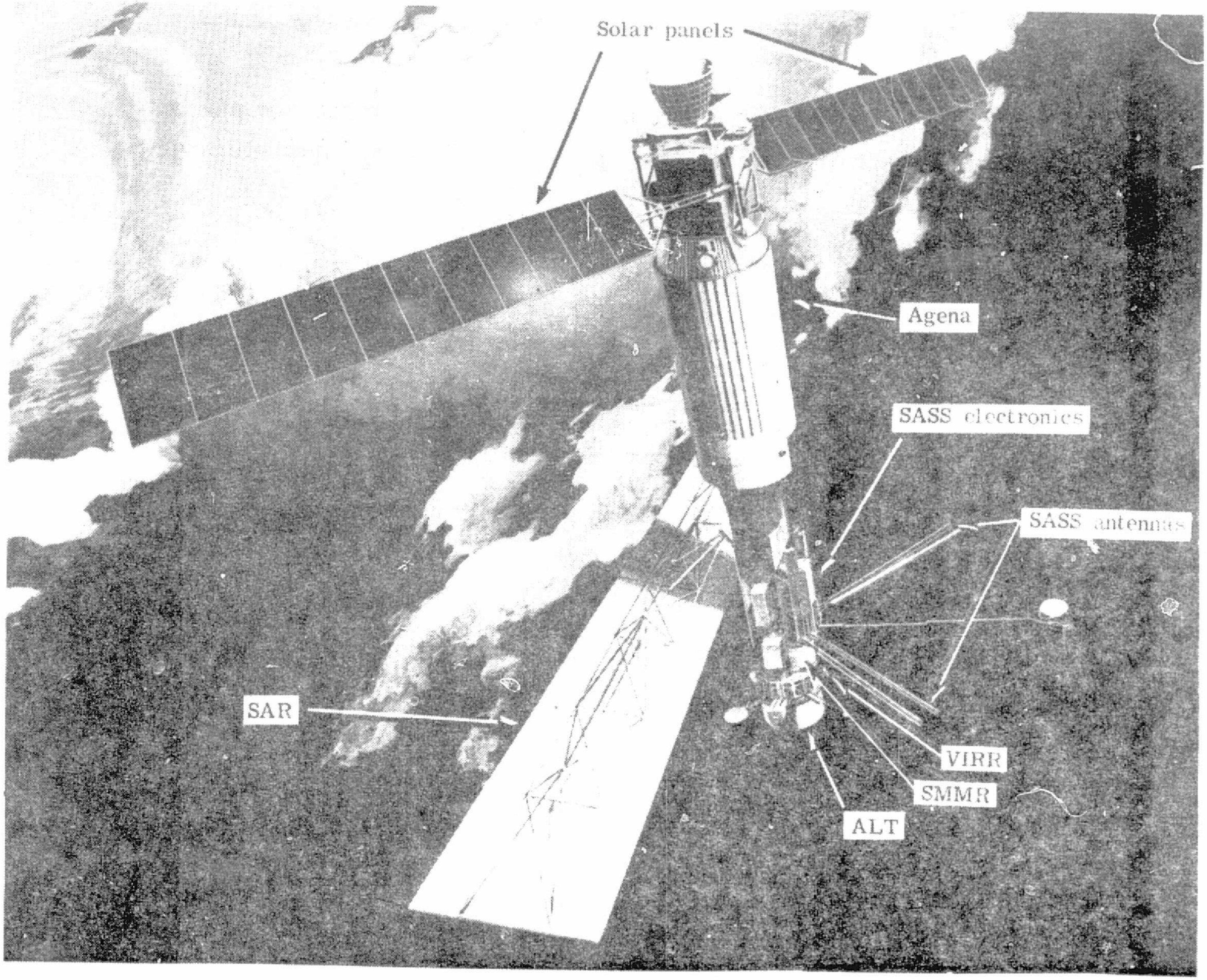

Figure 4.- SeaSat-A satellite.

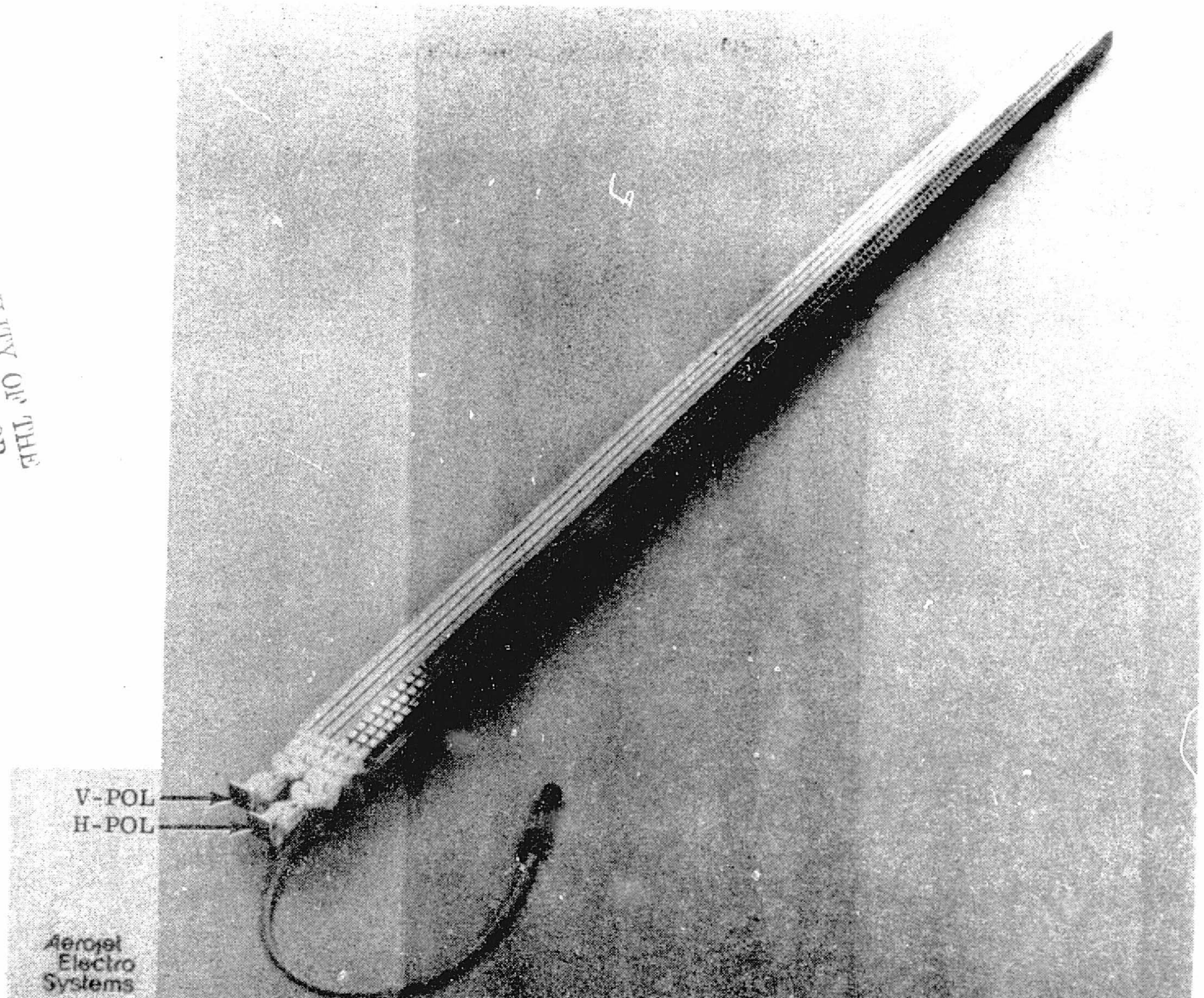

Figure 5.- SASS antenna assembly.

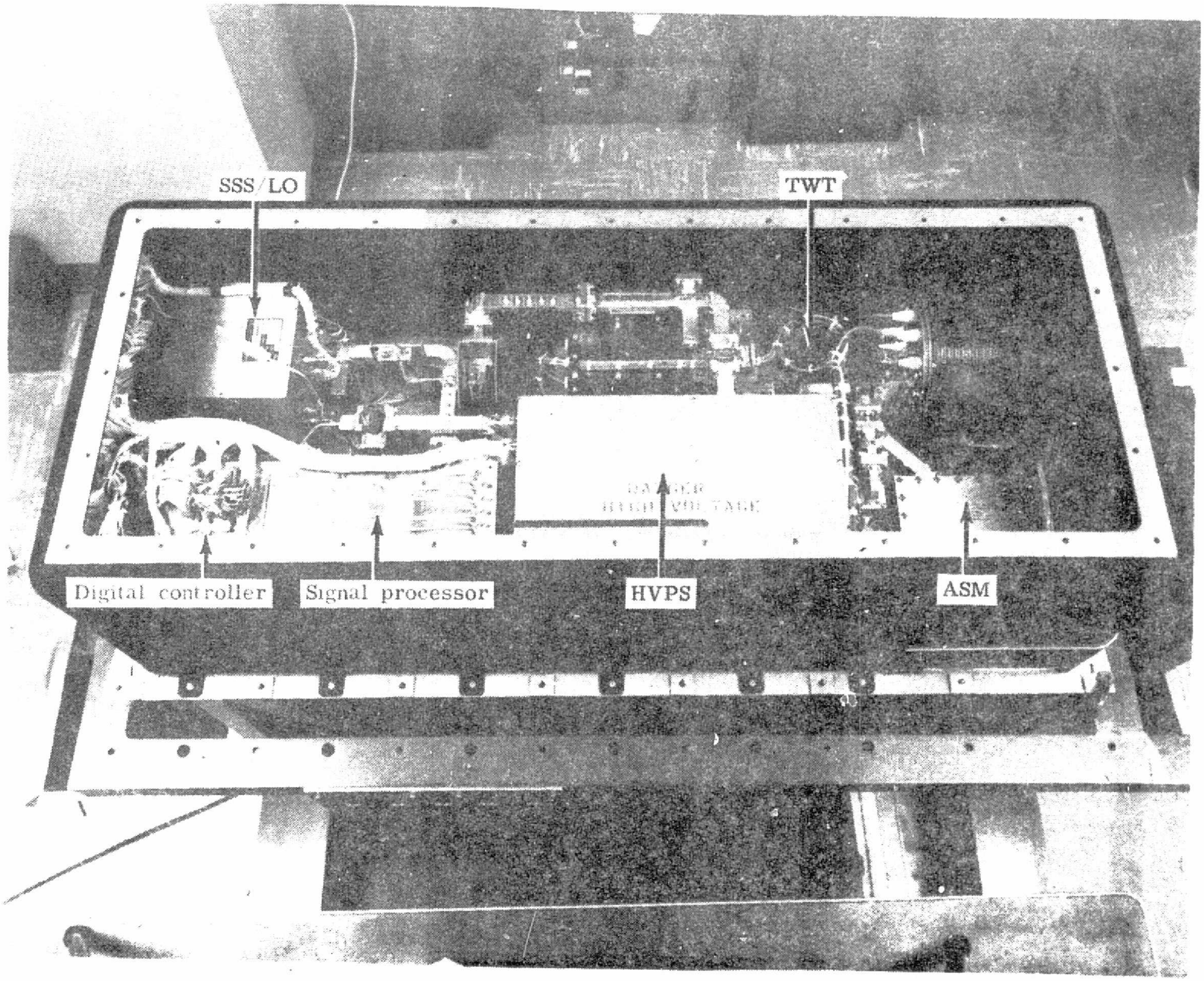

Figure 6.- Scatterometer electronics package.

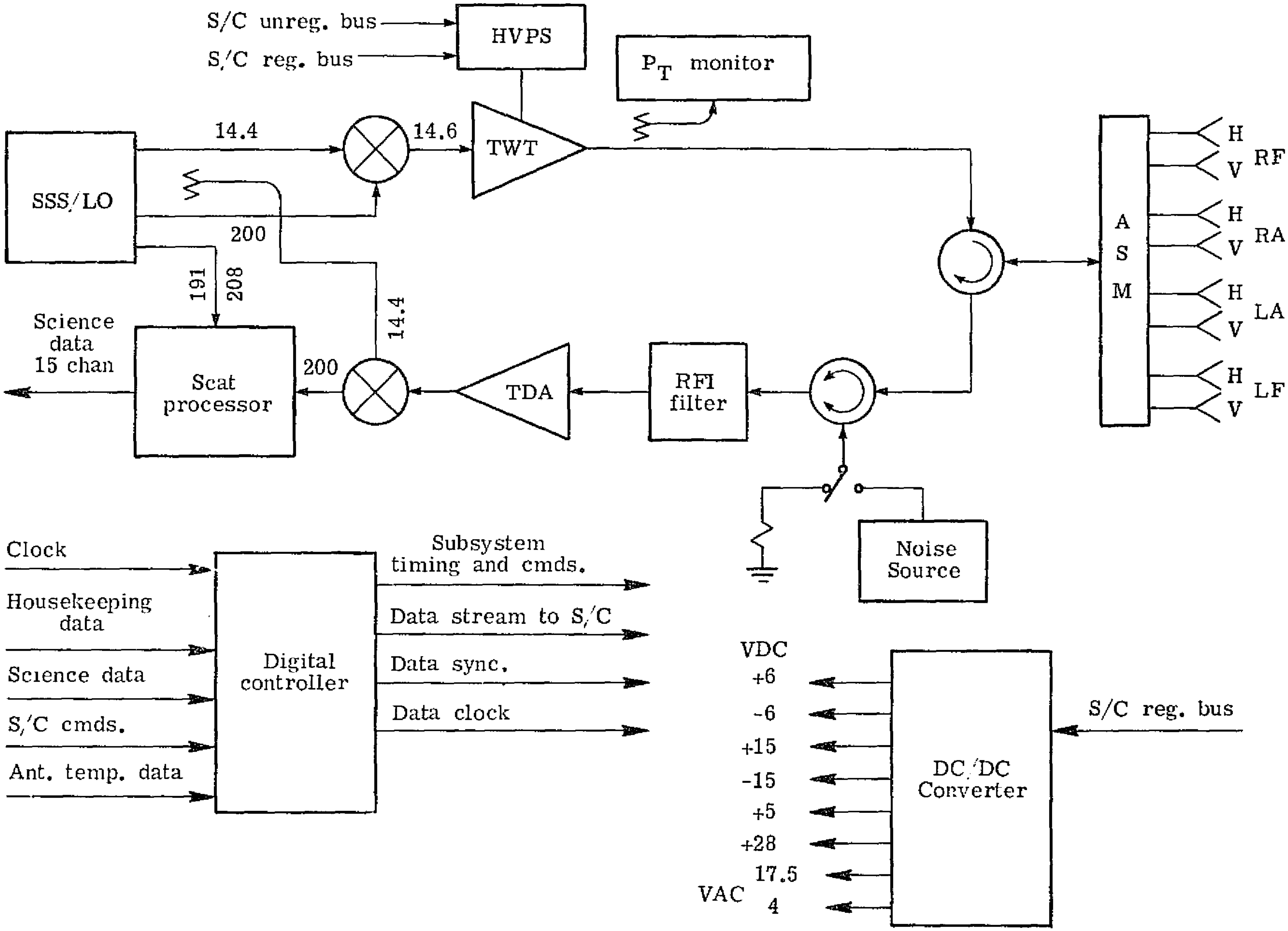

Figure 7.- SASS electronics block diagram

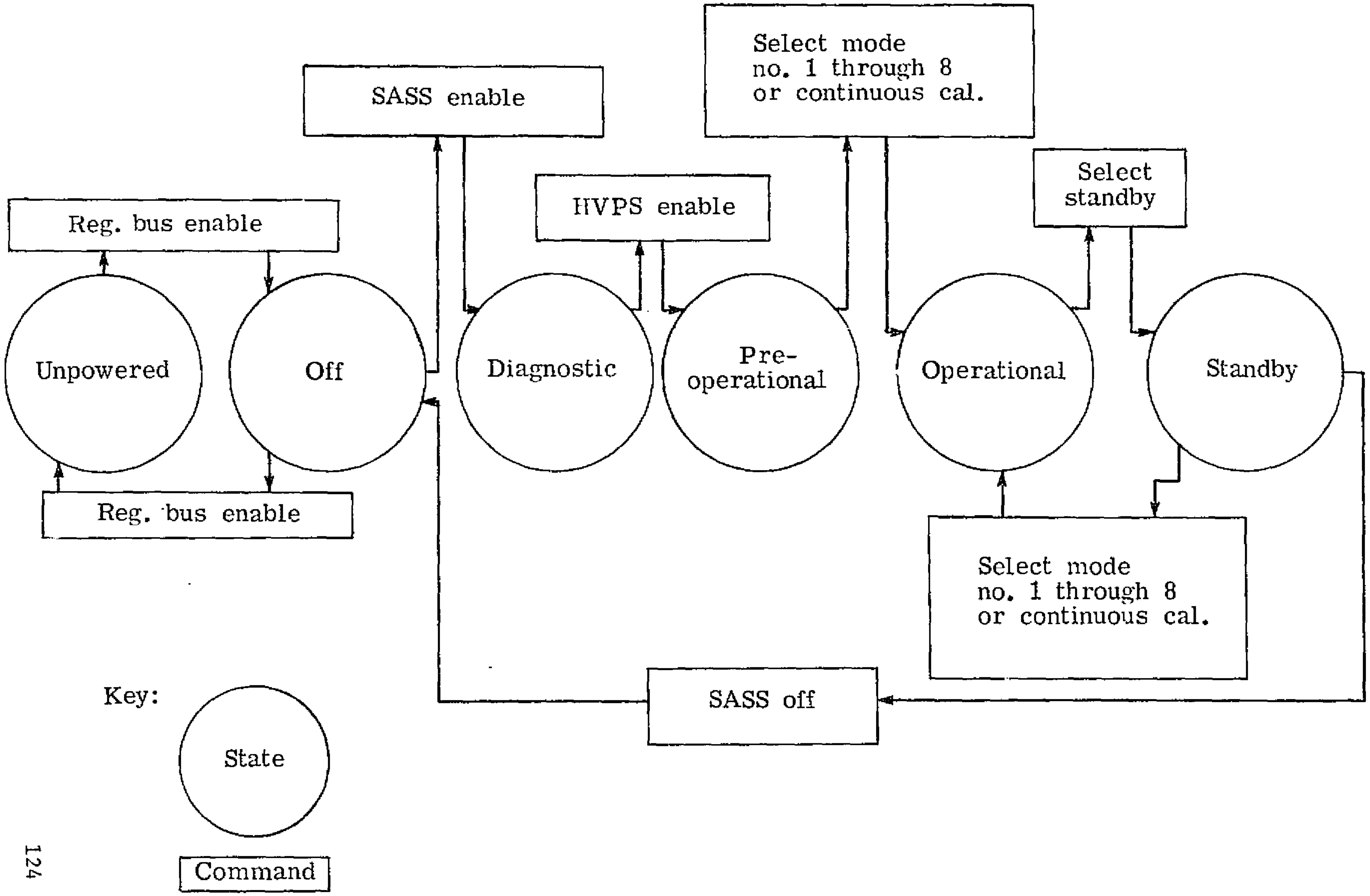

Figure 8.- Command sequence diagram.

Mode	Antenna Sequence*
1	4V, 1V, 3V, 2V
2	4H, 1H, 3H, 2H
3	4V, 4H, 3V, 3H
4	1V, 1H, 2V, 2H
5	4V, 4V, 3V, 3V
6	1V, 1V, 2V, 2V
7	4H, 4H, 3H, 3H
8	1H, 1H, 2H, 2H
9	CONTINUOUS CALIBRATE
10	STANDBY

$\triangleq$ Transmit vertical
Receive vertical

$\triangleq$ Transmit horizontal
Receive horizontal

Antenna numbering convention

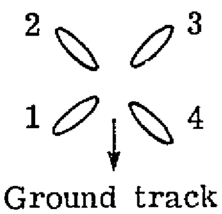

Figure 9.- SASS operating modes.

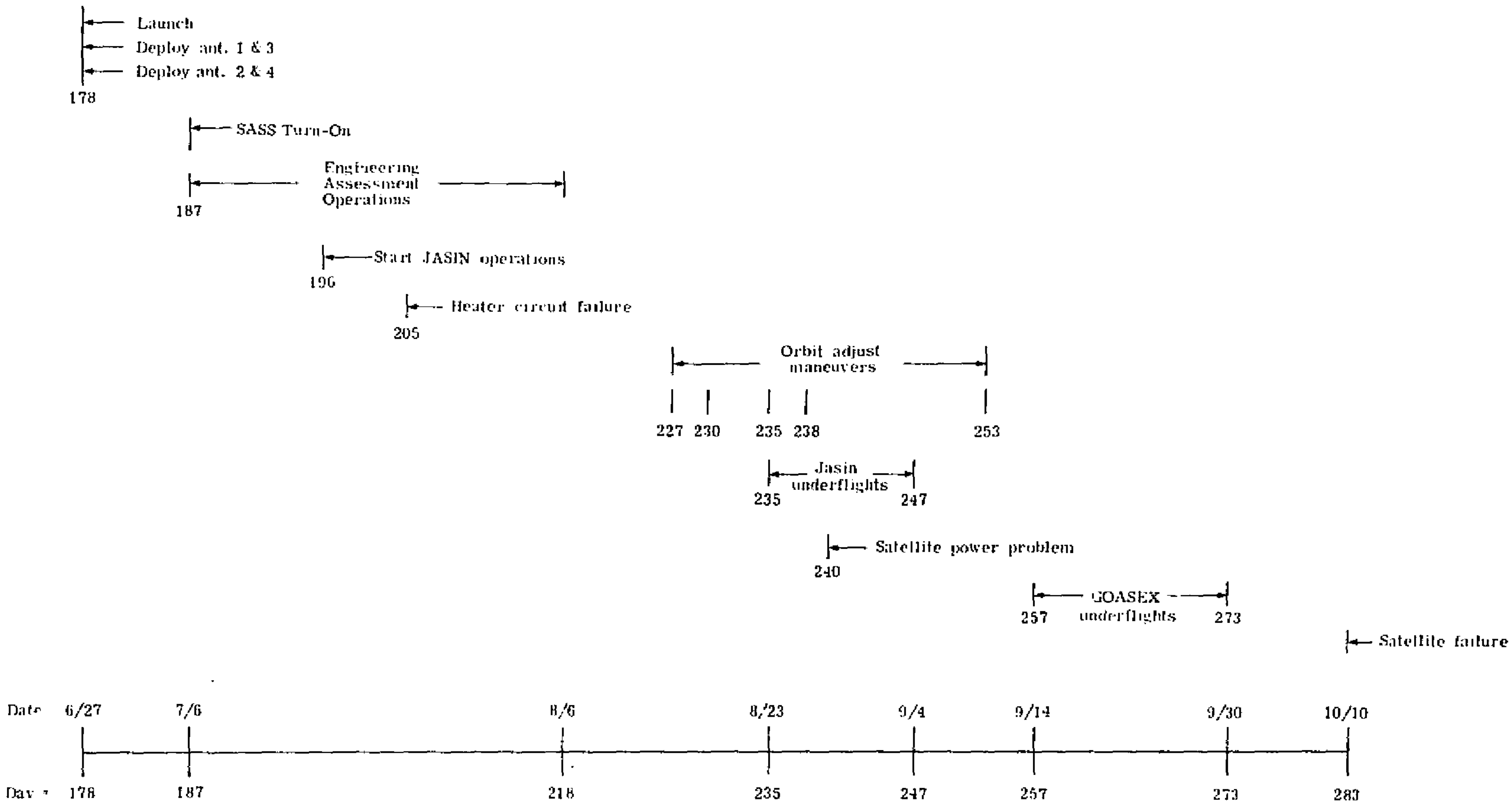

Figure 10.- Significant event flow chart.

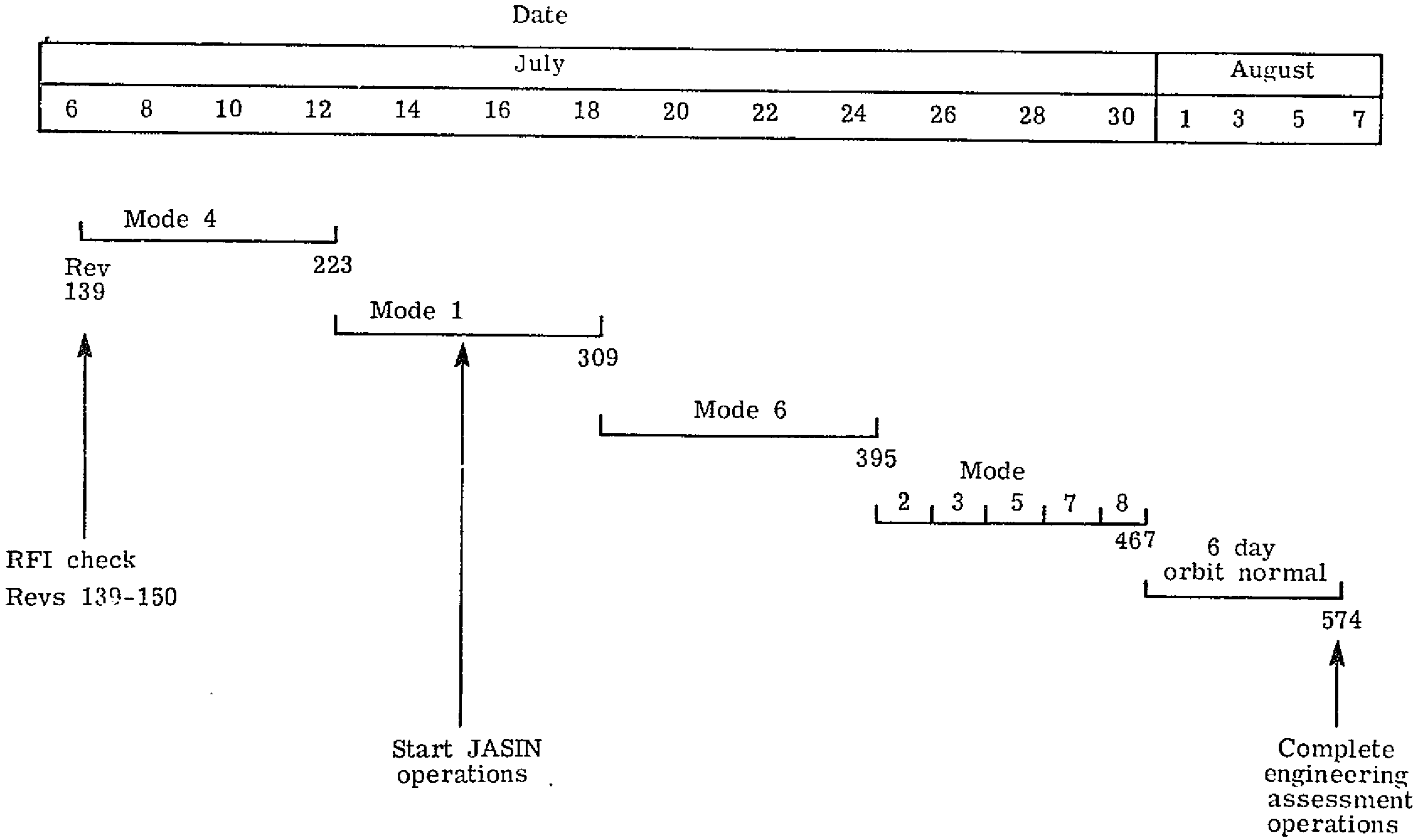

Figure 11.- Engineering assessment operations.

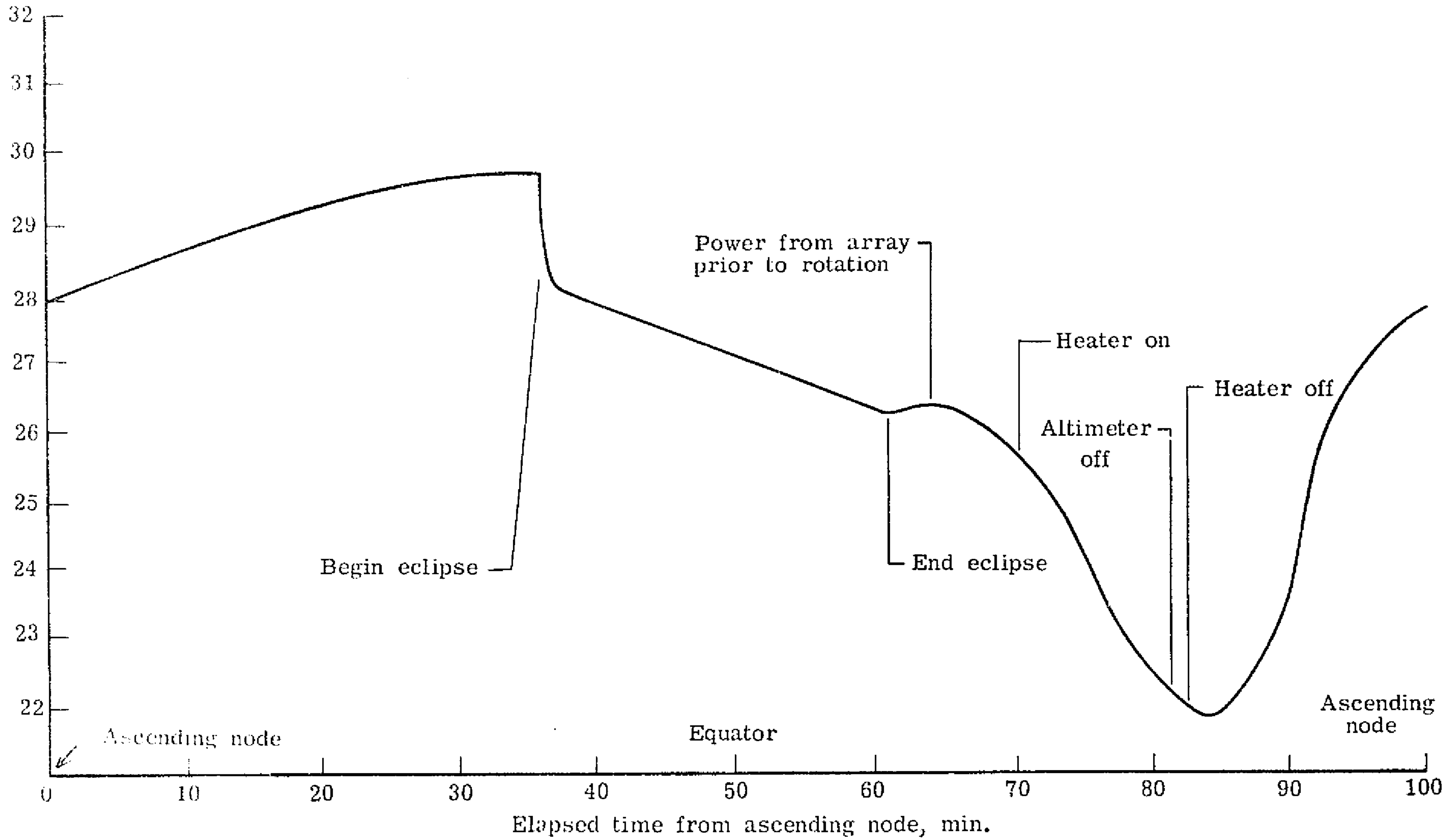

Figure 12.- Unregulated bus voltage on Rev 891.

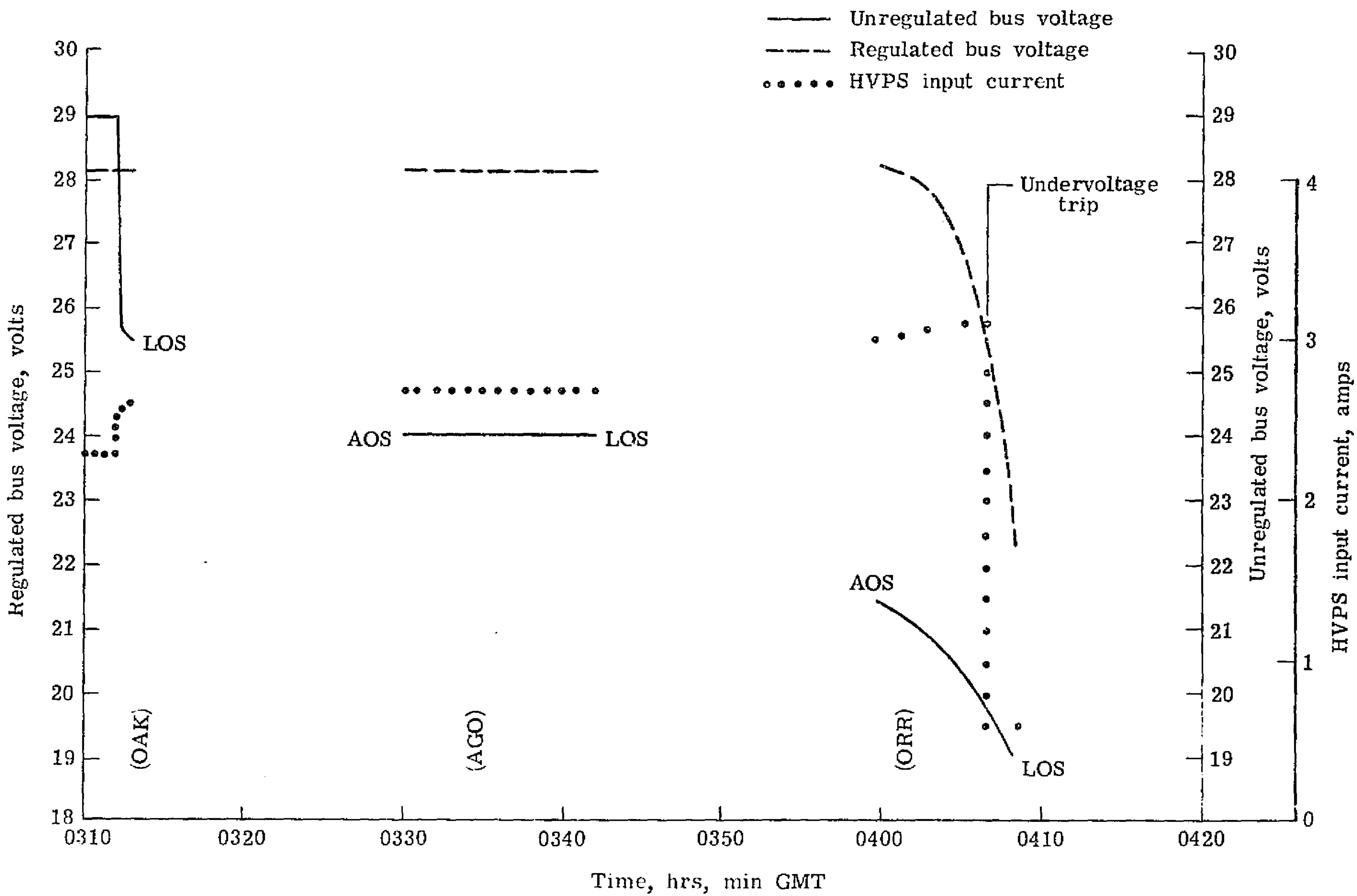

Figure 13.- SASS power parameters during failure

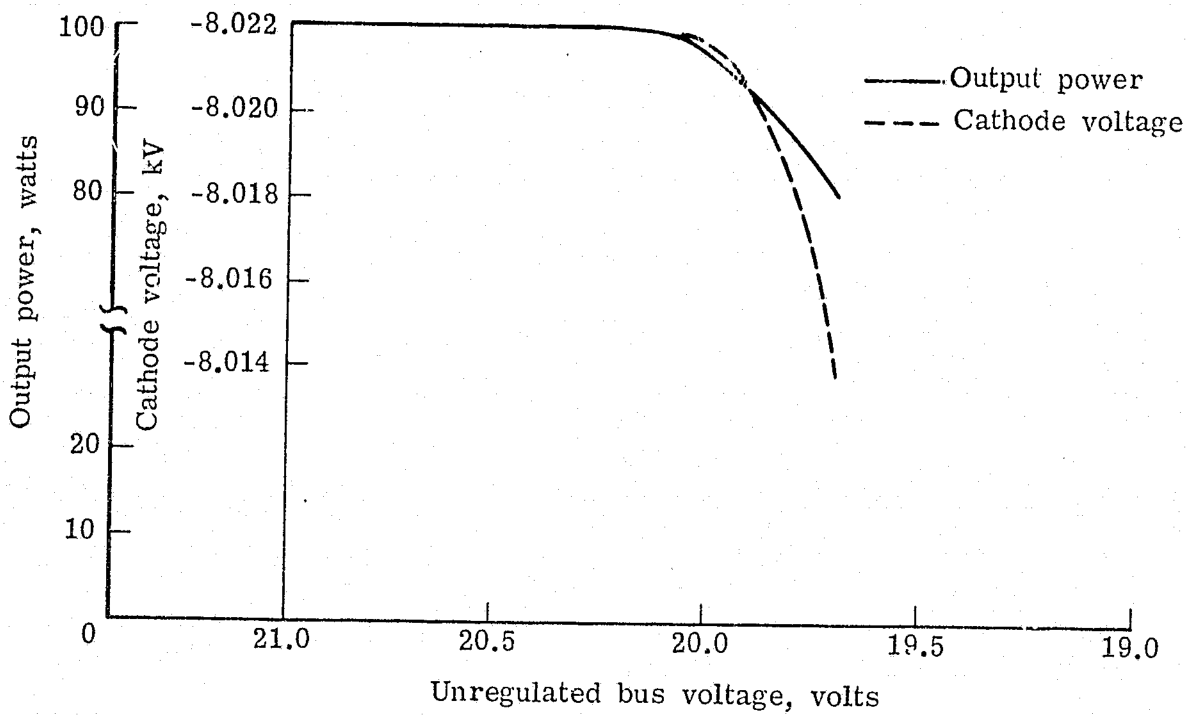

Figure 14.- Cathode voltage deregulation and output power drop during failure.

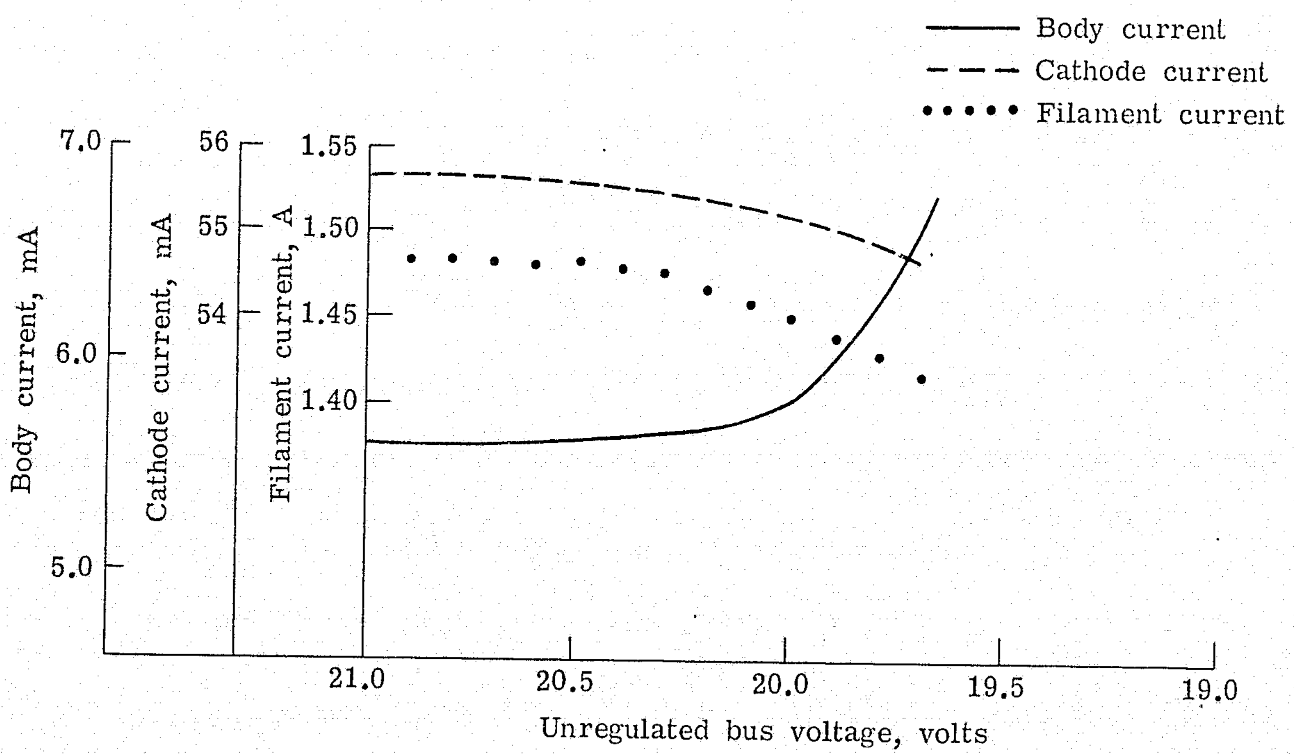

Figure 15.- Behavior of TWT currents during failure.

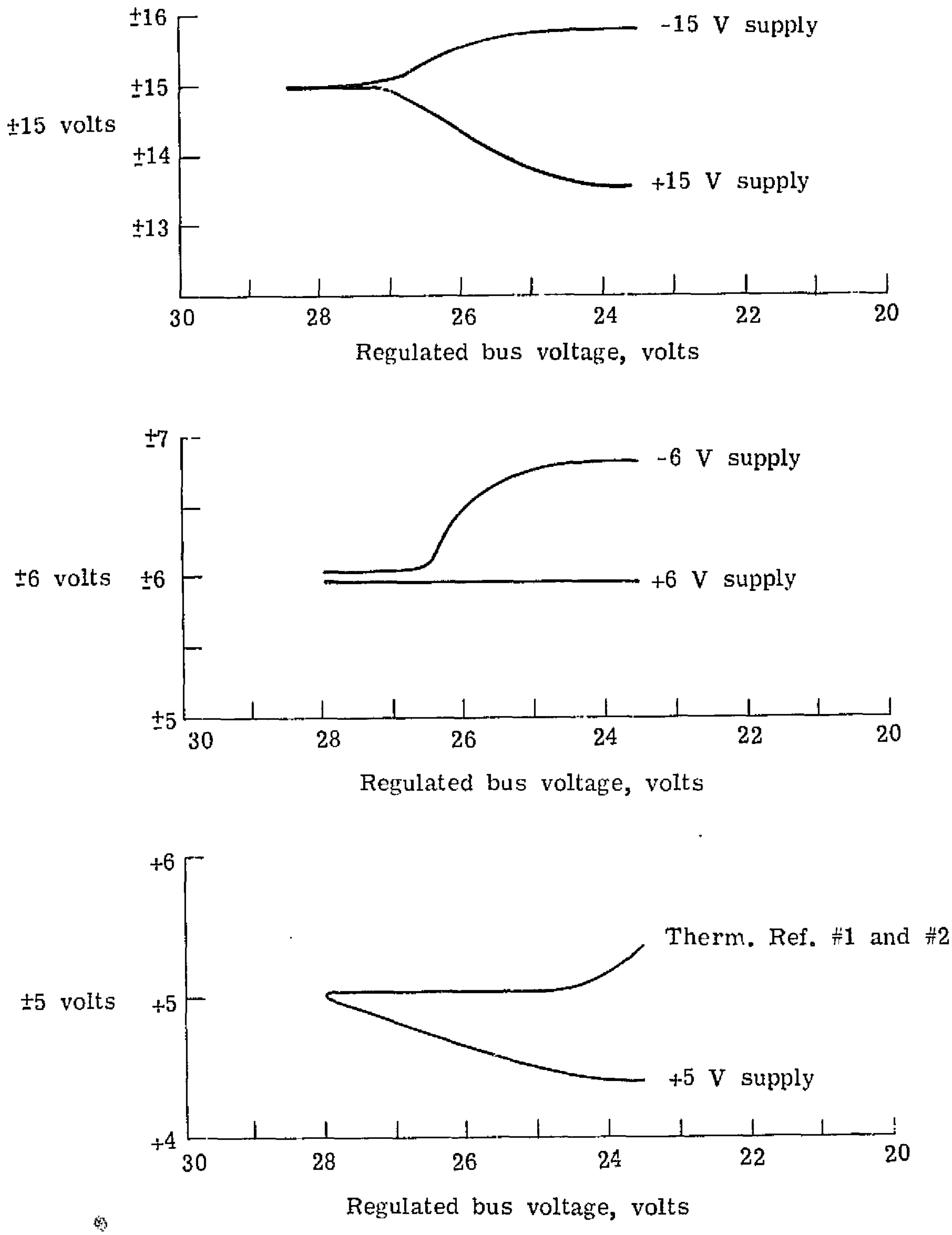

Figure 16.- SASS low voltage power supply behavior during failure.

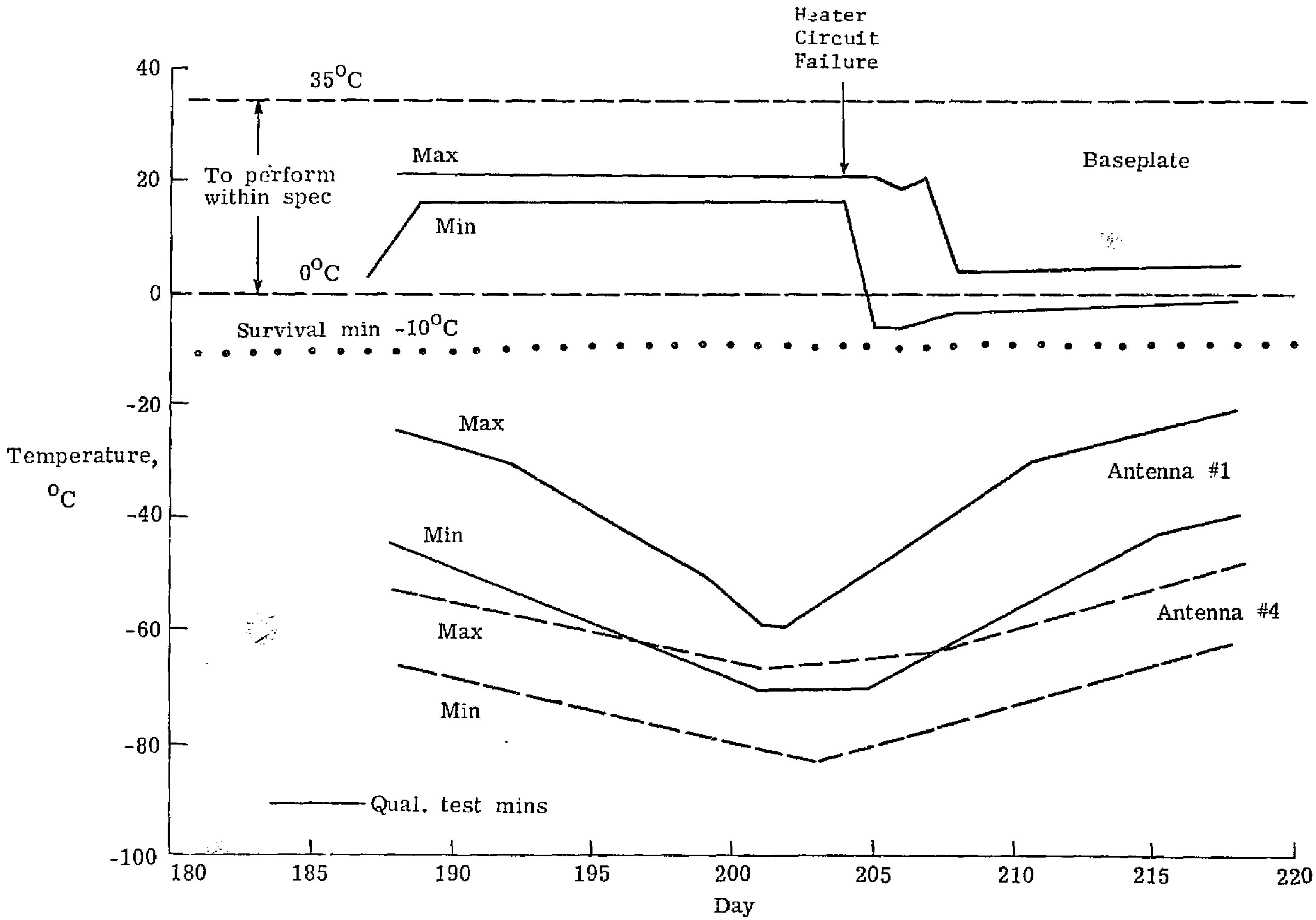

Figure 17.- Electronics baseplate and antenna temperature histories.

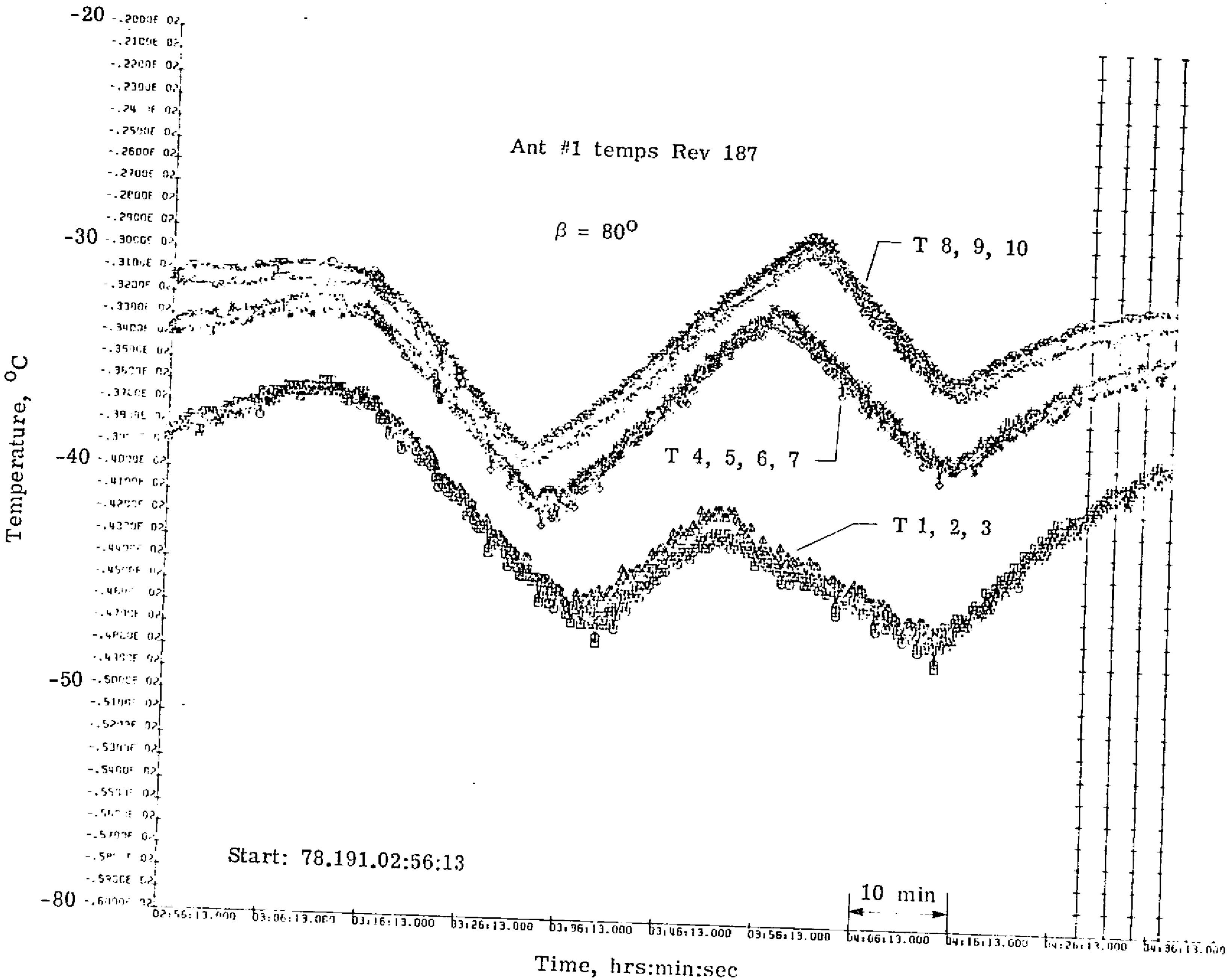

Figure 18.- Antenna assembly 1 temperatures for Rev 187.

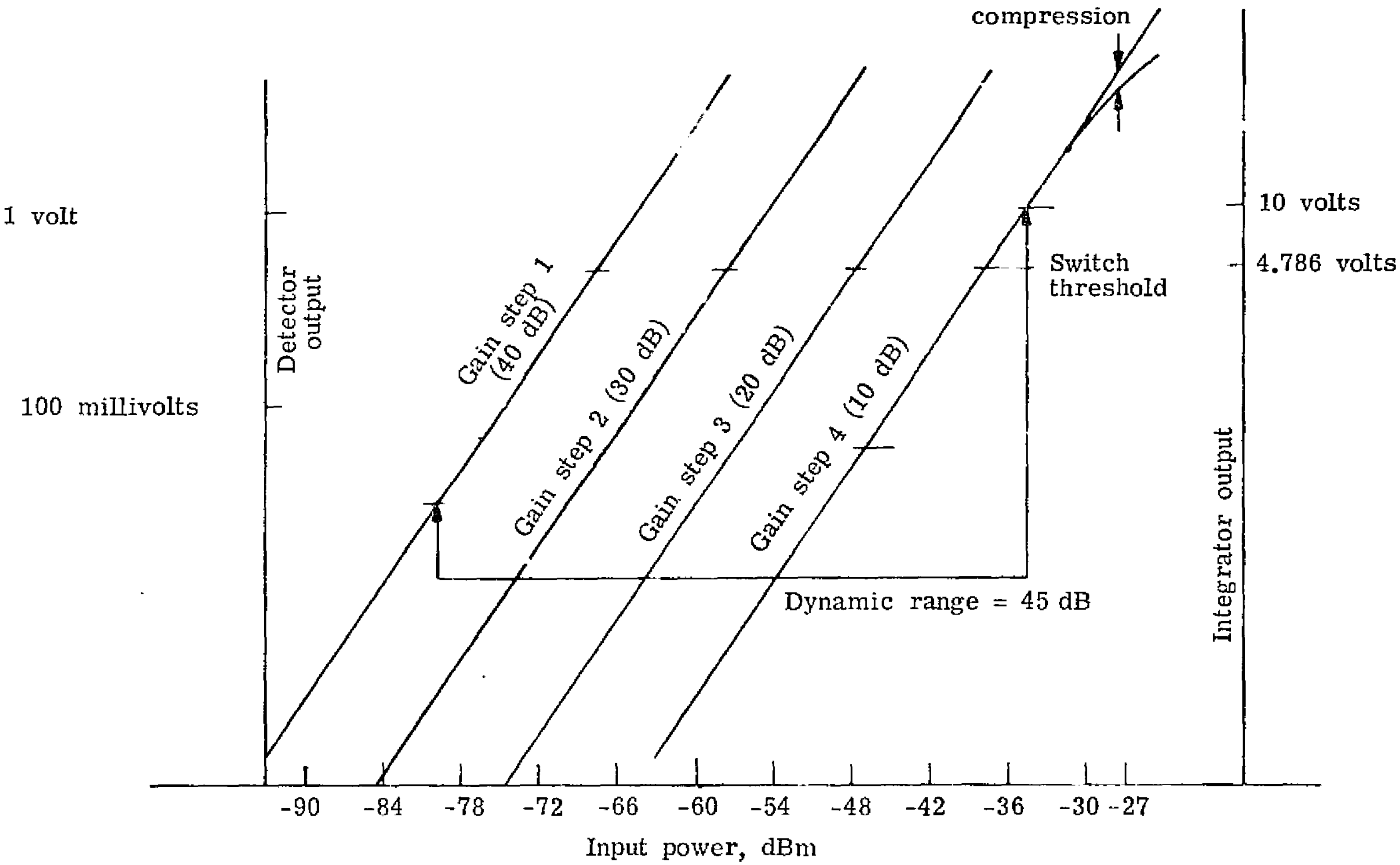

Figure 19.- Receiver gain characteristics.

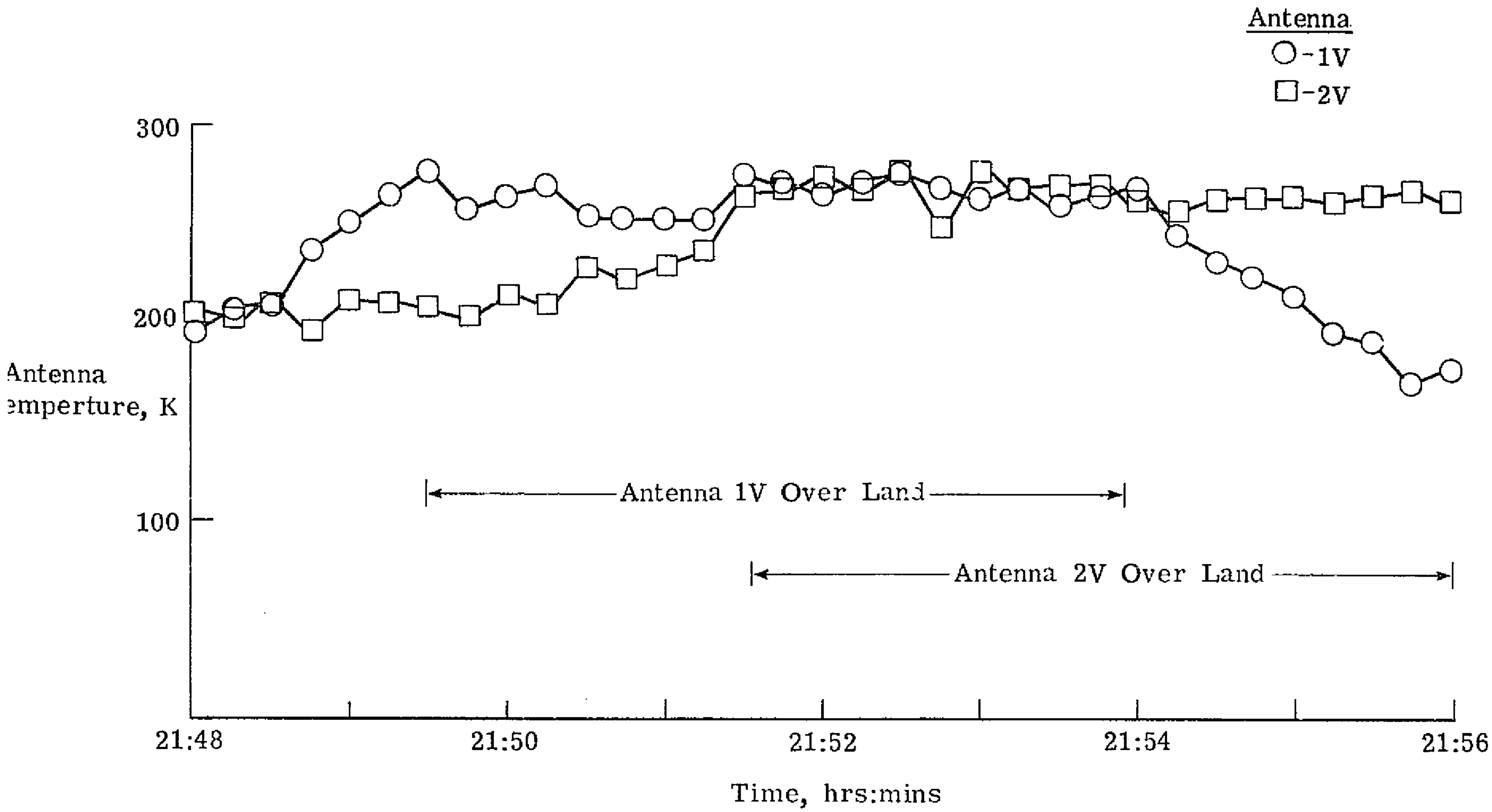

Figure 20.- Typical land/water antenna temperature profiles. Rev 141.

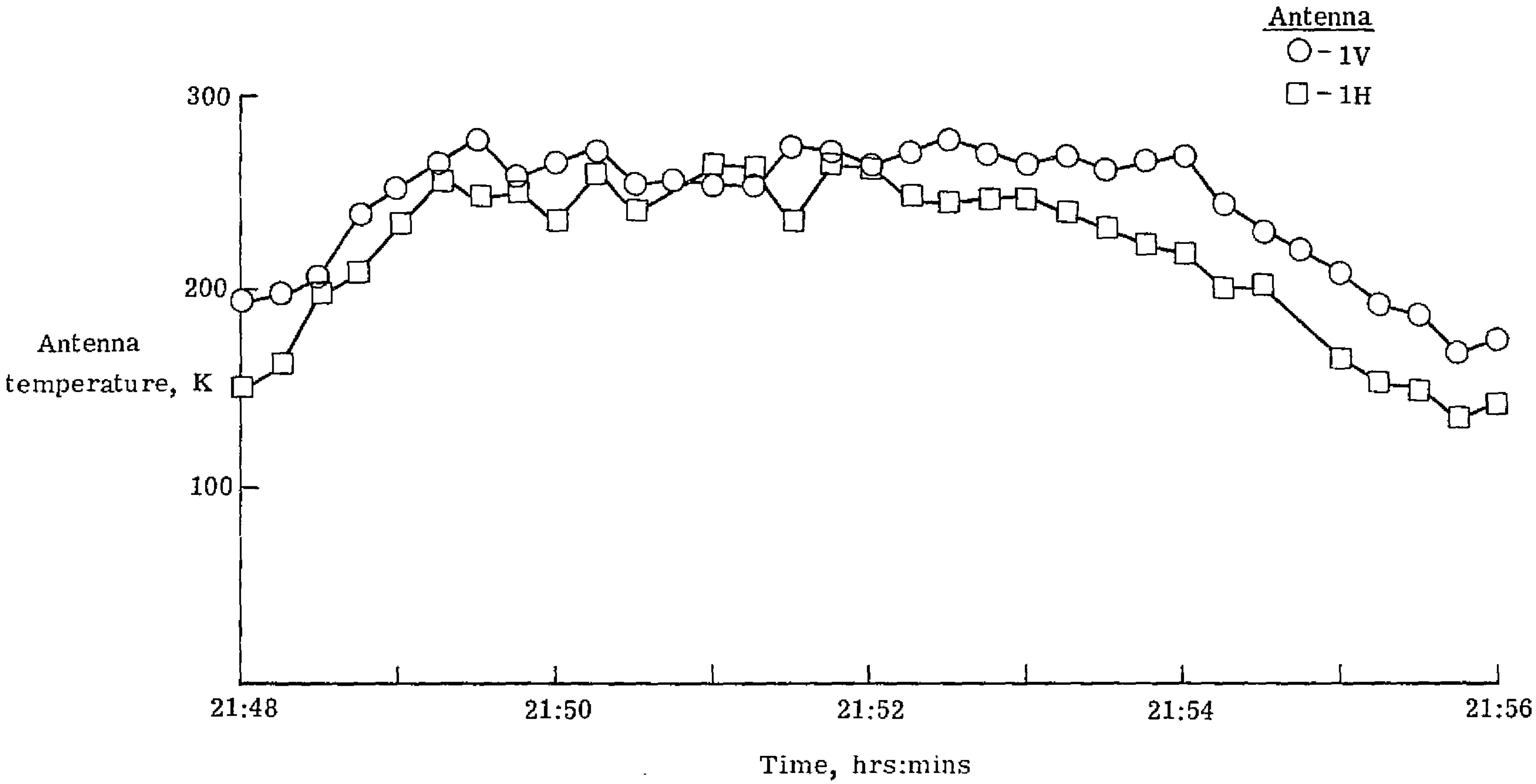

Figure 21.- Antenna temperature polarization characteristics, Rev 141.

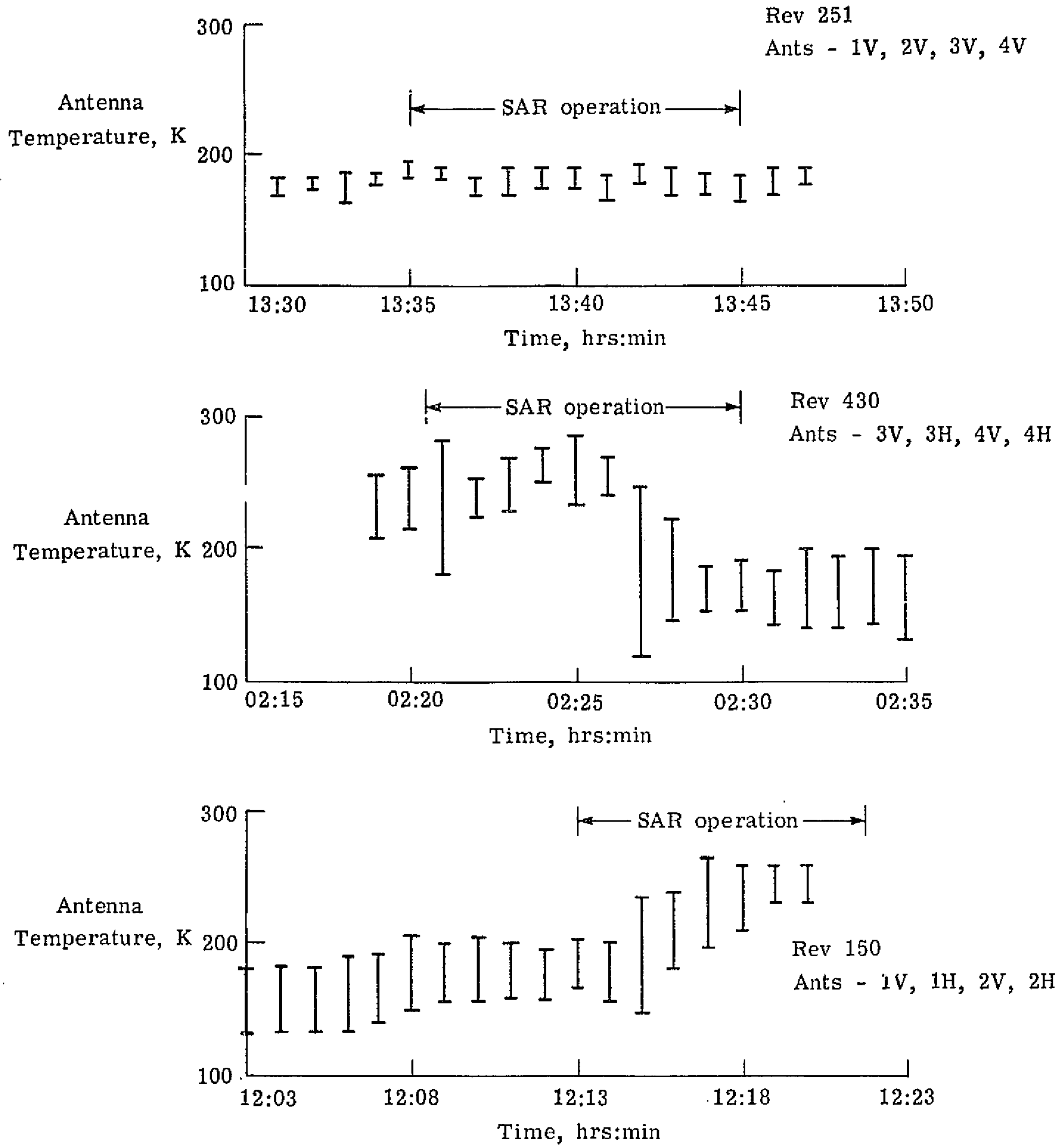

Figure 22.- Average receiver noise level test for RFI.

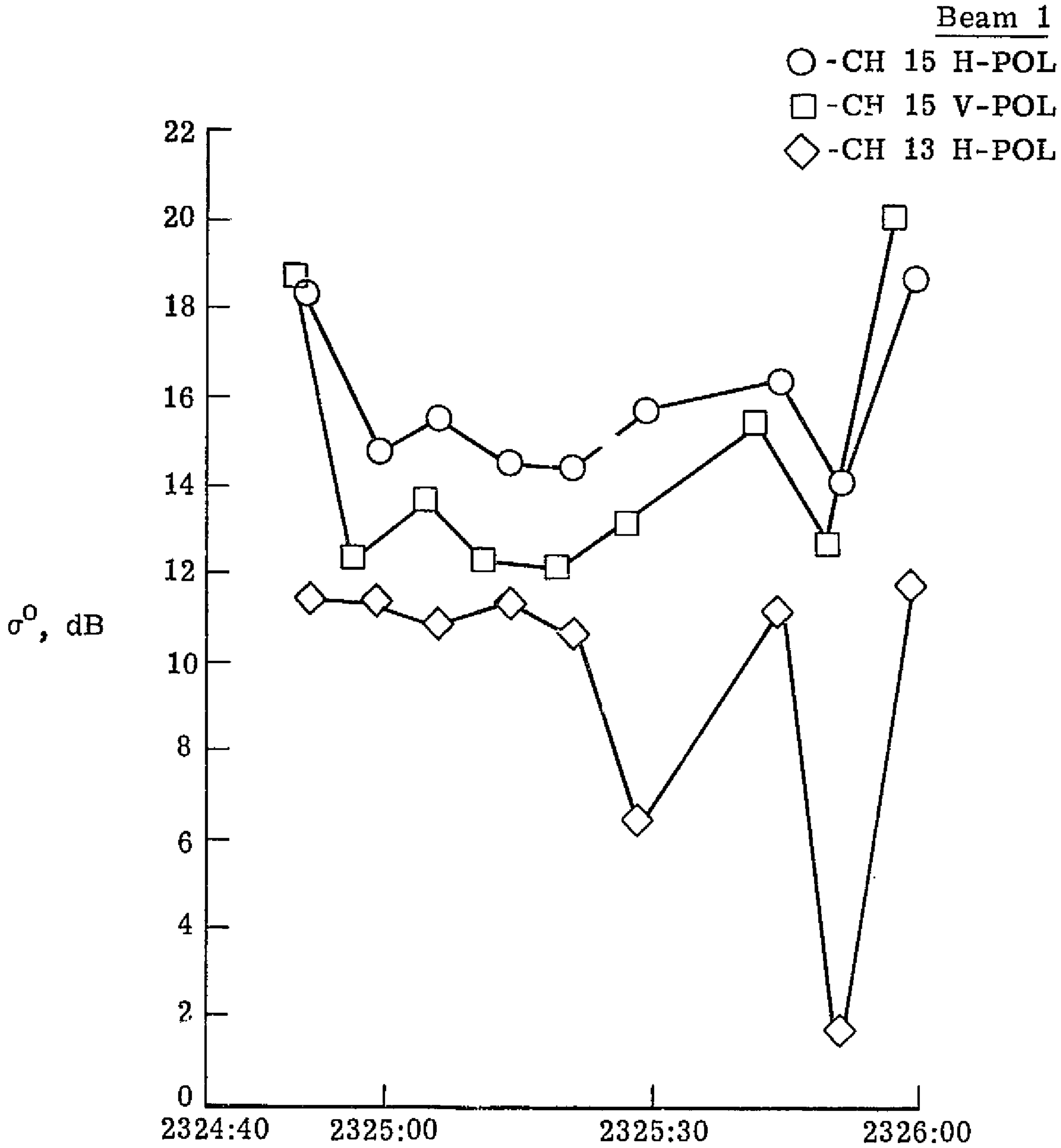

Figure 23.- σ^0 profiles for light surface winds on Rev 142.

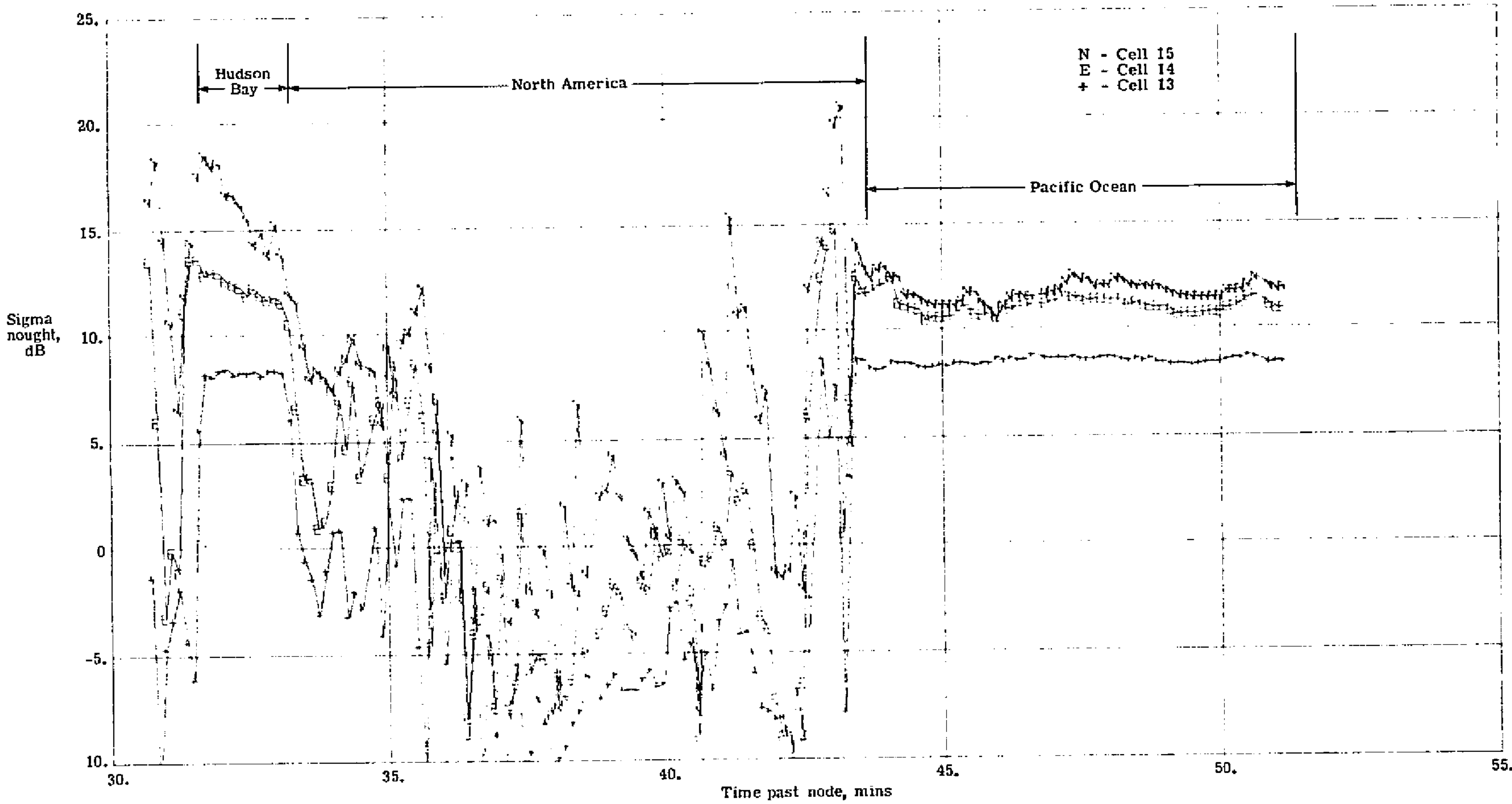

Figure 24,-σ° profiles for moderate surface winds, Beam 4, H-Pol.

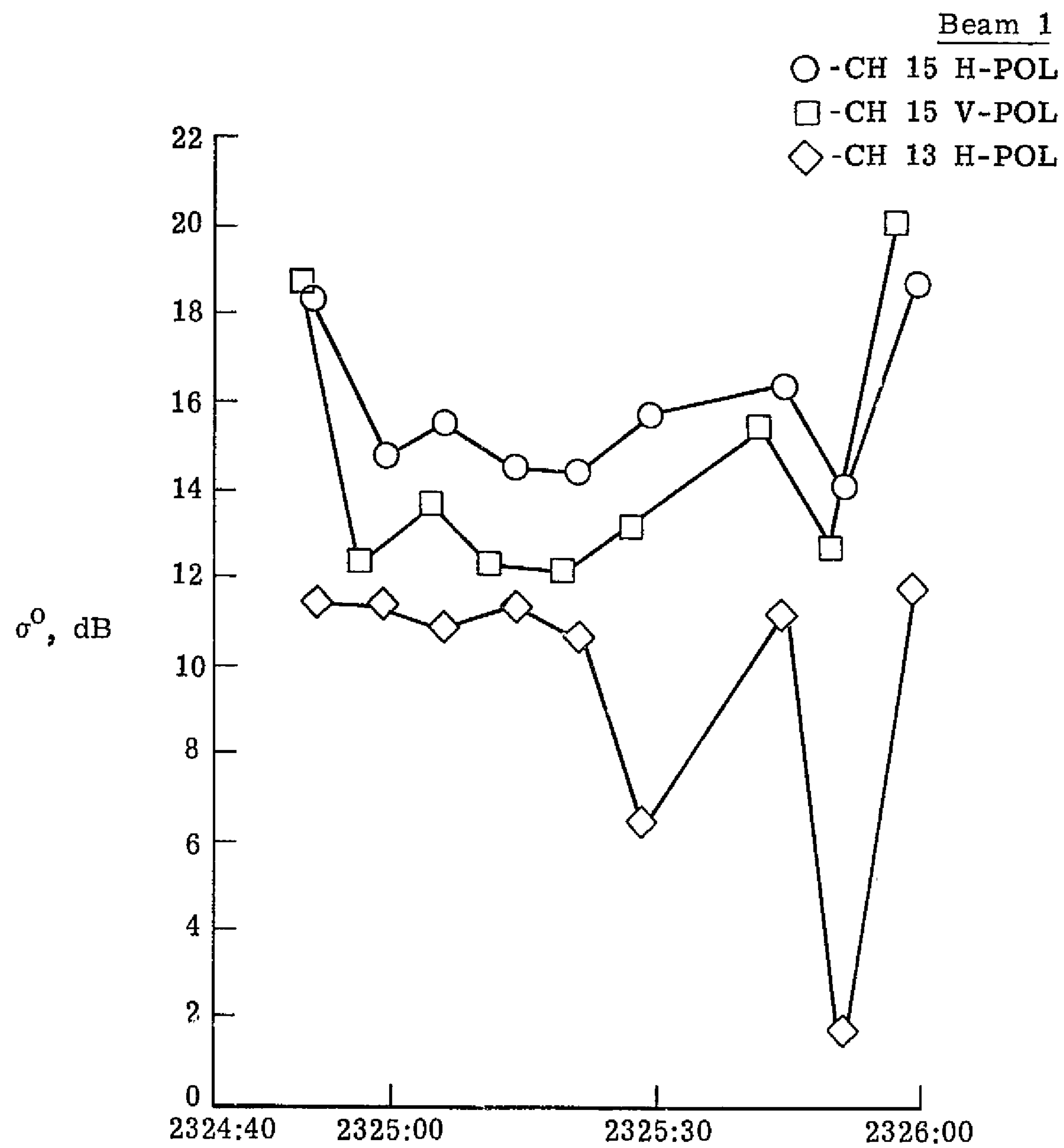

Figure 23.- σ^0 profiles for light surface winds on Rev 142.

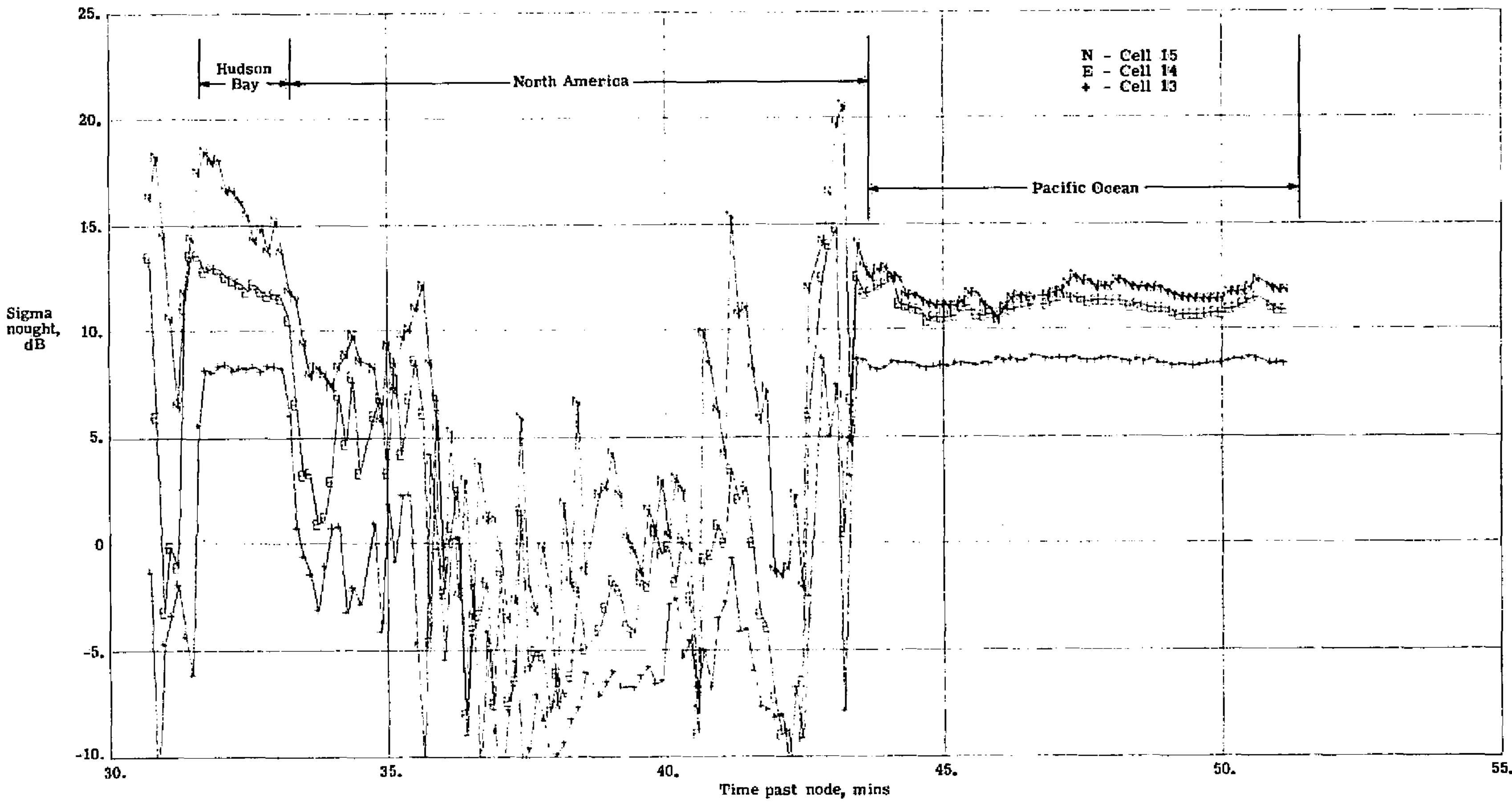

Figure 24,-σ° profiles for moderate surface winds, Beam 4, H-Pol.

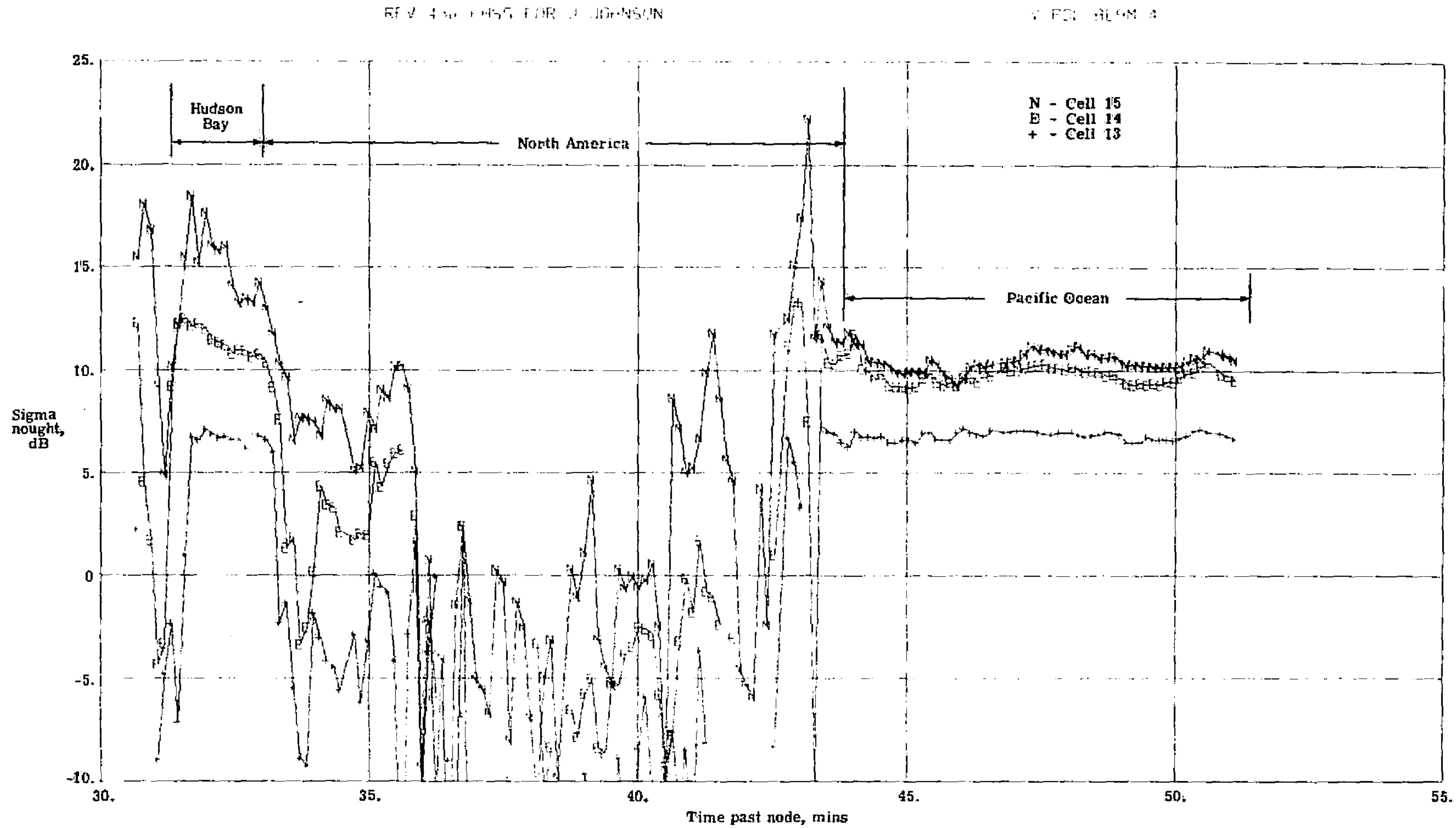

Figure 25.-σ° profiles for moderate surface winds, Beam 4, V-Pol.

1. Report No. NASA TM-80122	2. Government Accession No.	3. Recipient's Catalog No.
4. Title and Subtitle SeaSat-A Satellite Scatterometer Mission Summary and Engineering Assessment Report		5. Report Date May 1979
		6. Performing Organization Code
7. Author(s) James W. Johnson, Wendell H. Lee, Leon A. Williams		8. Performing Organization Report No.
9. Performing Organization Name and Address NASA Langley Research Center Hampton, Virginia 23665		10. Work Unit No.
		11. Contract or Grant No.
12. Sponsoring Agency Name and Address National Aeronautics and Space Administration Washington, D. C. 20546		13. Type of Report and Period Covered Technical Memorandum
		14. Army Project No.

15. Supplementary Notes

16. Abstract

The SeaSat-A satellite was launched on June 26, 1978 and operated in orbit through October 9, 1978. The SeaSat-A satellite scatterometer ocean surface wind field sensor began taking data on July 10, 1978 with virtually continuous operation for 95-1/2 days. This paper is a review of mission events significant to the scatterometer and a report on the hardware and software engineering assessment. The latter satisfies a JPL project office requirement to evaluate the scatterometer in orbit performance, in an engineering sense, and the performance of the JPL Instrument Data Processing System (IDPS) software to determine the quality of the data being gathered prior to geophysical processing. An evaluation of the Project Operations Control Center (POCC) software used to support mission operations is also included. It has been concluded that the POCC software met the original requirements and the IDPS software was acceptable for the given quality of the IDPS input data. Deficiencies in ground data handling and processing resulted in poor data quality that required extensive editing and filtering in the geophysical processing to attain acceptable error rates. It was also determined that the scatterometer hardware operated flawlessly throughout the mission meeting all of its electrical design goals and specifications with no detectable RFI effects from other SeaSat-A sensors.

17. Key Words (Suggested by Author(s)) SeaSat-A, Oceanography, Remote Sensing, Anemometer	18. Distribution Statement Unclassified - Unlimited; Subject Category 43

19. Security Classif. (of this report)	20. Security Classif. (of this page)	21. No. of Pages	22. Price*
Unclassified	Unclassified	144	$7.25

*For sale by the National Technical Information Service, Springfield, Virginia 22161